LIPID-BASED CANCER VACCINES

Elizabeth Ann Vasievich

A dissertation submitted to the faculty of the University of North Carolina at Chapel Hill in partial fulfillment of the requirements for the degree of Doctor of Philosophy in the UNC Eshelman School of Pharmacy.

Chapel Hill
2011

Approved by:

Rudolph Juliano, Ph.D.

Leaf Huang, Ph.D.

Russell Mumper, Ph.D.

Jenny Ting, Ph.D.

ABSTRACT

ELIZABETH ANN VASIEVICH: Lipid-Based Cancer Vaccines
(Under the direction of Leaf Huang, Ph.D.)

Each aim of this project ranges from vaccine formulation to whole-body response; starting from the structure-function relationship of the cationic lipid DOTAP (1,2-dioleoyl-3-trimethylammonium-propane) to the immunological action *in vivo*. The three aims of this work examine DOTAP; the structural specificity, development of a melanoma-specific formulation and development of a joint siRNA/peptide delivery vehicle.

The first aim in these studies investigates the impact of DOTAP's chiral center on a peptide based therapeutic vaccine in a murine cervical cancer model. The lipid, (R) or (S)-DOTAP was combined with an MHC Class I restricted peptide (E7), from the E7 oncogene in human cervical cancer. In this work, (R)-DOTAP/E7 was shown to act equally well as the racemic mixture in causing tumor regression, while (S)-DOTAP/E7 had a lesser effect. This data was supported by other studies evaluating the cell-mediated anti-tumor response, and in each, (R)-DOTAP/E7 showed greater efficacy.

The second aim investigates the development of a peptide/lipid melanoma vaccine with a different antigenic peptide that poses unique formulation challenges. The amphipathic Trp2 peptide antigen was formulated to address poor aqueous solubility, and yielded stable vaccine particles when mixed with (R)-DOTAP. (R)-DOTAP/Trp2 delivered in high Trp2 doses to tumor-bearing mice showed enhanced tumor growth

delay compared to lower Trp2 doses, which was supported by additional immunological assays.

The third aim seeks to enhance the versatility of the delivery vector with added siRNA therapy. Formulation of tri-modal particle, including (R)-DOTAP adjuvant, melanoma antigen (Trp2 peptide) and siRNA against PD-L1 (RTP particles) expanded the versatility of the previously developed (R)-DOTAP/Trp2 vaccine. PD-L1 siRNA was incorporated to dampen the inhibitory signal that DCs express when activated, that can inhibit T cell function. The examination of the structure and activity of these particles *in vitro* and *in vivo*, led to further understandings of the vaccine. In a solid melanoma model, delivery of RTP showed a tumor growth delay statistically significant compared to particles with control siRNA.

In closing, (R)-DOTAP is the immunologically active enantiomer, showing efficacy in cervical cancer and melanoma models, with the potential to deliver a variety of peptide antigens and siRNA, showing tumor growth delay.

To Harold

ACKNOWLEDGEMENTS

I would like to thank my advisor, Dr. Leaf Huang, for his mentorship and support throughout my education at UNC. He taught me the crucial design of experiments, encouraged me through my academic progression, gave me many opportunities to mentor other students and to collaborate, pushed me to write and publish reviews and manuscripts, encouraged me to deliver lectures to PhD and PharmD students alike, funded a flow cytometry training course at BD and he supported my pursuit of leadership positions within the school. Most crucially, he supported me in pursing my career goals. His dedication to his lab and the extreme devotion of time to his students is a testament to his incredible character.

I also thank my committee members, Drs. Juliano, Mumper, Needham and Ting for their critical review of my progress, suggestions and encouragement during the advanced years of my studies. Of note, I am particularly grateful to Dr. David Needham of Duke University, who taught me how to use my first pipet in the summer of 2005, interested and inspired me to the potential of liposomes as delivery vehicles and supported my progress through to PhD completion.

Dr. Feng Liu, our lab manager was a friend, ally, and brilliant scientific mind to consult on all aspects of my work. I often marveled to think how lucky I was to have a bench next to the first author of hydrodynamic delivery. Feng taught me many critical techniques in the lab and promoted a productive lab environment.

I was blessed to work with the many members of the Huang lab for the past five years. These colleagues saw the data first, from sitting with me at the flow, to looking at westerns straight out of the darkroom, or dendritic cells under the microscope. They were my teachers and my comrades. I must particularly thank those that taught me immunology first; Drs. Claire (Weihsu) Chen, Lisa McEwen and Willa (Wei-yun) Sheng. Also, Drs. Becky (Yunching) Chen, Star (Shyr-Dar) Li, Jun Li, and Al Wang, who helped me learn gene delivery and techniques to evaluate response. Dr. Srinivas Ramishetti guided me in my chemistry experiments and collaborated with me on much of the work presented here, providing an extra set of hands in an experiment. Teaching Dr. Ramishetti protocols and explaining the purpose of the experiments helped me gain a deeper understanding of this work. Miss Yuan Zhang, Miss Younjee Chung, and Miss Angela Yang also assisted on in tissue processing or imaging, with Y.Z. producing the TEM pictures in **Figure 3.2D, Figure 4.2**.

No child of science can be raised without a village, and the faculty and staff of the Division of Molecular Pharmaceutics and the larger Eshelman School of Pharmacy were instrumental in my success. I enjoyed serving with the Dean and the Graduate Education Committee, sitting in Dr. Cho's office to talk about life and chemistry, working with Amber Allen as the Graduate Student Organization president and chatting with Angela Lyght about the latest advances in my work. Drs. Michael Jay and Dhirin Thakker were both strongly supportive of my progress and often encouraged me along the way. The door of Dr. Boka Hadzija's office was directly across from our lab, and she would often

call me in to see how my work and how my life was going. The students of the Eshelman School of Pharmacy were guiding lights of scientific interest and character and I was lucky to share the path with them for a while. Arlene Bridges and the ADME Mass Spectrometry Center in the Department of Pathology and Laboratory Medicine at UNC are thanked for the use of their Mass Spectrometry instrument in Trp2 stability experiments. Judy Winston of the Kerr animal facility cared for each one of the mice in this body of work. Her dedication to the care of these subjects for the advancement of science through these experiments is greatly appreciated. Ricky Bunch of the housekeeping staff was a welcome face in the late hours of the lab, always offering encouragement and support.

My friends and family are greatly thanked. They rejoiced with me when the data was good, and the publications were accepted, and they comforted and encouraged me when the data was negative or the experiment failed.

In my first year of study, I was supported by the UNC Merit Assistantship. In subsequent years, I was supported by a Pre-Doctoral Fellowship in Pharmaceutics from the PhRMA Foundation and by Dr. Leaf Huang. The NIH funding (grant CA129421) helped support these studies, as well as funding from PDS Biotechnology, who obtained (R) and (S)-DOTAP from Merck KGaA for use in these studies.

TABLE OF CONTENTS

LIST OF TABLES

Table

LIST OF FIGURES

Figure

LIST OF ABBREVIATIONS

(R)-DOTAP	(R)-1,2-dioleoyl-3-trimethylammonium-propane
(S)-DOTAP	(S)-1,2-dioleoyl-3-trimethylammonium-propane
BMDC	bone marrow-derived dendritic cells
CCL2	chemokine C-C motif ligand 2, also known as MCP-1
CFSE	carboxyfluorescein succinimidyl ester
HPV	Human Papillomavirus
IFN-γ	Interferon gamma
i.t.	intratumoral
i.v.	intravenous
MCP-1	monocyte chemotactic protein 1, also known as CCL2
MDSC	myeloid derived suppressor cells
MHC	Major Histocompatibility Complex
ROS	reactive oxygen species
TAMs	tumor associated macrophages
TIL	tumor infiltrating lymphocytes
s.c.	subcutaneous
Tregs	T regulatory cells
Trp2	Tyrosinase-related protein 2 (also used to describe Trp2 peptide)

CHAPTER 1

INTRODUCTION

1.1 VACCINE NECESSITIES AND DELIVERY OF ADJUVANTS AND ANTIGENS USING CATIONIC LIPIDS

Three things are required in building an efficacious vaccine, and elicit an immune response in vivo. **Figure 1.1** describes the basic immunological process of vaccination to T cell activation for cell-mediated immunity (protection against infected cells, or even cancer cells). First, vaccines are essentially delivery vehicles, meant to (safely) mimic infection and establish immunological memory. This can occur via a depot effect that allows antigen to drain into lymph vessels and eventually lymph nodes, or cause local inflammation to recruit antigen-presenting cells (APCs) to the site of injection.

Second, vaccines require activation of APCs. Activation can occur through recognition of pathogen-associated molecular patterns (PAMPs) by Toll like receptors (TLRs) which can upregulate activation molecules and induce production of inflammatory cytokines and chemokines. TLRs specifically identify many of different conserved patterns both extracellularly and in endosomes. On the surface of the cell,

TLRs detect surface markers from bacteria, viruses or fungi, such as lipopolysaccharide (TLR4), viral hemagglutinin (TLR2), bacterial flagellin (TLR5). Inside endosomes, TLRs respond to single or double stranded DNA or RNA utiling TLR3, 7, 8 and 9. While "adjuvant" could be defined as any implement that enhances a vaccine's action, here we'll follow a more narrow definition of activation of APCs.

Finally, the body needs a signal of the infection or infected cells to recognize, called antigen, usually either a continuous or discontinuous peptide sequence.. How this antigen is presented to the immune system is important. The immune system responds differently to an infectious virus circulating through the blood, as compared to a virally infected cell. APCs present antigen differently to combat these two invaders, utilizing different Major Histocompatibility Complexes, either MHC I or MHC II. Circulating viruses or soluble antigen endocytosed by APCs will be processed into antigen fragments in the endosomal vesicle (never entering the cytoplasm), and presented on MHC II. Antigen presented on MHC II interacts with the T cell receptor (TCR) of $CD4^+$ T cells, leading to humoral immunity. In contrast, antigen in the cytoplasm (in the case of infected cells) is presented on MHC I, and interacts with the TCR on $CD8^+$ T cells (known as cytotoxic T lymphocytes, CTLs). CTLs lyse infected cells by releasing vesicles of Granzyme B and Perforin. Cross-presentation occurs when APCs endocytose antigen that subsequently escapes into the cytoplasm, therefore MHC I presentation can occur inducing a CTL response. Endosomal release and subsequent cross-presentation is crucial to creating CTL responses from antigen delivered by lipid carriers.

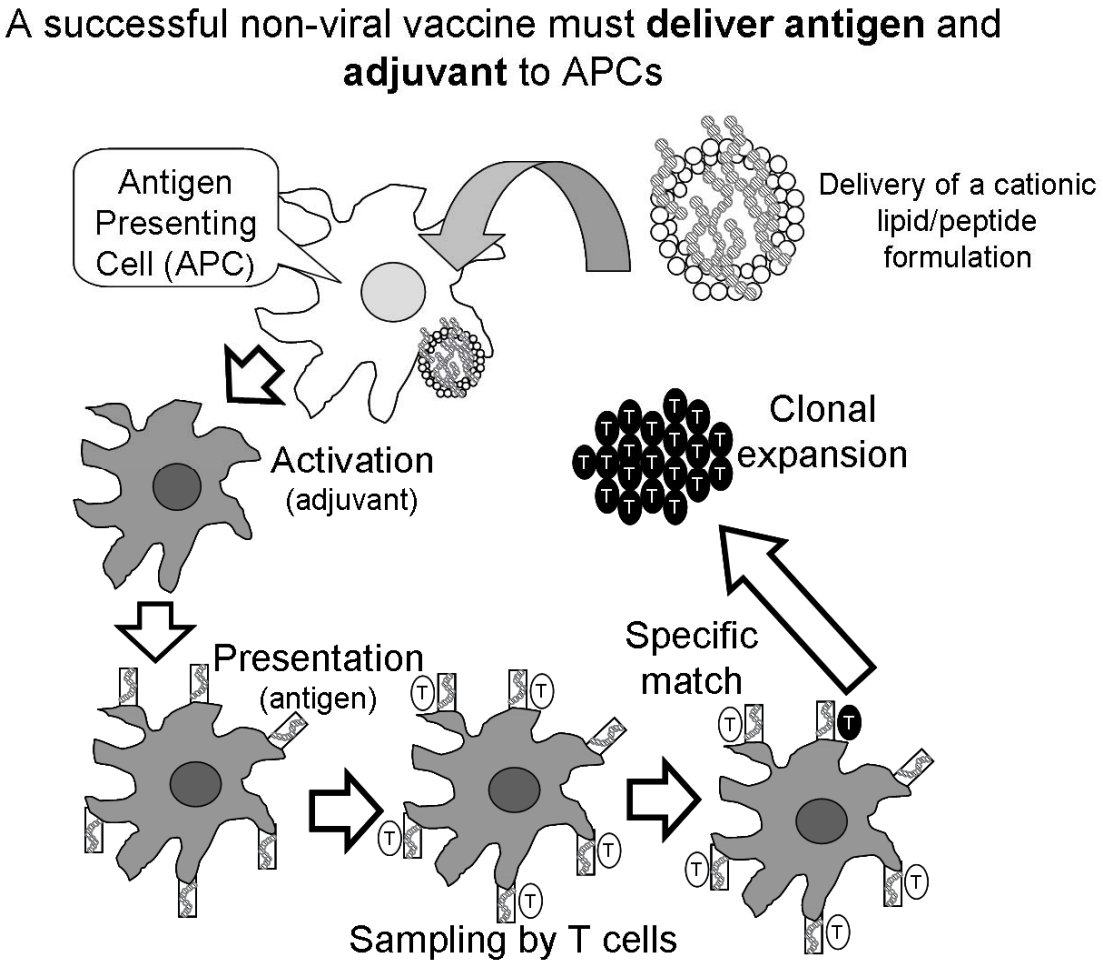

Figure 1.1 Requirements of an efficacious vaccine.
The cationic charge on some lipids allows for endosomal escape of antigen (with varying efficiencies), crucial for inducing cell-mediate immunity. A successful adjuvant seeking to elicit cell-mediated immunity should activate antigen presenting cells (APCs) and facilitate antigen presentation to T cells. In the figure, the schematic representation shows how the adjuvant works as vaccine. We've used the example of an antigenic peptide encapsulated in cationic lipid adjuvant. After the s.c injection of the vaccine, complexes can activate APCs through different mechanisms. After endocytosis, cationic lipids facilitate the intracellular release, allowing APCs to present the peptide via MHC class I to $CD8^+$ T cells. An activated T cell undergoes clonal expansion, generating many more T cells with the same T cell receptor specific for the antigen. T cells then circulates in the blood to surveillance the body for cells presenting the antigen they've been activated against. When the activated T cells find these infected (or cancer cells), they can kill them by releasing cytokines. Alternatively, when endosomal escape does not occur, antigen still may be presented, however now on MHC class II, and will elicit humoral, or antibody-based, immunity, most effective against soluble antigen or circulating pathogens.

Liposomes have been investigated as carriers of adjuvants and antigens for many years.[1; 2; 3] The delivery capacity of liposomes is well established, with a large available hydrophilic payload and a lipid bilayer capable of incorporating both lipid adjuvants and hydrophobic adjuvants or antigen. While lipids make poor antigens themselves for recognition by the immune system, they have been investigated as adjuvants. Monophosphoryl lipid A (MPL), shown in **Figure 1.2**, is the most well known lipid adjuvant, and appears in two U.S. marketed vaccines, Fendrix® and Cervarix®,[4; 5] for hepatitis B or HPV16/18, respectively. MPL is the immunologically active portion of lipopolysaccaride (LPS) from *Salmonella Minnesota*. Both MPL and LPS function as adjuvants to activate APCs through TLR4 on the surface of the cell.[6; 7; 8; 9] This action is well characterized and understood,[10] unlike the mechanism of other lipid adjuvants. Cationic lipid use in gene therapy has exposed interesting delivery properties allowing for intracellular delivery of antigen as well as some unique adjuvant properties. As delivery is a well established mechanism for liposomes, Chapter 1.2 will discuss cationic lipids' action as immunological adjuvants, particularly focusing on the advantages of using cationic lipids to initiate cell-mediated immunity.

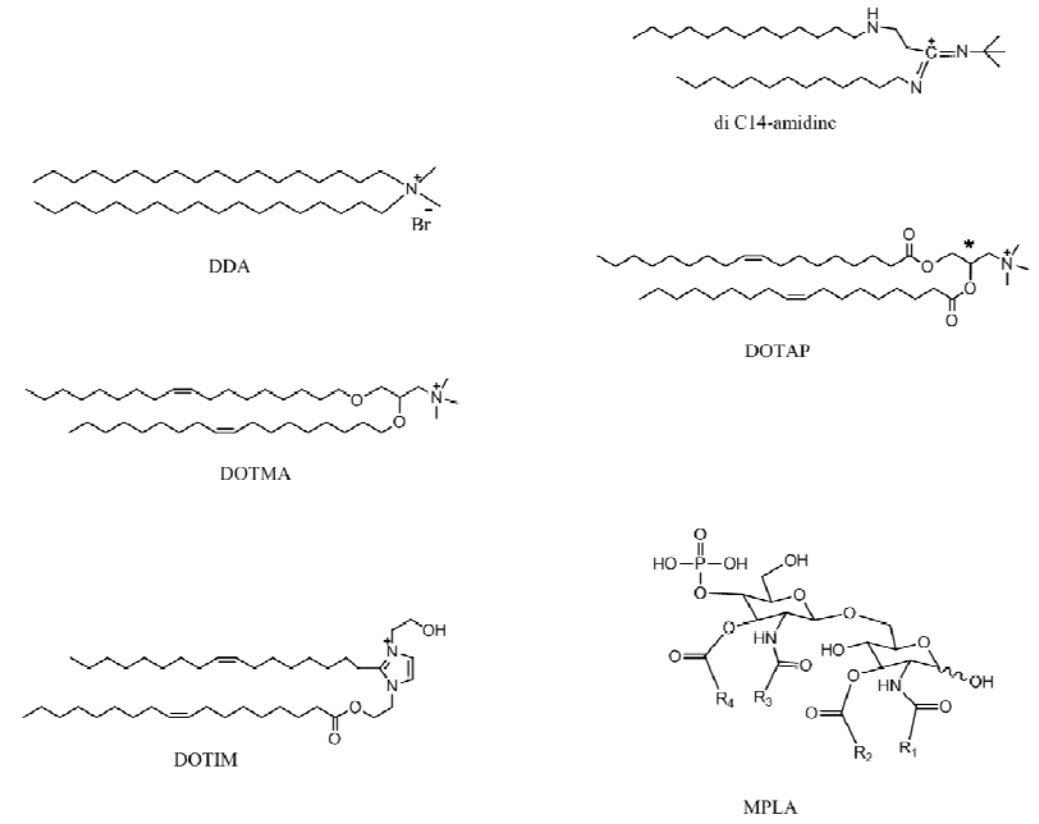

Figure 1.2 Different cationic lipids used in vaccine formulations (and MPL).
The joining of the acyl chains of DOTAP with the quaternary amine form a chiral center indicated with an asterisk (*). The enantiomers (R)-DOTAP and (S)-DOTAP are commercially available as chirally pure sterospecifically synthesized compounds (Merck KGaA) or as a racemic mixture (Avanti Polar Lipids).

1.1.2 Cationic Lipids as Delivery Vehicles

Complexes of cationic lipids used to condense (negatively charged) pDNA were found to be strongly immunostimulatory (mainly due to the unmethylated CpG motifs on the pDNA). However, the use of cationic lipids as delivery vehicles also releases their payload into the cytoplasm. The mechanism has been explained by ion-pairing between the negatively charged lipids in the internal layer of the endosome and the cationic lipids of the particle, therefore facilitating endosomal release.[11] The advantage of delivering an vaccine with such antigen release properties, is the ability to deposit the cargo into the cytoplasm. Thus, the antigen is directed to present via MHC class I, and stimulating cell-mediated immunity becomes a possibility. Other ways that cationic lipids can assist in delivery is to enhance antigen loading, by increasing the adsorption of anionic proteins.

Therefore, as a delivery vehicle, cationic lipids confer beneficial properties (as no other endosomal release strategy needs to be considered). Some cationic lipids are investigated for their vaccination delivery properties alone, formulating them with additional adjuvants to enhance any activity the cationic lipid may possess. A few examples of lipids that have been thus investigated include: DDA (as vesicles), DOTIM, DOTMA and DC-Chol (all shown in **Figure 1.2**).

1.1.2.1 DDA or DDAB or DODAB (dimethyldioctadecylammonium bromide)

DDA has two unsaturated 18 carbon chains and a simple headgroup consisting of a quaternary amine. In vaccine formulations, this lipid has shown contradicting results. Some have reported its immunostimulatory potential, while others attribute its vaccine efficacy to a depot effect, and thus formulate with an additional adjuvant to boost activity. We've presented first how DDA acts as a carrier, and later, how others have explained its adjuvant activity. Then we'll explain some possibilities for the differences.

A formulation termed cationic adjuvant formulation 01 (CAF01) is made from DDA and TDB (trehalose 6,6'-dibehenate) and has been widely tested in many different delivery mechanisms, including as a mucosal adjuvant.[12] CAF01 was attributed to function through TLR 2, 3, 4, and 7 independent pathways, in a MyD88-dependant manner.[13] However, the independent function of DDA was not isolated in these studies. DDA doesn't activate bone marrow-derived dendritic cells (BMDC) to upregulate MHC class II, CD40, CD80, CD86. Lipid cationic charge and antigen adsorption contribute to antigen deposition at the site of injection as seen with CAF01.[14]

However, some have generalized DDA to have "adjuvant" action by targeting particles to antigen presenting cells.[15] Increased particle size has shown faster localization to draining lymph nodes.[16] One comparative study, formulated three different cationic lipids, DDA and evaluated the appearance in draining lymph nodes. In comparative experiments, DDA/TDB/Ag and DC-Chol/TDB/Ag complexes showed an enhanced retention at the site of injection and increased recruitment of monocytes to the site of injection. This was correlated with the smaller sized formulations for DDA and DC-Chol at ~500nm and ~300nm, compared to ~700nm for the DOTAP formulation. The larger sized DOTAP formulations showed the fastest accumulation of lipid and antigen in the

popliteal lymph node (draining from a quadriceps i.m. injection), indicating faster drainage from the site of injection and faster exposure to APCs.

1.1.2.2 DOTIM (octadecenoyloxy(ethyl-2-heptadecenyl-3-hydroxyethyl) imidazolinium)

DOTIM has been investigated in vaccine formulations ranging from influenza to cancer. Formulated with cholesterol and pDNA it is termed, "CLDC" cationic lipid-DNA complexes, or JVRS-100 (for commercial purposes), this complex has shown efficacy in tumor growth delay in an orthotopic glioblastoma model without an associated antigen.[17] However, the lipid alone (or the pDNA alone) did not have any effect on tumor volume (after i.v. administration). This is surprising as pDNA is known to activate TLR9 in APCs through its unmethylated CpG motifs. The JVRS-100 formulation was also successful in a transgenic model expressing the hepatitis B virus (HBV), breaking tolerance with humoral (IgG titer) and cell-mediated (IFN-γ with restimulation) responses.[18] Again, in model, JVRS-100 was not able to induce antibodies against HBV. Finally, in a separate application, JVRS-100 was combined with Fluzone®, a commercially available seasonal influenza vaccine.[19] JVRS-100 was added to Fluzone® by mixing and tested in mice and non-human primates. While JVRS-100 had no activity (the non-specific activation shown previously was not apparent in any figures), the mixture of JVRS-100 + Fluzone® caused increased humoral and cell-mediated responses compared to Fluzone® alone, even allowing for protection from antigenic drift.

In these studies, DOTIM/Chol/pDNA structures have shown the ability to bolster the immune activity, either acting as non-specific immunostimulators (glioblastoma), carriers for hepatitis B surface antigen, or Fluzone®. However, as mirrored in the

glioblastoma study, the DOTIM lipid is not a strong enough antigen to have any anti-tumor effect on its own. The non-specific cell-mediated effect cannot be replicated in the viral protection studies of HBV and influenza. Thus, we suspect, DOTIM was included in this formulation solely as a carrier for pDNA, with cholesterol included to stabilize the bilayer by reducing fluidity.

1.1.2.3 DOTMA (N-(1-(2,3-dioleyloxy)propyl)-n,n,n-trimethylammonium)

DOTMA/Chol, like DDA, has been used as a carrier of nucleotides, including CpG oligos and pDNA. Complexing with modified oligos, particle sizes are small, around 120nm, ideal for i.v. or i.p. injection.[20] DOTMA/modified CpG oligo complexes were able to prevent peritoneal metastases as well as induce large amounts of TNF-α in *ex vivo* treated macrophages. This indicates that tumor progression (to metastases) was prevented by a strong inflammatory response by the lipid/modified CpG oligo combination. (Control groups indicated it was the modification of the oligo from a phosphodiester (PO)-CpG, to a phosphorothioate (PS)-CpG, that caused the increase in inflammation). In studies of intratracheal administration of DOTMA/Chol/pDNA, it was found how DOTMA and the pDNA each enhance the immune response.[21] It was found that pDNA contributed to the IFN-γ and IL-12 secretion, and DOTMA alone did not induce IL-12. DOTMA was responsible for TNF-α secretion as well as acute cellular influx. The carrier aspect of DOTMA is also associated with the non-specific inflammation of TNF-α production. However, TNF-α can have toxic effects that act very quickly and safer vaccine components are needed to ensure cytokine storms are kept at bay while an efficacious vaccine can install immunological memory.

1.1.2.4 DC-Chol (3β-(N-(N',N'-dimethylaminoethane)-carbamoyl]cholesterol hydrochloride)

Gao and Huang developed DC-Chol, as a cationic lipid for gene delivery, however it has been tested in vaccine formulations as well.[22; 23] Cholesterol doesn't form liposomes alone; it is usually formulated 1:1 with a neutral lipid to form bilayer vesicles. When DC-Chol was combined with split inactivated influenza vaccines, antigen binding and immune stimulated was increased, compared to neutral cholesterol.[24] Cryo-TEM pictures showed that DC-Chol combined with the split virus were liposomes, indicating the formation of virus-like particles. DC-Chol stabilized the split virus and increased the antigen adsorption to grater than 75 %. These particles also showed increased humoral and cell-mediated immunity, compared to neutral carriers of the vaccine, or antigen alone. However this could be due to increased particle uptake due to the cationic charge as well as increased antigen loading. Increased antigen loaded in an i.v. DC-Chol vaccine formulations (with the adjuvant Quil A, and antigen OVA protein) was shown to elicit equal humoral responses to alum.[25] In these same studies, where DC-Chol was used to create a implantable vaccine, the immune response was no different than formulations using cholesterol (neutral charge). This could indicate the importance of delivery in this adjuvant's immune stimulating properties. In one test in humans, DC-Chol was an ineffective adjuvant via mucosal delivery in humans (nasal or vaginal) as a protective HIV vaccine (using the protein gp160 as an antigen).[26] Contradictory to all previous studies, Brunel et al showed that one large (500uL) s.c. injection of DC-Chol with HepB surface antigen, strong cell-mediated and humoral immunity were elicited and able to break tolerance in a resistant mouse model.[27] Separate investigators found that even after multiple s.c. immunizations, DC-Chol formulated with HepB surface antigen were unable

to stimulate a greater immunity than antigen alone.[28] DC-Chol has not shown versatility as an adjuvant via multiple delivery routes. However, in regards to antigen loading, DC-Chol (like many other cationic lipids) can greatly increase the antigen loading in the vehicle by interacting with negatively charged antigens by charge-charge interactions or interacting with other carrier lipids by decreasing the bilayer flexibility and permeability.

1.1.3 Cationic Lipids Multi-tasking as Adjuvants and Delivery Vehicles

Some cationic lipids are immunostimulatory by themselves, and as such, multi-task as both the delivery vehicle and the adjuvant. While the mechanism of action is not known for all cationic lipids, the adjuvant activity of many have been studied, including: DOTAP, DDA (as bilayer fragments), and diC14-amidine (all shown in **Figure 1.2**).

1.1.3.1 DOTAP (1,2-dioleoyl-3-trimethylammonium-propane)

DOTAP was first investigated as a non-viral gene therapy delivery agent, as an analog of DOTMA. As hypotheses regarding cytosolic release of nucleic acids from a DOTAP/gene complex involve the lipid ion-pairing to negatively charged membrane lipids, it is reasonable to assume that peptides and proteins might reach the cytosol as well from DOTAP-aided delivery. MHC class I-specific immunity against virally infected cells can be elicited from delivery of a protein with DOTAP.[29] DOTAP/antigen vaccinations have shown higher T cell activity (*in vitro* cytotoxicity to targets) as well as *in vivo* tumor regression than treatment with Complete Freund's Adjuvant (CFA).[29; 30]

Bone marrow-derived dendritic cells (BMDCs) are a common model for mechanistic studies on APCs, as are RAW264.7 and DC2.1 macrophage and dendritic

immortalized cell lines, respectively. DOTAP liposomes have been extensively studied in BMDCs. They have been shown to generate ROS in a dose-dependant manner, as well as requiring this ROS for ERK and p38 activation as well as cytokine induction.[31] CCL2, CCL3, and CCL4 are induced after DOTAP treatment to BMDCs.[32] Upregulation of activation markers, CD80/CD86 has been reported after DOTAP treatment, in both *in vitro* and *in vivo* applications.[30; 31] However, *in vitro* toxicity is apparent at high concentrations of DOTAP.[31; 33]

Very often, investigation of cationic lipids in gene delivery applications has lead to investigation of DNA vaccines, or protein antigen delivery. LPD, or lipid-polycation-DNA has been developed by our group to deliver DNA, siRNA, protein and peptides, utilizing DOTAP as the lipid component.[34; 35; 36; 37; 38; 39] However, the CpG motifs of the DNA had been linked to pro-inflammatory cytokines. However, it was found that LPD was able to stimulate natural killer (NK) cell activity in a CpG independent manner.[40] Indeed, it has been shown that DOTAP does not induce TNF-α, and thus although able to elicit a strong immune response, is not associated with undue inflammation.[41] Further work by Chen et al. exposed that complexes of DOTAP and an exogenous peptide alone was able to upregulate activation markers on DCs in draining lymph nodes and cause complete tumor regression in a murine cervical cancer model.[30] DOTAP has also successfully elicited cell-mediated immunity with a protein adjuvant.[42]

Interestingly, commercially available DOTAP is a racemic mixture. Stereospecific synthesis, by Merck KGaA, has conducted stereospecific synthesis of (R)-DOTAP and (S)-DOTAP for evaluation as adjuvants. Our recent work has shown that (R)-DOTAP is the active enantiomer in adjuvant activity, able to elicit similar tumor

regression as the racemic mixture when utilized as an adjuvant in an exogenous antigen.[33] (R)-DOTAP was able to show preferential *in vivo* CTL killing, and specific activity of nearly 30 % of $CD8^+$ TIL against the immunized tumor-specific peptide antigen. MPL analogs have been synthesized to investigate the stereospecificity as well. Similarly, stronger agonistic activity of the R,R,R,R-MPL analog, was shown compared to R,S,S,R-configuration, activity, but still acting on the TLR4 receptor.[43] This indicates the possibility that, although the exact mechanism of action that separates the DOTAP enantiomers is unknown, it is likely they act through the same receptor or mechanism, except (S)-DOTAP with a lesser affinity compared to (R)-DOTAP. This was shown in tumor growth delay (not regression), in (S)-DOTAP/antigen tumor-bearing mice, statistically significant from both the complete regression caused by (R)-DOTAP formulations or untreated mice with large tumors. (R)-DOTAP should be further investigated as an adjuvant promoting cell-mediated immunity as it contains the immune stimulation and cargo delivery properties necessary.

1.1.3.2 DDA or DDAB or DODAB (dimethyldioctadecylammonium bromide)

Unique formulation strategies with DDA have led to some interesting vaccines. With probe sonication in low ionic strength buffer, DDA vesicles are broken into bilayer fragments (BF), which have been investigated alone or as coating agents for solid particles (like silica or polystyrene sulfate).[44] An advantage of utilizing the solid core technique for formulation allows for a possible decrease in the amount of lipid needed. Interestingly, no difference was detected in Th1 or Th2 cytokines from mice treated with DDA vaccine formulations with or without a solid core (ie. silica or polystyrene sulfate) using a 18kDa-hsp antigen. DDA also elicited cytokine production from cells when

complexed with a different antigen, indicating that it is neither the "APCs like aggregates" theory, nor the specific molecular surfaces the DDA/Ag complexes that controls activation. Thus, it must be possible that there is direct recognition of DDA by APCs. When compared to alum, known for its ability to induce humoral immunity, alum performed about the same as DDA+Ag (with or without a silica core). However, when examining cell-mediated immunity, DDA+Ag (with or without a silica core), performed better than alum, indicating a multi-modal immunity that could be elicited.[45] Another consideration is efficacy in the two branches of immunity could indicate incomplete endosomal escape, and activation of APCs through a surface receptor (rather than in the cytoplasm).

The formation of the bilayer fragments are through sonication using a titanium probe. Methods indicate that titanium fragments are allowed to settle in the sonicated solution for 1 hour, at which time the supernatant containing DDA BF is removed. It is possible that while DDA has not shown activity alone (and thus the development of CAF01 formulations), that by chance utilizing this titanium probe to create bilayer fragments, what is actually being created is a colloid system of titanium particles and excess DDA. This would explain why DDA BF works as adjuvants, while DDA alone must be formulated with an additional adjuvant to produce efficacious immune responses.

1.1.3.3 diC14-amidine (3-tetradecylamino-tert-butyl-N-tetradecylpropionamindine)

diC14-amidine is a potent immunostimulator as well as delivery agent that stimulates dendritic cells through TLR4, in both MyD88-dependent and Toll/IL-1R-containing adaptor inducing interferon IFN-β (TRIF)-dependent pathways.[46] MPL, a simpler component of LPS that still signals through TLR4, and diC14-amidine both share similar

hydrophobic structures with C12-C14 chains and 2 C14 chains respectively. Treatment with diC14-amidine causes large amounts of inflammatory cytokines, including TNF-α and IL-12p40, in contrast to DOTAP and DDA. As expected, NF-κB as well as ERK1/2, JNK and p38 MAP kinases are associated with DC activation by diC14-amidine. Earlier work has shown that mannan coating of diC14-amidine/DNA vaccine formulations greatly increases efficacy, particularly when measuring a cell-mediated response.[47] The well-characterized nature of this adjuvant allows for careful use in clinic, perhaps even pairing with a cargo or application that necessitates or could counteract the strong inflammation elicited.

1.1.4 Conclusion

Many types of liposomes (charged and uncharged) have been utilized in stimulating the immune system.[48; 49; 50] Cationic lipids allow for flexibility in delivery of polyanionic cargos such as pDNA and CpG oligonucleotides, encoding therapeutic cytokine genes, or antigen itself, or utilization of the TLR9 activity of CpG oligos. More importantly, some cationic lipids can both stimulate and deliver, with a variety of antigenic cargoes, and elicit cell-mediated response that has not yet been shown by any FDA approved adjuvants.

1.2 THE SUPPRESSIVE TUMOR MICROENVIRONMENT: A CHALLENGE IN CANCER IMMUNOTHERAPY

In the past few years, the public's perception of vaccines has radically changed. The retraction of Andrew Wakefield's landmark 1998 publication in the Lancet that had correlated the development of autism with vaccinations and primarily the preservative thimerosal, had less impact than a scientist could hope. [51; 52; 53; 54] Rather, the emergence of preventative vaccines such as Gardasil™ and Cervarix™ that vaccinate against strains of the Human Papillomavirus (HPV) attributed to cause 70 % of cervical cancers, and Dendrion, a therapeutic vaccine that utilizes personalized medicine to treat prostate cancer have created renewed energy and interest in vaccines and immunotherapy, particularly for cancer treatment.

Gardasil™ is a quadravalent vaccine, immunizing against four different strains of HPV (6, 11, 16, 18), and is approved for women and men ages 9-26. Gardasil uses amorphous aluminum hydroxyphosphate sulfate as the adjuvant and uses a yeast expression system to manufacture the protein antigens. These protein antigens (from the four different HPV strains) are a major viral capsid protein, called L1, thus when introducing the proteins to the immune system, with the help of an adjuvant, the immune system can recognize the virus in circulation and kill the infected cells before it is able to mutate cervical epithelial cells (or any others) into cancer.

Cervarix™ is a similar formulation, delivering the viral capsid proteins with an adjuvant for prevention of HPV infection, however has several distinct differences. Cervarix is a bivalent vaccine (against HPV16 and 18) and therefore is only approved for women (ages 10-25), uses a baculovirus (insect cell) expression system to manufacture antigens, and a different adjuvant (AS04 (3-O-desacyl-4'-monophosphoryl lipid A (MPL) adsorbed on to aluminum (as hydroxide salt)).

As mentioned previously, Gardasil™ is an example of a cancer vaccine that uses aluminum hydroxide as an adjuvant. Until recently, alum was the only approved FDA adjuvant, utilized in nearly every marketed vaccine. AS04 is the second adjuvant to be approved in the US, and only appears in one vaccine (Cervarix). It builds upon the success of aluminum hydroxide, quite literally, with monophosphorylated lipid A conjugated to aluminum hydroxide.

However even with the recent successes, a good cancer vaccine has a great deal to overcome. It is not adequate to simply contain a strong adjuvant, specific antigen and particle form to make it attractive to the immune system. In some cases, an effective Th1 response can be measured (via IFN-γ levels), however, the tumor remains.[55] Stromal cells have a strong impact on the tumor microenvironment and how the immune system interacts with the tumor.[56] Several different types of hematopoetic non-vascular stromal cells can be present and protect the tumor from discovery and elimination. Removal or suppression of these inhibitory cells can enhance the tumor recognition and regression by the immune system as shown in **Figure 1.3**. Chapter 1.3 will present different types of hematopoetic non-vascular stromal cells and their affect on the tumor microenvironment, as well as strategies to overcome these effects.

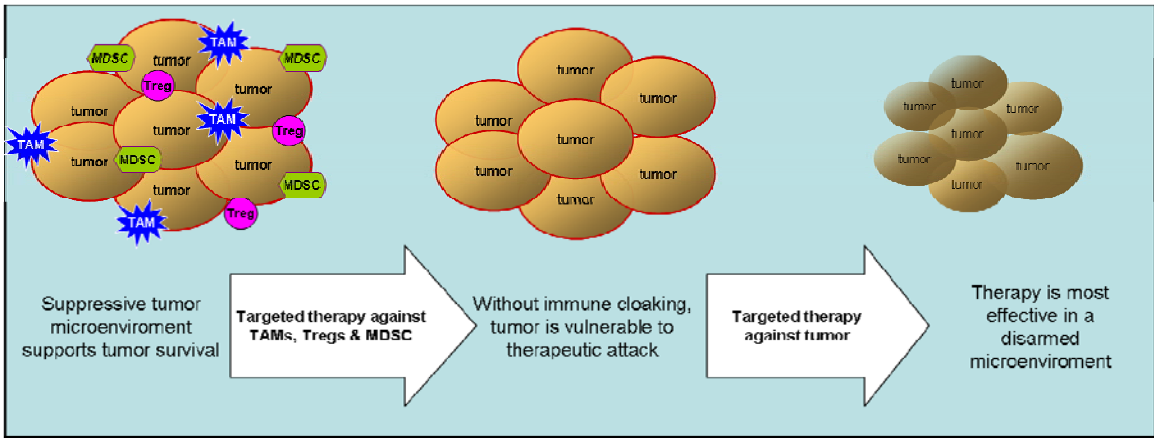

Figure 1.3 The suppression of the suppressive tumor microenvironment.
By disarming the suppressive immune cell sentries in the tumor, the tumor becomes vulnerable to attack and destruction. This chapter will focus myeloid-derived suppressor cells (MDSC), tumor-associated macrophages (TAM), and T regulatory cells (Tregs).

1.2.1 Tumor Associated Macrophages (TAM)

1.2.1.1 Overview

Chemokine (C-C motif) ligand 2 (CCL2), also known as monocyte chemotactic protein-1 (MCP-1), has a strong influence in the recruitment of macrophages and lymphocytes into tumor interstitum. This chemokine is released by macrophages and some tumors, recruiting macrophages and lymphocytes into the tumor microenvironment. While it may seem that macrophages in the tumor may be beneficial, tumor associated macrophages or TAMs, release growth factors and angiogenic factors encouraging the survival of the tumor. However, some studies have shown increased recruitment of cytotoxic T lymphocytes in environments with tumor expression of CCL2. Also, care should be taken in interpreting the results of some of the studies with human cancers in nude mice, as the authors infer a particular immune effect, when the subject (or mouse) has a compromised immune system.

In biopsies of cervical cancer patients, a correlation has been found between the amount of CCL2 mRNA expression by cervical tumor cells and the number of TAMs. Lack of CCL2 expression in 16 % of samples correlated with "increased cumulative relapse-free survival, increased cumulative overall survival, less post-operative surgery, reduced vascular invasion and smaller tumor size (<40mm)." Loss of heterozygosity (LOH) at 17q11.2 in six samples corresponded with the absence of CCL2 mRNA. The authors conclude that TAMs support tumor progression, "presumably by promoting angiogenesis and production of growth factors."[57]

Levels of cellular stress such as smoking or cancer have shown to sensitize some cells to produce more CCL2 when stimulated with LPS. Although CCL2 levels were seen

to be similar in a group containing patients with non-small cell lung cancer, healthy smokers and healthy non-smokers, these levels were seen to increase (in the supernatants) when peripheral blood mononuclear cells (PBMCs) were stimulated with LPS. Compared to baseline, CCL2 levels increased 28.5 fold in non-small cell lung cancer patients, 15 fold in healthy smokers and 13-fold in the group of non-smokers.[58] This sensitivity could explain the difference in the role of macrophages in a tumor microenvironment compared to a less severe inflammatory environment.

CCL2 was transfected into a human gastric carcinoma model (both ectopic and orthotopic) that did not previously express CCL2. CCL2 transfectants induced tumor growth, tumorigenicity, lymph node metastasis, ascites, TAMs in and around tumors, and significantly higher microvessel density.[59] In a xenograft prostate cancer model, CCL2 was shown to contribute to the regulation of TAM infiltration and enhanced angiogenesis within the tumor.[60] CCL2 concentration has been shown to increase with tumor stage (severity of tumor) and correlate with TAM accumulation in human colorectal cancer.[61]

Recombinant adenoviruses (rAds) expressing an herpes simplex virus thymidine kinase (HSV-tk) gene delivered in concert with a rAd expressing CCL2 showed suppression of mouse colon cancer tumor growth and has been attributed, by the authors, "exclusively associated with the recruitment of monocytes/macrophages, T helper 1 (Th1) cytokine gene expression and cytotoxic activity of the splenocytes." The tumor itself did not intrinsically express CCL2 before treatment. The propagation of TAMs into tumors did increase following delivery of the CCL2 gene in contrast to delivery of the CD80 gene.[62] The study concluded that suppression of the tumor was directly correlated

with macrophage presence in the tumor. However this is not congruent with the many other reports of CCL2 inducing negative effects of TAMs.[62]

The concept of positive feedback is an important one to consider with chemokine induction in the tumor microenvironment. In biopsies of human head and neck squamous cell carcinoma, TAMs secreted CCL2 as well as IL-6.[63] Both cytokines have shown to upregulate anti-apoptotic proteins and inhibit the caspase cascade.[64] If both the tumor and the TAMs are secreting CCL2, there is an amplification loop to recruit more and more macrophages to the tumor and surrounding area, increasing the negative effects from the secreted cytokines and chemokines by the macrophages.[65] In fact, IL-6 and CCL2 themselves have been shown to promote mutual induction, protection from apoptosis and polarization towards the M2 type macrophage.[64] The M2 phenotype act in an immunosuppressive manner, secreting IL-10 and transforming growth factor-β (TGF-β). In contrast,, M1 type macrophage are immunostimulatory, producing inducible nitric oxide synthase, IL-12 and TNF.[66; 67] Transition of TAMs from the M1 to M2 phenotype can be induced via HIF-1α knockout.[68]

1.2.1.2 Solving the Tumor Associated Macrophage (TAM) Problem

Inhibition of CCL2 has been of great interest lately as many negative effects have been elucidated regarding TAMs and CCL2. Gene therapy delivered to a human malignant melanoma (B16-F1) has shown that delivering a dominant negative CCL2 mutant gene (7ND) over expressing 7ND protein reduced TAMs, tumor angiogenesis, and tumor growth. Also, levels of TNFα, interleukin-1α (IL-1α) and vascular endothelial growth factor (VEGF) decreased in the tumor, attributed to less TAMs infiltrating the tumor.[69] In

another study, inhibition of CCL2 in human melanoma xenografts reduced tumor growth and macrophage recruitment resulting in necrotic tumor masses.[70]

Ability to switch the phenotype from M2 to M1 would solve the TAM problem and allow the infiltrated macrophages to become powerhouses of destruction. An adenovirus containing CCL16 (AdCCL16) and CpG was delivered intratumorally; the anti-IL10R antibody was given i.p., and complete regression in the majority of large tumors was observed.[71] A few hours after treatment, tumor macrophages switched from M2 to M1 type secreting TNF, IL-12, and nitric oxide and even dendritic cells in the tumor had upregulated costimulatory molecules and secreted IL-12 and TNF. The presence of inhibitory M2 type macrophages was reemphasized as the delivery of AdCCL16 alone was not able to cause tumor regression. However, one weakness of this study is the delivery aspect, with three separate injections needed (by two different delivery routes) to create the desired effect, therefore more work should be done to further refine the delivery of this treatment.

Specific delivery to M2 macrophages could be achieved by targeting the mannose receptor. Part of the change to the M2 phenotype caused by CCL2 or IL-6 is a significant increase in the mannose receptor (CD206).[64] Mannose can be conjugated or incorporated to treatments to target therapies to M2 polarized macrophages. Alternatively, targeted immunotherapy against TAM surface markers could cause selective clearance of this population, A DNA vaccine for legumain, an asparaginyl endopeptidase overexpressed by TAMs, increased the number of mice surviving a lethal tumor challenge and decreased the number of remaining metastases.[72]

1.2.3 Myeloid Derived Suppressor Cells (MDSC)

1.2.3.1 Overview

Myeloid derived suppressor cells (MDSC) are often $CD11b^{+}Gr\text{-}1^{+}$, but are broadly defined and have many functions.[73] Not only are these two markers found on neutrophils, but also immature dendritic cells, monocytes and early myeloid progenitors. MDSC are immunosuppressive, and also promote neovascularization. In humans, MDSC are $CD34^{+}CD33^{+}CD13^{+}$.[74] When directly exposed to a murine ovarian cancer cell line, MDSC express high levels of CD80 (but not CD86).[75] As with all immune cells, new subpopulations are constantly being defined and re-defined; MDSC are no different, with mononuclear or MO-MDSC, and low-density polymorphonuclear cells or PMN-MDSC. MO-MDSC was shown to function through STAT1, IFN-γ or nitric oxide (NO), whereas PMN-MDSC required IFN-γ, but not STAT1 or NO.[76]

The appearance of MDSC has been documented in many different cancers including mouse mammary carcinoma[77], 4T1[78; 77], and murine colorectal (MC38/CEA2)[79]. It has been shown in breast cancer that $CD11b^{+}Gr\text{-}1^{+}$ are recruited into tumors with type II TGF-β receptor gene (*Tgfbr2)* deletion.[78] Recruitment of MDSC to tumors has also been shown by several different chemokines including CXCL12, SDF-1α, CCL2, CXCL5 and KIT ligand.[80] Secretion of TGF-β1 by MDSC in the tumor microenvironment has been shown to promote metastasis in breast cancer.[78] In human breast cancer, numbers of MDSC was proportional to the clinical stage and lymph node metastasis (with stage III having more than stage I/II, and >3 metastases having more MDSC than <3.[81]

Immature myeloid cells inhibit $CD8^+$ T cells in direct cell-cell contact, show increased amounts of reactive oxygen species (ROS) caused by accumulation of H_2O_2. Also, MDSC have increased ROS production in the presence of stimulated Ag-specific T cells (stimulated with their specific Ag and producing IFN-γ.[82] MDSC are inversely correlated with NK function in the liver and the spleen and have been shown to inhibit NK cell production of IFN-γ by MDSC membrane-bound TGF-β1.[83]

In a tumor that produced IL-1β, accumulation of $CD11b^+Gr\text{-}1^+$ cells correlated with poor prognosis.[84] Not only does IL-1β attract MDSC to tumors, but GM-CSF and VEGF as well. $CD34^+$ cells showed accumulation in Lewis lung carcinoma tissues selectively (rather than the surrounding tissues), entirely attributed to the secretion of VEGF.[85] High expression of GM-CSF in the tumor causes increased numbers of MDSC and immunosuppression.[86; 87]

Not surprisingly, MDSC do not act alone. MDSC and macrophages communicate in the tumor via cell-cell contact, with macrophage production of IL-12 decreasing dependent on MDSC production of IL-10.[88] The over expression of CD80 on MDSC allowed for the suppression of antigen specific immune responses in concert with T regulatory cells (see section 1.2.4).[75]

1.2.3.2 Solving the Myeloid Derived Suppressor Cell (MDSC) Problem

The simplest fix is to remove the draw that recruits the MDSC into the tumor interstitum in the first place. Resection of large tumors producing IL-1β restored immune activity, while treatment with IL-1R agonist reduced tumor growth.[84]

Another less elegant solution is to remove the suppressive cells from the body, and convert them *in vitro* to a tumor fighting immune cell type. Isolated $CD11b^+Gr\text{-}$

$1^{+}CD31^{+}$ suppressor cells can be converted *in vitro* to myeloid dendritic cells with exposure to IL-4 and GM-CSF.[86] This could facilitate removal of the suppressive MDSC, *ex vivo* priming of the newly formed dendritic cells with tumor antigen, and re-dosing of the activated DCs to the patient. However, an effective method to extract the MDSC from the tumor interstitum does not yet exist, and thus the need for new and innovative treatments to combat MDSCs.

Formalin-inactivated herpes simplex virus (HSV) delivered to a murine system of colorectal cancer inactivated MDSC through B cells. It was shown that expansion of MDSC required B cell production of angiogenesis factors such as VEGF-A, and neuropilin-1 (NRP-1).[89] Delivery of *all-trans*-retinoic acid (ATRA) to patients with metastatic renal cell carcinoma reduced the number of immature myeloid suppressor cells, if the patients retained a high plasma concentration of ATRA >150 ng/mL.[90]

Combination therapy is a popular approach to combat MDSC cells' effect on tumor growth. Delivery of IL-7 and IL-15 after radiofrequency thermal ablation reduced tumor growth, metastasis and numbers of MDSC in murine breast tumors.[77] Another example is the delivery of 5-fluorouracil and leucovorin together with a DC vaccine reduced the numbers of both MDSC and T regulatory cells (another suppressive immune cell to be discussed in detail later) in a murine colorectal cancer model.[79] Decrease of MDSC in the microenvironment and tumor control of colorectal tumors (inoculated with intrahepatic injection) was achieved by delivery of an adenovirus coding IL-12 in conjunction with oxaliplatin. The IL-12 expression cassette was developed to be mifepristone inducible, thereby allowing control of IL-12 dosing. With this treatment, an increase in the $CD8^{+}$/Treg ratio was also observable.[91]

While this review has focused on the effect of regulating these suppressive cells in the tumor microenvironment, it is useful to note that eradication of the suppressive cells from anywhere in the body can elicit a therapeutic response. Gemcitabine was able to decrease splenic MDSC in large tumor bearing mice, while increasing the anti-tumor activity of $CD8^+$ T cells and NK cells.[92; 88] This was further augmented by an intratumoral injection of adenovirus containing IFN-β.[92]

1.2.4 $CD4^+CD25^+FoxP3^+$ Regulatory T cells

1.2.4.1 Overview

T regulatory cells (Tregs) are positive for surface markers CD4, CD25 (IL-2 receptor) and an intracellular marker, FoxP3. Additionally, these cells have high surface expression of cytotoxic T-lymphocyte-associated antigen 4 (CTLA-4) and glucocorticoid-induced TNFR-related protein (GITR).[93] These cells have been found to accumulate in metastatic melanoma tumors and prevent tumor regression, even when CTL are present.[94] Although their function has not been completely elucidated, the presence of Treg cells have been linked to poor tumor regression and can be induced by immunostimulatory treatments.[30; 95]

Presence of Tregs in tumor tissue is cancer specific. Early-stage non-small cell lung cancer and late-stage ovarian cancer patients were first observed to have Treg infiltration.[96] Tregs are rarely seen in enucleated chorodial melanoma,[97] however they are found in human prostate cancer and more common in the peripheral and transition zones than in the core of the tumor.[98] In gliomas, infiltration of Tregs was correlated with Heme oxygenase-1 (HO-1) mRNA and progression of the disease.[99] Increased populations of

Tregs have been found in hepatocellular carcinoma, and even in non-tumorous liver that contains primary hepatic tumors.[100]

Tregs have been shown to migrate towards IL-6 and IL-8-producing tumors by induction of CXCR1 by IL-6.[101] TAMs also secrete IL-6 promoting Treg recruitment to the tumor interstitium. Similarly, TAMs and tumor cells producing CCL22 recruited $CCR4^+$ Tregs in ovarian cancer and glioblastomas.[102; 103] NK depletion in mice bearing Lewis Lung Carcinoma (LLC), has shown increase in expression of CCL22 and correlated with increased levels of Tregs.[104] In both human and mouse models of pancreatic cancer, tumors produce CCL5 that recruits $CD4^+FoxP3^+$ Tregs to the tumor.[105]

Tregs contain high levels of cytotoxic T lymphocyte (CTL)-associated antigen 4 (CTLA-4) which binds with CD80/86 on APCs. This interaction induces production of indoleamine 2,3-dioxygenase (IDO) in APCs,[106] which interferes with the activation of T cells. Some types of Treg cells have been defined as secreting IL-10 and TGF-β but not IL-4 or IL-2.[107] IL-10 production can inhibit proliferation of $CD4^+$ cells.[108] The exact mechanism of suppression is unknown, and the myriad of phenotypes makes specification difficult, however, it is well established that presence of Tregs in tumor interstitum correlates with poor prognosis.

1.2.4.1 Solving the Regulatory T cell (Treg) Problem

Coexpression of surface CD25 and intracellular FoxP3 (on CD4+ cells) has been used to characterize the Treg population. However, CD25, also known as the IL-2 receptor (IL-2R), is upregulated on activated T cells, thus designing drugs against CD25 may have off-target. Preclinically, delivery of anti-CD25 antibodies have shown success in increasing the life span of tumor bearing animals in a variety of tumor types, including

glioma and pancreatic cancer. [99; 109; 110] In one study on glioblastomas, survival was found to be tumor burden dependent, indicating there is some limit to the strength of an unstimulated immune response.[109] Daclizumab is a humanized monocolonal antibody against CD25. In a small clinical trial, it has been used in metastatic breast cancer patients to clear $CD25^{+}Fox3^{+}$ cells from circulation, to allow for a more preferable environment to dose a peptide vaccine and elicit a CTL response.[111]

A simpler way to target CD25, the IL-2 receptor, is with IL-2. Denileukin diftitox, is a fusion protein combining IL-2 and diphtheria toxin. In a pilot study, after multiple doses of denileukin diftitox, T-cell response to carcinoembryonic antigen (CEA) was observed.[112] In treating melanoma, after dosing with denileukin diftitox numbers of Tregs, $CD4^{+}$ and $CD8^{+}$ T cells decreased, but T cell repopulation included $CD8^{+}$ T cells specific for melanoma antigens. After at least one cycle of denileukin diftitox, five out of sixteen patients experienced melanoma regression, some with metastatic lesions (NCT002996889).[113] When denileukin diftitox was compared against cyclophosphamide and anti-CD25, cyclophosphamide provided the greatest degrease in Tregs, but also reduced the population of $CD8^{+}$ T cells. Denileukin diftitox reduced more than half of the Tregs, with anti-CD25 having a lesser but longer lasting effect.[114]

Other experimental treatments have varied approaches and outcomes. With the positive effect CD25 agonists and antibodies have performed, it is not surprising anti-CTLA4 antibodies were also tested. Treatment consisting of chronic administration of anti-CTLA4 antibodies was unable to deplete Tregs or impair function in a B16 melanoma model, and actually allowed the population of Tregs to expand in percentages and absolute numbers.[115] A simple vaccine of DOTAP and peptide antigen has been

shown to decrease the number of Treg cells and cause regression of existing tumors.[30] In one case, the addition of low dose CpG to an immune stimulatory complex (ISCOM) vaccine decreased the population of Tregs. Delivery of a CCR5 inhibitor (TAK-779) in pancreatic adenocarcinoma limits Treg migration to the tumor, as well as produces tumors smaller than control subjects.[105]

1.2.5 Conclusion

With the growing promise of gene delivery, and the plasticity of immune cells and lineage, it is important to consider the target genes that could be modified to reverse the suppressive immune environment. **Table 1.1** notes several genes discussed in this review that play important roles in the immune regulation of the tumor microenvironment. As can be seen, most of the proposed strategies involve using siRNA to down-regulate the target gene. The only up-regulation desirable is the expression of a dominant negative mutant of CCL2. Thus, delivery of specific siRNA or plasmid DNA to the immune cells in the tumor interstitium is highly desirable. It presents a new challenge to the gene therapy community.

While a great deal of work has been done in creating treatments to overcome the tumor microenvironment, a great deal still remains. While all cell types reviewed in this article deal with hematopoetic stromal cells, a recent publication in Science by Kraman and colleagues explore mesenchymal stromal cells and the inhibitory nature with the expression of fibroblast activated protein–α (FAP-α). The study showed that the removal of FAP-α expressing cells permits the efficacy of a therapeutic vaccine in a solid tumor model.[116] While the model of expression is transgenic and artificial, the importance of

FAP-α lends insight to yet another method utilized by tumors to prevent immune recognition. Whatever the method of immune suppression the tumor employs, it seems that any therapeutic cancer vaccine that hopes to be efficacious must simultaneously be able to switch the immune system on, and switch the tumor microenvironment off.

Table 1.1 Target genes in the suppressive tumor microenvironment.

Gene/Protein	Target Cell(s)	Strategy
CCL2	TAMs	siRNA to ↓ expression
IL-6	TAMs	siRNA to ↓ expression
dominant negative CCL2 mutant gene (7ND)	TAMs	Gene transfer to ↑ expression
CCL16	TAMs	Gene transfer to ↑ expression
IL-10	TAMs, Tregs	siRNA to ↓ expression
Heme oxygenase-1 (HO-1)	Tregs	siRNA to ↓ expression
Transforming growth factor-β (TGF-β)	TAMs, MDSC, Tregs	siRNA to ↓ expression
STAT1	MDSC	siRNA to ↓ expression
Indoleamine 2,3-dioxygenase (IDO)	APCs	siRNA to ↓ expression
IL-6, IL-8, CCL22	Tumor (to prevent TAM recruitment)	siRNA to ↓ expression
CXCL12, SDF-1α, CCL2, CXCL5, KIT ligand, IL-1β, GM-CSF, VEGF	Tumor (to prevent MDSC recruitment)	siRNA to ↓ expression
CCL5	Tumor (to prevent Treg recruitment)	siRNA to ↓ expression

1.3 CHEMICAL VECTORS FOR DELIVERY OF NUCLEIC ACID BASED DRUGS

1.3.1 Introduction

The blossoming field of gene therapy is a clever way to regulate the proteins in a tissue by making the host cells produce (or silence) the protein of interest by its own mechanism. One could consider it protein "dosing," and it can be used to treat many genetic and acquired disorders including cancer. Many different types of nucleic acid based drugs can be delivered, such as plasmid DNA, oligonucleotides, and various forms of RNA interference (RNAi): siRNA, shRNA or miRNA (short interfering RNA, short hairpin RNA or micro RNA). Delivery vectors range a wide gamut of biomaterials, the two largest classifications being viral and non-viral. While viral vectors are able to produce the highest gene transfection efficiency,[117] complications with immune response push our interests towards the newer field of non-viral vectors, also called chemical vectors, including cationic polymers, liposomes and peptides, among others. While many different vectors can be used to control size of payload, transfection efficiency and immune response, the delivery route is also an important consideration because the treatment needs to be efficient, simple to administer and suitable to the application. This chapter will briefly review systemic barriers to gene delivery via chemical vectors, then discuss different vehicles used in nucleic acid delivery. Targeting moieties and triggered release will also be reviewed as ways to enhance systemic or local delivery. Finally, delivery of nucleic acids with chemical vectors in recent clinical trials will be covered.

1.3.2 Barriers to Delivery of Nucleic Acids

1.3.2.1 Anatomical

In systemic circulation, the first barrier encountered is the blood stream. The blood contains serum proteins, nucleases and macrophages that can aggregate, degrade or phagocytose the delivery vector, respectively, even before it reaches the tissue of interest. Naked plasmids have been shown to have a half-life of 1.2 minutes for supercoiled pDNA, 21 minutes for open circular pDNA and 11 minutes for linear pDNA in rat plasma.[118] However, in the same study, complexing pDNA with cationic liposomes (DOTAP:DOPE, 1:1 w/w), prevented degradation and allowed the supercoiled plasmid to be detected after 5.5 hours.

Clearance by the reticuloendothelial system (RES) is of great concern, and particle size often determines by what organ (liver, kidney or spleen) and how quickly the particle will be cleared from the blood. Extended plasma circulation is desired to allow a majority of the injected dose to reach the target tissue. Poly(ethylene glycol) (PEG), a hydrophilic inert polymer has been conjugated to many chemical vectors to extend circulation time, such as liposomes, patented by Lasic's group, later termed Stealth® liposomes.[119; 120; 121; 122] Once in the vasculature of the target tissue, the delivery vector must leave the blood stream and transverse into the interstitial space of the tissue.

Tumor vasculature is inherently disorganized, immature, and tortuous due to the presence of discontinuous endothelium and an incomplete basement membrane. The blood vessels in the tumor attempt to supply tumor cells with nutrients, and cannot grow fast enough to fully develop. The Enhanced Permeability and Retention (EPR) effect is

often utilized in cancer therapy to deliver drugs to the interstitum of tumors, skipping the usual barrier of transversing the endothelium.[123; 124; 125; 126] However, this permeability is not universal in tumor vasculature. Heterogeneous permeability of tumor endothelium and interstitum was shown in window chamber experiments using by Rhodamine-labeled stealth liposomes.[127] Doxil® (a commercial formulation of doxorubicin encapsulated in stealth liposomes), showed increased accumulation in tumor tissue compared to normal tissue in humans.[128]

While the EPR effect is useful in many tumor microenvironments, other methods have been developed to further enhance the delivery. For efficient delivery, the vector may be targeted to the specific tissue of interest by ligand attachment on the vector, to target a receptor on the cells in the tissue of interest or by triggering release at the desired site. These two topics will be discussed in depth later. Being able to discriminate between target and non-target cells is crucial to ensure specific expression of the nucleic acids delivered.

1.3.2.2 Cellular

Once at the plasma membrane, the chemical vector must be endocytosed to enter the cell. Endocytosis can occur by many routes including macropinocytosis, clathrin-mediated and non-clathrin mediated endocytosis and entry via caveolae.[129] Polyplexes of polyethyleneimine (PEI) complexed with pDNA were shown to attach to cell surfaces, migrating into clumps, and then endocytosed.[130] It has been postulated that cationic lipid carriers can enter cells through fusion with the cell membrane however, much more evidence exists for endocytotic pathways.[131] However, Douglas et al, have recently published results arguing that endocytosis is cell-line dependent. The authors report that

after clathrin-mediated endocytosis, complexes follow the endo-lysosomal pathway, which initiates the proton-sponge effect for release (to be discussed later, in the section entitled 'Triggered Release'). Further, the author's report that caveolin-mediated endocytosis leave the complexes trapped in vesicles that become "transfection-incompetent."[132] In the endosome, the nanoparticle or naked plasmid must escape before being degraded upon fusion of a lysosome with the current endosome.[133]

Once the particle or naked plasmid is in the cytoplasm, it faces additional intracellular barriers. Diffusional mobility of plasmid DNA is limited due to the cytoskeleton, particularly actin and molecular crowding in the cytoplasm.[134] Intracellular mobility of DNA was shown to be size dependent. Double stranded DNA >250 bp had significantly decreased diffusion compared to DNA of 100 bp or less.[135] Active cytosolic nucleases can degrade the plasmid. However, if the nucleic acids being delivered function via an RNAi mechanism, they need travel no further than the cytoplasm where crucial enzymes such as RISC and Dicer reside. Entry into the nucleus by the plasmid is rate limiting, and can only be achieved when the cell divides or through nuclear membrane pores, which have size limitations on what can enter or exit. Nucleus localization sequences (NLS) can be conjugated to pDNA to facilitate entry through the nuclear pores,[136] which can increase in size from 9 to 39 nm from docking of appropriate NLS.[137] However, most delivery systems rely on non-specific entry to the nucleus.[135]

1.3.3 Major Classes of Delivery Vectors

1.3.3.1 Introduction

Cationic moieties are able to condense DNA, RNAs, and other oligonucleotides, through the ionic interaction of the nucleic acid's negatively charged phosphate backbone, with cationic charges, which can come from lipids, polymers, or peptides. These different classes of delivery vectors have been developed with individual limitations on size, charge ratio, nucleic acid capacity, and toxicity.

1.3.3.2 Cationic Lipids

Cationic liposomes were first used for DNA transfection by Felgner et al. in 1987 with the introduction of the cationic lipid, N-[1-(2,3-dioleyloxy)propylJ-N,N,N-trimethylammonium chloride (DOTMA).[138] Soon after, DOTMA's ester analogue DOTAP (1,2-dioleoyl-3-trimethylammonium-propane) also saw popularity as a cationic lipid used in drug delivery.[29; 139]

Lipoplexes are a popular chemical vector delivery technique, due to the relatively low immune response accompanying their delivery. These vectors combine cationic lipids with DNA to produce a complex, a product of the interaction of the negatively charged phosphate backbone and the positively charged lipid head groups. Transfection has been shown to be a function of charge ratio (lipid:DNA). Using a 4:1 charge ratio, the *in vivo* transfection of IL-12 plasmids was improved by conjugating albumin to the exterior of the lipoplex in combination with intratumoral (i.t.) delivery.[140] The lipids used were 1-palmitoyl-2-oleoyl-*sn*-glycero-3-ethylphosphocholine (EPOPC) and cholesterol (chol) in a 1:1 ratio. Albumin was added to the outside of the membrane, to enhance the escape of DNA from the endocytotic pathway, since it has been described to undergo a

low-pH induced conformational change, acquiring fusogenic properties.[141] Similar to IL-18, IL-12 enhances the proliferation and cytotoxic activity of both T and NK cells and induces the production of IFN-γ. Also delivered (in a separate experiment) by this albumin conjugated lipoplex was the "suicide" gene, HSV-tk, which when delivered with the prodrug ganciclovir (GCV), converts into a toxic active metabolite that causes cell death. The attachment of albumin greatly increased the transfection efficiency of the lipoplex at all charge ratios (4:1, 2:1 and 1:1). This study showed that 4 i.t. injections of these plasmids over several days at 40 μg each (with HSV-tk accompanied by intraperitoneal (i.p.) injections of GCV) showed significant tumor growth delay in a subcutaneous TSA model (a mouse mammary adenocarcinoma, which is highly aggressive, immunogenic and has a high proliferation capacity) compared to the control injection of buffer. Complete tumor regression was seen in one member of the immunogene therapy group (one of six). Even after 4 i.t. injections of the control plasmid, some growth delay was seen, the authors attributing this to cytosine-phosphate-guanine (CpG) motifs in the plasmid that elicited a slight immune response. Higher T-lymphocyte infiltration was seen from control plasmids verses untreated mice, showing the immune response from even an empty plasmid. However, albumin coated lipoplexes containing the IL-12 plasmid (40 μg) showed significant tumor regression, high T-lymphocyte infiltration and extensive necrotic and hemorrhagic areas. Also, with both formulations (with and without albumin) this study demonstrates a frequent problem of high transfection in the lung, rather than the target tissue.

LPD, which stands for "liposome-polycation-DNA," was developed by Huang's group, and uses cationic liposomes differently than other groups. While most cationic

liposomes condense nucleic acids in layers, with the cationic bilayers associating with negatively charged nucleic acids, making a multilamellar liposome, LPD is different. LPD first condenses nucleic acids with a polycation such as polylysine or protamine, making a solid particle, and then mixes that solution with charged liposomes, which effectively coat the surface of the solid DNA-polycation core. LPDII complexed DNA and polylysine at a ratio of 1:0.75, then trapped in folate-targeted anionic pH-sensitive liposomes. LPDII is coated with PEG conjugated to folate, to help the particle evade RES detection and target folate over-expressing cells such as KB cells.[142] The particle's charge depends on the lipid/DNA ratio, and at high lipid/DNA ratios, the anionic particles are formed, while at low lipid/DNA ratios, cationic particles are formed. The cationic particles were found to have high transfection but to not be tissue specific, whereas the anionic particles showed a receptor dependent transfection activity.

In another, more recent formulation of LPD, three different siRNA sequences were co-formulated in each LPD to cause simulatenous silencing of three important proteins in cancer survival: MDM2, c-myc and vascular endothelial growth factor (VEGF).[143] The LPD were made with DOTAP as the cationic lipid, protamine as the polycation, protected against RES uptake by a PEG and targeted using anisamide to the sigma receptor on murine lung metastasis. A 70-80 % reduction in cancerous nodules in the lung was seen in the targeted treatment group compared to control.

1.3.3.3 Cationic Polymers

Polyethylenimine (PEI) is a cationic polymer commonly used in gene delivery to create "polyplexes," indicating the complexation of DNA and a polymer. Linkers made of PEG, an inert hydrophilic polymer, can also be added to prevent uptake by the RES.[144] Because

of the enhanced release from the endosome due to the proton sponge effect, cationic polymers have been popular in gene delivery. However, the toxicity of the vector is often an issue at high molecular weights. Polyplexes have also been conjugated to targeting ligands, either directly to the PEI, or to a PEG linker on the PEI such in the case of RGD peptide.[144]

Focal adhesion kinase (FAK) is a protein kinase in cell cycle progression and cell migration. Modified PEI (M-PEI) was used to transfect tumor cells and tissues with a FAK siRNA plasmid (psiFAK) to down-regulate tendency of metastases forming in the mouse model from left hind footpad model using B16F10 (mouse melanoma). After i.t. delivery of psiFAK, the tumor showed no metastases in the lungs and lymph nodes in any mouse (n=6), compared to PBS or either control plasmid (pLuc or pKH3). Primary tumors also experienced a statistically significant growth delay, and survival time when treated with psiFAK as compared to the controls.[145].

In addition to modified PEI, linear and branched PEI have also been used in i.t. gene delivery. Coll et al. has compared three routes of delivery (i.v., intracystic and i.t.) to human non-small cell lung carcinoma (NSCLC) using a Luciferase plasmid to discover the best method of polyplex administration with linear PEI.[146] A charge ratio of 10 polymer:DNA provided the best *in vivo* transfection, causing increasing expression from 24 to 96 hours. When delivering intravenously to solid tumors, minimal expression was seen in the highly vascularized tumors, independent of size. However, a nearly 3-fold increase in expression was seen in the normal lung tissue, making these nanoparticles useless for solid tumor delivery if injected i.v., not even benefiting noticeably from the EPR effect. A common lung metastasis model was used here that consists of i.v. injection

of tumor cells which are caught in the lung and create many nodules therein. After an i.v. injection of these PEI particles, only tumor-free mice expressed Luciferase and no expression was seen in tumor loaded lungs. However, using other delivery routes, these particles were effective. In several cancers, including some ovarian and gliomas, the tumor wall expands to create a liquid filled cavity. In a cyst-forming tumor mouse model H358NL, after draining the internal liquid (up to 5mL), a small volume of polyplexes were delivered into the cyst cavity.[146] This method of delivery showed high transfection and long-lasting expression and could also be used post-surgery, after the bulk of the tumor had been removed and some residual tumor cells remained. The authors found that the volume injected i.t. with a normal syringe traveled to the periphery of the tumor. A micro-pump technique was developed to deliver i.t. at a rate of 20μL/min. This method showed high and long-lasting expression of the transgene, where normal syringe injection was not effective. However, free plasmid injection was inefficient with the micro-pump, and more effective with the normal syringe injection, indicating that the hydrostatic pressure induced from normal i.t. injection possibly aided in delivery.

Rozema et al. introduced a multifuntional polymer for delivery of siRNA to hepatocytes.[147] Named "Dynamic PolyConjugates", these particles utilize an endosomolytic polymer, an amphipathic poly(vinyl ether) termed PBAVE, composed of butyl and amino vinyl ethers. This polymer has the ability to connect to targeting ligands to reach the cell of interest, poly(ethylene glycol) to evade the RES, as well as the nucleic acid payload. Once inside the endosome and the pH drops, a pH-labile bond connecting the targeting ligand and PEG is cleaved, exposing many positive charges and inducing the proton sponge effect, drawing water into the endosome until it bursts, allowing the

siRNA to escape into the cytoplasm. This vector has a mechanism for many of the challenges of delivery, and lives up to its dynamic name, able to change as each event presents itself.

The Davis group introduced a cationic cyclodextran-containing polymer for condensing pDNA in 1999 showing comparable transfection to PEI and Lipofectamine formulations *in vitro*.[148] Aims were to decrease toxicity during transfection, and the cyclodextran formulation showed no signs of toxicity at a 70:1 (+/-) charge ratio in the presence of 10 % serum. Later development of this system included conjugation of an adamantane-terminated modifier to PEG to stabilize the particle and maximize plasma circulation time, as well as conjugating the modifier to targeting ligands such as transferring.[149; 150; 151] Characterization of the particle's formulation showed that size can be "dialed in" between 60 and 150 nm, similarly with a zeta potential ranging between 10 and 30 mV depending on how the formulation is made and modified.[151]

Water soluble lipopolymers (WSLP) are another class of polymers used for nucleic acid delivery.[152] Branched PEI was conjugated to a hydrophobic lipid anchor. Single or repeated i.t. injections of WSLP containing IL-12 plasmid were compared to see the tolerance of the method and the efficacy on tumor regression and survival in a CT26 colorectal model. The studies also showed that the complexes could be retained in the tumor for up to 24 hours. The WSLP/pIL-12 plasmid complexes performed better against the controls of no treatment, free plasmid and 25K PEI/pIL-12 in both 4 and 8 day repeat i.t. injections. After 45 days, 60 % of the treatment group that received WSLP/pIL-12 every 4 days were alive, compared to 40 % of the group that was treated with WSLP/pIL-12 every 8 days, while all members of the single injection and control

groups had reached study endpoints by day 33 and 26, respectively. However, the repeat injection method did cause some side effects. After six weeks of injections (either every 4 or 8 days), the majority of mice in these groups could no longer receive injections because of increased tumor necrosis.

1.3.3.4 Cationic Dendrimers

Cationic dendrimers are built of positively charged molecules, usually amino groups, branching out from a central core. Each increased addition of branches is termed a new "generation." Several consistencies are seen across dendrimer transfection research. Increased generation yields increased transfection, but also increased toxicity. Even dendrimers delivered alone (not complexed with DNA) can induce host cell DNA damage.[153] Also, because cationic dendrimers can contain many positive charges, as they are formed from cationic monomers polymerized outwards from a central core, the proton sponge effect can be observed with dendrimers as well.[154] Endocytosis of dendrimers complexed with nucleic acids (dendriplexes) varies across cell lines.[155; 156] Dendriplexes have been shown to internalize through a cholesterol-dependent mechanism, [155] but in other cells, cholesterol depletion does not seem to have an effect in cells which express few caveolae (HeLa and HepG2).[156] These cells, as well as endothelial cells endocytosed dendrimers complexed with DNA (dendriplexes) even with inhibition of clathrin-independent, phagocytic and macropinocytic pathways. It was discovered by the same group (Manunta et. al), that an increased rate of uptake occurred with over-expression of caveolin 1.

Issues with cationic dendrimers such as transfection efficiency and cytotoxicity increasing in tandem, have been solved somewhat by Zhang et al. The research group

conjugated polyamidoamine (PAMAM) dendrimers to the surface of poly(D,L-lactide-*co*-glycolide) (PLGA) microspheres. Plasmid DNA was trapped by these particles by incubating PAMAM-coated PLGA microspheres (positively charged) with negatively charged pDNA. Unmodified PLGA microsphere were made by double emulsion and solvent evaporation of a mixture of PLGA to pDNA.[157]

The core of the dendrimer can be modified, giving a different branching pattern and thus amino group density, dictated by the number of reaction centers available on the core.[158] The core that builds a less dense dendrimer, has been shown to require a higher generation to effectively condense DNA. A trimesyl core that gives three places for dendrimer building to begin, while pentaerythritol gives four, and inositol gives six. Trimesyl core dendrimers required generation six dendrimers to effectively condense DNA, while pentaerythritol and inositol only required generation five dendrimers. However, interestingly, the trimesyl core generation 6 dendrimers were smaller (100-300 nm) than the pentaerythritol or inositol generation 5 dendrimers (>600 nm), as well as showing greater transfection. In trimesyl core dendrimers, as commonly reported with all dendrimers, cytotoxicity did increase with generation, however, the toxicity was much less than that of PEI.[158]

1.3.3.5 Cell Penetrating Peptides (CPP) and DNA mimics

Cell penetrating peptide-based drug delivery systems have been developed to administer genes to tumors. Morris et. al. have developed an amphipathic peptide, Pep-3, suitable for either i.t. or i.v. delivery, with slight modifications to overcome systemic barriers when delivered intravenously.[159] Plasmids that target antisense cyclin B1 (HypNA-pPNA) were

delivered to a xenograft animal tumor model (PC3, human prostate carcinoma) as a DNA mimic.

The studies also showed that peptide binding of DNA mimics and uptake of the complex into cells are dependent on the hydrophobicity and charge of the peptide, respectively, with a minimum of four cationic charges require within the hydrophobic domain. The greatest growth delay over all the groups was seen with i.t. delivery of 5μg of the Pep-3 DNA mimic, outperforming even 1 μg of the same complex delivered, showing a dose dependency. To evade the immune system in systemic circulation, Pep-3 was coated with poly(ethylene glycol) (PEG). The newly coated Pep-3/DNA mimic/PEG nanoparticle was delivered intravenously at 10 μg and saw similar tumor growth delay as 5 μg Pep-3/DNA mimic delivered i.t. As not exemplified in previously studies, this chemical vector had similar growth delay effects from i.t. and i.v. delivery after some minor vector modifications.

The rabies virus glycoprotein (RVG) has been conjugated to siRNA to transverse the blood-brain barrier.[160] RVG targets the nicotinic acetylcholine receptor (AchR) on neuronal cells, enabling the entry of virus particles. The virus protein (RVG) was conjugated to a chain of nine D-arginine residues as a spacer, then to siRNA, which allowed transfection specifically in neuronal cells (Neuro-2a) *in vitro*. *In vivo*, after i.v. delivery, particles were found in the brain but not the liver or spleen and showed a high level of FITC fluorescence. Finally, after infecting NOD/SCID mice with flaviviral encephalitis and injecting an antiviral siRNA sequence conjugated to RVG, survival was significantly extended.

1.3.3.6 Naked DNA

Degradation of free plasmids by rat plasma has been shown to have a half-life of 1.2 minutes for supercoiled pDNA, 21 minutes for open circular pDNA and 11 minutes for linear pDNA.[118] However, in the same study, complexing pDNA with cationic liposomes (DOTAP:DOPE, 1:1 w/w), allowed the supercoiled plasmid to be detected after 5.5 hours.

Other than hydrodynamic injection, (a large volume quickly injected, efficient in delivery to the murine liver), naked DNA plasmid delivery has seen little success in i.v. delivery.[161] Eliminating many barriers encountered in systemic circulation, it makes sense to assume that i.t. injection would show greater transfection efficiency and anti-tumor effects for naked plasmids. Intratumoral delivery of a naked interleukin (IL-18) plasmid was delivered to CT26 tumors established in the liver.[162] CT26 is an undifferentiated murine adenocarcinoma that models colorectal cancer, the most common site of metastasis being the liver. Tumors were established by injection of CT26 into the lower left lobe of the liver. IL-18 protein was found in all subjects injected with either the control vector or IL-18 plasmid, but significantly higher levels in the 50 μg plasmid-injected group. Mice treated with the control vector did not generate a CT26-specific T cell response, while those treated with the IL-18 producing plasmid contained a significant number of IFN-γ (interferon gamma) producing $CD4^+$ T cells and had significantly lower tumor growth. While most studies use solid tumor models in the hind flank of mice, this study shows the versatility of i.t. injection as it can also be administered to a solid tumor within a major organ within the body cavity.

1.3.4 Targeted Delivery

1.3.4.1 Introduction

Attaching a ligand specific to the tissue of interest increases localization of the nanoparticle to that tissue. Many different receptors are over-expressed in tumor tissues making the corresponding ligands desired as targeting agents. Also, hepatocytes express the asialoglycoprotein receptor in high amounts, making galactose and asialofetuin, desired ligands for targeting in that application.

1.3.4.1.1 Galactose

Galactose can be used as a targeting agent to the asialoglycoprotein receptor (ASGP-R) on mammalian hepatocytes.[163] Asialofetuin, the receptor's natural ligand can also be used. N-acetylgalactose (NAG) has been conjugated to the end of endosomolytic polymers to target the vehicle to hepatocytes for pDNA delivery.[147] Galactose has also been conjugated to liposomes for delivery of oligodeoxynucleotides (ODN).[164]

1.3.4.2 Targeting solid tumors and/or metastasis

1.3.4.2.1 Transferrin

Transferrin is an iron-binding glycoprotein often used as a targeting ligand. Expression of transferrin receptors on the cell surface is upregulated in quickly dividing cells due to their need for iron. Transferrin receptor density can be increased by treating cells with the cell-permeable iron chelator desferrioxamine.[165] Transferrin targeting was used to deliver a reporter plasmid using polylysine or protamine to human leukemic cells, K-562, termed "transferrinfection".[165] Other systems targeting immune cells have used transferrin as a ligand, such a liposome targeting to rabbit bone marrow precursor cells.[166] In addition to K-562 cells, transferrin targeting has been efficient with neuroblastoma Neuro-2A cells,

melanoma H225 and 16F10 cells, with increased expression in all cell lines, some as high as 1000 to 10,000 fold.[117] Joshee et al. showed that adding pDNA to a mixture of transferrin and DOTAP/DOPE (1:1) cationic liposomes yielded significantly higher transfection in Panc-1 cells than the formulation where pDNA and cationic liposomes were mixed first, then mixed with transferrin, although zeta potentials of the formulations were similar (around -33mV). When conjugating gold nanoparticles to transferrin and adding pDNA to the gold-transferrin and cationic liposome mixture, both the labeled transferrin and pDNA colocalized at the perinuclear space and in the nucleus, suggesting cotransport intracelluarly and into the nucleus.[167] Transferrin has been conjugated to many different chemical vectors including: cationic cyclodextran polymers,[149; 150] polylysine and protamine,[165] PEI,[117] and liposomes[166; 168]. Anti-transferrin receptor single-chain antibody fragments have similarly been used to target the upregulation of these receptors.[162] The cationic liposome decorated with these anti-transferrin receptor single-chain antibody fragments was able to target solid tumors and metastasis.

1.3.4.2.2 Folate

Folate receptors are over-expressed in many tumors including ovary, kidney, uterus, testis, brain, colon, lung, myelocytic blood cells, as well as KB cells, a nasopharyngeal epidermal carcinoma cell line.[169; 170; 171; 172; 173; 174; 175; 176; 142] Lee's LPDII used polylysine to complex DNA, then coated with a pH-sensitive anionic lipid, as well as the folate ligand as a targeting mechanism to KB cells.[142] It was shown that transfection was controlled by charge for the cationic particles (low lipid/DNA ratio), and by folate ligand for the anionic particles (high lipid/DNA ratio). KB cells also showed high uptake of neutral liposomes encapsulating doxorubicin targeted using folate conjugated to a PEG

linker, secured to the lipid bilayer with a cholesterol anchor.[177] Wang and Low indicated that folate should be conjugated to the carrier at the γ-carboxyl group terminus, as not to interfere with the receptor-ligand binding pocket.[178] Folate has also been conjugated to PEI[179] and polylysine[180] for gene delivery.

1.3.4.2.3 Sigma Receptor

Sigma receptors are expressed on many normal tissues within the body, including the heart, liver, endocrine glands, kidneys, lungs, gonads, central nervous system and ovaries.[181; 182; 183] Novakova et al. showed that in a rat heart, gene expression of sigma receptors can be upregulated by intense stress stimuli, with hypoxia and immobilization showing the greatest upregulation, and exposure to cold showing no effect on gene expression at all.[183] Hypoxia is an environment found in many tumors, thus the upregulation of sigma receptors under these conditions correlate with an upregulation of sigma receptors found in several cancers. Across both human and rodent cancer lines, tumors show an upregulation of the sigma receptors making substrates for the receptor efficient targeting moieties. Vilner et al. tested 13 different rodent and human cell lines, and found that all tumors except one (human MCF-7 breast adenocarcinoma) expressed some level of sigma receptor 1 and 2. MCF-7 did not express the sigma receptor 1 at all. Other cell lines tested include: T47D breast ductal carcinoma, NCI-H727 lung carcinoid, A375 melanoma (amelanotic), ThP-1 leukemia, U-138MG glioblastoma, SK-N-SH neuroblastoma, LNCaP.FGC prostate, C6 glioma (rat), NB41A3 neuroblastoma (mouse), N1E-115 neuroblastoma (mouse), NG108-15 mouse neuroblastoma X rat glioma (hybrid), S-20Y neuroblastoma (mouse).[184] Other studies have discovered other cancer

cell lines lacking the sigma receptors include HeLa, KB, HepG2 and Chinese hamster ovary cells.[133]

Ligands for the sigma receptor are diverse and include haloperidol, reduced haloperidol, fluphenazine, perphenazine, trifluoperazine, BD737, LR172, BD1008, SH344, trifluperidol, thioridazine, and (-)-butaclamol.[185] Often these ligands can be conjugated to delivery vectors to target cells with over-expressing sigma receptors. Haloperidol has been conjugated to the distal end of PEG linked to a phospholipid and used to deliver a reporter gene to MCF-7 cells, showing a 10-fold increase in expression, compared to the untargeted lipoplex. Administration of spironolacetone (a sigma receptor down regulator) with the lipoplex showed a 10-fold lower gene expression than those cells not treated with spironolacetone.[133] Benzamides have been shown to be sigma receptor ligands.[186] Huang's group first used anisamide, a benzamide ligand that has shown great affinity for sigma receptors, in targeting stealth liposomes loaded with doxorubicin to DU-145, a human prostate adenocarcinoma cell line, by conjugating anisamide to the distal end of PEG.[187] The group has also used anisamide to target LPD to the human NCI-H460 lung cancer line[188; 189] and has shown targeting effects in B16F10 (murine melanoma cells) as a metastatic cancer model.[190]

1.3.4.2.4 RGD

The sequence of RGD (arginine-glycine-aspartic acid) attaches to many proteins in the extracellular matrix and on the cell surface specifically being a ligand for integrin receptor $\alpha_v\beta_3$.[191] Attachment of RGD influences cell growth, migration and differentiation.[192] When targeted with RGD-PEG-PEI or RGD-PEI complexes, saturable binding was shown in Mewo human melanoma cells, and low binding was shown in

A549 human lung carcinoma cells.[191] When the PEG spacer was not used, transfection of the Mewo cells was increased 1-2 fold, however, attachment of RGD to polyplexes using a PEG spacer delivering pDNA against vascular endothelial growth factor (VEGF), showed increased delivery to tumors, growth delay and increased survival rate.[144]

1.3.4.2.5 Intratumoral Delivery

Local injection is a promising treatment option especially in the case of solid tumors and has been taken advantage of for gene delivery with chemical vectors, owing to the inherent lower transfection ability seen with chemical vectors compared to viruses. Intratumoral (i.t.) delivery evades many of the barriers that i.v. delivery faces, as the delivery vector starts in the tumor interstitum. However, in i.t. delivery there is rapid plasmid DNA clearance from the tumor interstitium that can be attributed to the leaky vasculature, and local drug diffusion may cause non-specific toxicity.[152] Also, i.t. delivery is only practical where direct injection is possible, such as solid tumors and, to an excised tumor cavity or in the case of cystic fluid filled tumors that have been drained, to treat the residual tumor cells as suggested by Coll et. al..[146] Many of the genes delivered i.t. center around immunogene therapy, producing large amounts of cytokines to recruit T and NK (natural killer) cells to the tumor (and only the tumor, hence the direct injection method), to produce a localized immune response.

Intratumoral injection may not be the most realistic treatment for all tumor types, but for solid tumors it is able to deliver nearly the entire volume of injection to the tumor interstitum without depending on the EPR effect. Although i.t. gene therapy is not a viable method for treating metastasis, unless the metastasis can be localized, as in the liver as most i.t. delivered drugs have no cancer cell targeting mechanism, or mechanism

to evade RES detection so they are quickly cleared from the bloodstream.[162] As shown in previous sections, many of the same vectors employed in i.t. delivery of nucleic acid based drugs have been used in i.v. delivery, with slight modifications increasing the targeting properties and extending systemic circulation time. Intratumorally administered gene therapy can become a combined therapy when incorporated with a mechanical delivery enhancement method, such as electroporation, ultrasound or use of a micropump injector, showing superior transfection of tumor cells *in vivo*. Although not the standard of administering drugs, i.t. administration of these gene therapies might become a way to compensate for the relative low transfection efficiency of chemical vectors compared to viruses, especially with the enhancement from being combined with a mechanical delivery method.

1.3.5 Triggered Release

1.3.5.1 Introduction

Triggered release is an important aspect of gene delivery. Triggered release can include anything from facilitated escape from endosomes, temperature or pH sensitive carriers or a mechanical method such as electroporation or ultrasound. Mechanical methods can trigger release by permeating cell membranes or breaking open delivery vectors and are often used in concert with intratumoral delivery due to the local application of the mechanical method.[193; 194; 195; 196; 197; 198] Using mechanical methods to facilitate gene delivery is a broad subject and out of the scope of this chapter, however, many quality reviews have been written on the subject.[199; 200; 201]

1.3.5.2 Proton Sponge Effect

Boussif et al. first coined the term for the "proton sponge effect" when describing PEI in endosomes, but it has been shown to be true for many different chemical delivery vectors.[202] This phenomenon occurs when cationic delivery vectors (reported for polymers, lipids and dendrimers), enter an endosome. The large buffering capacity of non-protonated amino groups or other proton acceptors causes a large influx of hydrogen ions. As protons enter the endosome, so do chloride anions to maintain the electro-neutrality. Water also diffuses in via osmosis to keep the osmotic pressure the same inside and outside the endosome. This influx of water causes the endosome to burst, releasing the delivery vector into the cytosolic space. This mechanism has been verified in cultured cells.[203]

Cationic lipids can have interactions with negatively charged endosomal lipids (such as phosphatidylserine), and create non-lamellar structures, possibly disrupting endosomes and allowing for escape into the cytoplasm.[204] Also, greater generation dendrimers conjugated to PLGA particles showed greater buffering capacity, which the authors pointed towards increased proton-sponge effect, or triggered release from endolysosomal compartments by lysis of endolysosomes as water diffuses through the membrane to compensate the large number of positive charges and the lower pH.[157]

Sakae et al. used PEI/pDNA complexes coated with PEG-Suc (PEG-Succinic acid), using negatively charged carboxylate groups as proton acceptors, and showed an increase in the buffering capacity compared to polyplexes coated with another anionic modified PEG, called PEG-C. While PEG-C accepted 41 μmol of protons between pH 7.4 and 5.5, PEG-Suc accepted 66 μmol. The pK_{a1} and pK_{a2} values of PEG-Suc were 4.00 and 5.24, respectively. The addition of PEG-Suc reduced the zeta potential from

+37.8 mV for the PEI/pDNA complexes to -24 to -34 mV. A greater amount of PEG-C was needed to achieve the same negative zeta potential as with PEG-Suc [205]. While much focus has been given to cationic chemical vectors for gene delivery, this paper shows, in a new light, the potential of negatively charged chemical vectors to deliver *in vivo*, based on the proton sponge effect.

1.3.5.3 Magnetofection™ (Magnetic Delivery)

Buerli et al. presented a protocol for magnetofection reporting procedures used in the laboratories of Fritschy (University of Zürich, Switzerland), Medina (INMED/INSERM, Marseille, France) and Fuhrer (Univeristy of Zürich, Switzerland and Mount Sinai Medical Center, New York, US). The magnetofection reagent used by all three groups is CombiMag with a magnetic plate for delivery of cDNA and short hairpin RNA (shRNA) into rat hippocampal neurons (embryonic day 18/19). CombiMag is obtained from OZ Biosciences. The protocol shows effective double-magnetofection of pyramidal and GABAergic interneurons, with expression of two genes in one neuron.[206]

Scherer et al. showed that by using superparamagnetic iron oxide nanoparticles coated with poly(ethyleneimine) (TransMAG^{PEI}, obtained from Chemicell, Berlin, Germany) associated with chemical vectors (as well as viral vectors and naked plasmids), showing an increased expression of the luciferase reporter gene delivered. Particle sizes ranged from 400-1000 nm. All the chemical vectors used (PEI, AVET-PEI, GenePorter, and Lipofectamine) showed increased luciferase activity after 10 minutes of magnetofection with magnetic field compared to standard transfection (4 hours incubation) in both NIH3T3 and CHO-K1 cell lines. Magnetofection (use of transMAG^{PEI} particles associated with the carrier), without magnetic field never produced

significantly greater gene expression over the standard transfection. Of the chemical vectors used, Lipofectamine™ showed the greatest enhancement in expression, with 971 fold greater expression with magnetofection and applied magnetic field compared to standard transfection.[207]

Xenariou et al. used TransMAG^{PEI} to deliver Lipofectamine™ 2000 or a cationic lipid (GL67) complexed with pDNA *in vitro*, showing a 300 fold and 30 fold increases in Luciferase gene expression respectively, compared to the vectors/pDNA without TransMAG^{PEI} after exposure to a magnetic field. However, delivering to nasal epithelium of mice *in vivo*, the control particles, GL67/pDNA had significantly higher luciferase gene expression (50 fold) than TransMAG^{PEI}-GL67/pDNA complexes; also, the formulation precipitated *in vivo*. When the precipitate was removed, and treatment with the supernatant was also completed, no significant difference existed between the groups of treatment with the supernatant and the precipitates, or between use of the magnet and without. *In vivo* magnetofection was also low in TransMAG^{PEI}-pDNA complexes with and without the magnet compared to naked pDNA.[208]

Lee et al. used PolyMAG, a superparamagnetic iron oxide nanoparticle, for transfecting mouse embryonic stem cells. PolyMAG consists of a superparamagnetic nanoparticles (tsMAG-PEI) coated with PEI, complexed to pDNA with free PEI. Significant increases in transfection efficiency of GFP were seen with magnetofection (PolyMAG) compared to the control vector, FuGENE6. A magnetic field was applied by placing the plates on MagnetoFactor plate device for 15 minutes at 37ºC, then returned to incubate at 37ºC. After 50 subpassages in culture, the mouse embryonic stem cells that underwent magnetofection still expressed GFP.[209]

1.3.5.4 Hyperthermic Delivery

Hyperthermia is often used in drug delivery to increase vasodilation in the tumor, increasing the EPR effect. Clinically, temperatures in the range of 40-44ºC are used for local, regional, part body, or full body hyperthermia.[210] Chemical vectors have been made with thermosensitive materials such as lipids and polymers to facilitate release of nucleic acids (and other drugs) before, during or after heat is applied.

Chen et al. showed a reduced transition temperature of K_8-ELP(1-60) block copolymer particles after complexing with pDNA from 71.5 to 44.9ºC, bringing the particle into a clinically relevant hyperthermic temperature range. ELP is an elastin-like polypeptide with 60 repetitive pentapeptide units, which aggregates above it's transition temperature facilitating release, while K_8 signifies a cationic oligolysine used to complex and condense the pDNA. However, while the development of a temperature sensitive block copolymer gene delivery vehicle was produced, and showed delivery of GFP plasmids in MCF cells *in vitro*, hyperthermic triggered release was not established. Release profiles were determined by concentrations of heparin sodium, an anionic protein found in the body. Still, the future of this block copolymer is bright, having a clinically relevant transition temperature and functional activity.[211]

Zintchenko et. al. produced a block copolymer with PEI and poly(N-isopropylaryamide) (PNIPAM), which when complexing pDNA made uncharged particles of about 150-200 nm that aggregated to sizes of a few microns after 15 minutes of incubation, releasing pDNA at temperatures between 37 and 42ºC. Neuro2A cells were transfected and showed almost 2 orders of magnitude higher gene expression after several cycles through the polymer's transition temperature. The studies showed that

hyperthermia was able to facilitate the rate at which the particles aggregated, but not the rate of uptake into cells. The enhanced gene expression was attributed to larger size of the aggregated thermosensitive particles in comparison to the control PEI-PEG copolymers, which lead to a greater osmotic pressure inside the endosomes, greater amount of PEI to facilitate the protein sponge effect and thus more DNA released into the cytoplasm.[212]

1.3.5.5 Reductive Agents

Sulfhydryl cross-linked chemical gene delivery systems have been developed to facilitate protection of DNA and triggered release. By creating peptides with one to four cystine residues, McKenzie et al. reported a greater ability to create sulfhydryl bonds and by including many lysine residues, the peptides could achieve an appropriate cationic charger to complex with DNA.[213] Five peptides presented in the paper (such as Cys-Trp-Lys_{18}) were able to spontaneously oxidize after binding to pDNA, causing interpeptide disulfide bonds, decreasing the particle size, and preventing dissociation of DNA in the presence of concentrated sodium chloride. These five peptides fully condensed DNA at a peptide to DNA ratio of 0.3-0.4 nmol of peptide/μg of DNA, with a charge ratio of 2:1 (+/-). Release of DNA was triggered by the reducing environment of the endosome and cytosol, reducing the sulfide bond, showing a 5-60 fold increase in DNA expression compared to uncross-linked peptides. Kwok et al. showed *in vivo* delivery of sulfhydryl linked PEG-peptide/glycopeptide DNA nanoparticles with large biodistribution to the liver. In this study, peptides with the most positive zeta potentials (18.1 to 21.5 mV) showed greatest distribution to the hepatocytes, and those with the most negative zeta potential (-16.1 to -13.0 mV) had the greatest accumulation in Kupffer cells (macrophages of the liver).[214]

Lee and colleagues used degradable nanogels made of hyaluronic acid (HA) to deliver siRNA triggering release as a function of glutathione (GSH) concentrations [215]. Glutathione is a major reducing agent found in the cytoplasm, and triggered the release of siRNA from the hyaluronic acid nanogels that were crosslinked with disulfide linkages. When 10 mM of GSH was used, 100 % of siRNA was released in 60 minutes, compared to only 5.8 % siRNA released when 0 mM GSH was used. The HA/siRNA nanogels were also shown to be non-toxic, have GFP expression in HCT-116 silenced comparable to the silencing of PEI/siRNA complexes *in vitro* and finally, significantly better silencing of GFP as compared to PEI/siRNA complexes in the presence of serum *in vitro*. The hyaluronic acid nanogels also had specific endocytosis mediated by the CD44 receptor.[215]

1.3.5.6 Biotin-Avidin

The strong affinity of biotin for avidin has been well established. Xiong and colleagues developed a nanoparticle that takes advantage of this to trigger release of DNA. The carrier consisted of avidin conjugated to PEG, and biotin conjugated to PEI. PEI complexed the plasmid DNA, the biotin bound the avidin, and the PEG was included to protect the carrier from clearance by the RES. The group found that conjugating PEI to biotin decreased the binding affinity to avidin, making it possible for dissociation of biotin from avidin *in vivo* in a biotin-rich environment. Localization *in vivo* to tumor interstitium was attributed to the enhanced permeability and retention (EPR) effect. After polyplexes had accumulated in tumor interstitium, additional biotin could be delivered either orally or intravenously to bind with the avidin-PEG molecules, triggering release of the PEG shell from the PEI-pDNA complex. This also allows the polyplex to associate with the cell membrane, encouraging endocytosis.[216]

1.3.5.7 Electrochemical

DNA conjugated to gold nanoparticles have elicit interest in electrochemically triggered release. Wang et al. in a proof-of-concept experiment showed that it was possible to immobilize non-thiolated layers of dsDNA or ssDNA on gold nanoparticles, and release the DNA by controlling the electric potential.[217]

1.3.6 Recent Clinical Trials Using Nucleic Acids

1.3.6.1 Introduction

When searching for "gene therapy" clinical trials on www.clinicaltrials.gov, a website maintained by the NIH as a "registry of federally and privately supported clinical trials conducted in the United States and around the world[1]," nearly 1500 trials were returned. However, the majority of these trials had been flagged because genotyping, gene expression analysis, or gene expression profiling was included in the studies' aims. Other trials included delivery vehicles such as adenoviruses, adeno-associated viruses, lentiviruses, retroviruses, or cell based therapy, where immune cells were transformed with a virus to express a certain protein and re-injected into the body. Although these fields are older and more developed that those of non-viral, chemical vectors, some chemical vectors appeared on this list in less than two percent of the clinical trials, ranging from phase 1 to phase 4. In the following section, clinical trials have an associated number (i.e. (NCT00000000). These clinical trials can be found online by going to www.clinicaltrials.gov/show/NCT00000000, where NCT00000000 is the NCT identification number associated with the trial.

[1] www.clinicaltrials.gov

1.3.6.2 Naked Nucleic Acids in Clinical Trials

1.3.6.2.1 Naked DNA

In phase 1 studies at the Seoul National University Hospital, Korea, IL-2 plasmids are being used as an immune adjuvant to vaccinate patients with HIV antigens. A human mutant plasmid called GX-12 contains both human IL-2 and HIV-1 antigen genes. An i.m. injection of GX-12 is delivered in combination with highly active antiretroviral therapy (HAART). (NCT00517569).

Plasmid encoding vascular endothelial growth factor (VEGF) has been delivered to the heart to promote angiogenesis and vasculogenesis to treat myocardial ischemia and angina pectoris. In phase 1 and 2 trials, at the Cardiac Catheterization Laboratory, The Heart Centre, University Hospital, Rigshospitalet, Copenhagen, Denmark, VEGF-A165 plasmid was used to treat chronic myocardial ischemia. This treatment was also combined with granulocyte colony stimulating factor (G-CSF) therapy, recruiting bone-marrow derived stem cells to regenerate the cardiac tissue at the sight of damage, promoting angiogenesis and vasculogenesis. (NCT00135850). Similarly, at Northwestern University, in phase 1 trials, phVEGF165 is being delivered by intramyocardial injection into the heart, and G-CSF is also administered treating patients with ischemic heart failure. (NCT00279539). In an effort to enhance vasculogenesis, VEGF has been delivered with another growth factor, basic fibroblast growth factor (bFGF). In phase 2 trials at the Institute of Cardiology Warsaw, Poland, plasmid coding human VEGF-A165/bFGF was injected into ischemic myocardium of refractory coronary artery disease patients. These two important angiogenic growth factors, bFGF and VEGF-A were

combined into one plasmid (bicistronic). This therapy aims at stimulating neoangiogenesis to increase myocardial perfusion. (NCT00620217).

In phase 2 trials at 35 locations across the U.S., recombinant plasmid DNA coding for VEGF2, (pVGI.1) is administered using an experimental cardiac direct injection catheter (Stiletto™) system for patients with angina pectoris. (NCT00090714).

DNA encoding VEGF has also been used to treat critical limb ischemia, leg ulcers, peripheral artery disease and diabetic neuropathy. At over 30 study locations, in a phase 3 trial, plasmid XRP0038/NV1FGF (delivering phVEGF165) is being used for critical limb ischemia (CLI) patients with skin lesions. (NCT00566657). At three locations across the U.S., in a phase 1 study, a VEGF plasmid (pVGI.1) is i.m. injected into leg muscles to treat moderate to high-risk critical limb ischemia, and leg ulcers. VEGF treatment is being tested to see if it improves rest, pain and/or heals ulcers in the legs of patients with peripheral artery disease. (NCT00304837).

At centers in Boston and New York, VEGF DNA is being delivered in the form of pVGI.1 to express VEGF2 to treat diabetic neuropathy in the legs. The study is in phase 1 and 2 trials. (NCT00056290). In phase 1 trials by Diabetes and Glandular Disease Research Associates, San Antonio, Texas, plasmid hVEGF-A is used to treat diabetic neuropathy. The plasmid, named SB-509, by Sangamo BioSciences, is administered as an i.m. injection. (NCT00110500).

A phase 1 and 2 trial at Memorial Sloan-Kettering Cancer Center in New York, New York, is using sargramostim, also known as granulocyte-macrophage colony stimulating factor (GM-CSF). DNA is used as an adjuvant for a multi-epitope vaccine to treat melanoma. DNA is injected subcutaneously (s.c.) on day 0 and the vaccine delivered

on day 5, also s.c. This study is treating stage IIB, stage IIC, stage III, or stage IV melanoma. (NCT00085137).

In Connecticut, a phase 1 trial is underway to treat leaky bladder problems. The plasmid, hMaxi-K will be given as a single administration into the bladder through a catheter. Changes in incontinence episodes, maximum bladder capacity, urgency episodes and participant quality of life will be analyzed, among other variables. (NCT00495053).

Turner syndrome and SHOX (short stature homeobox) deficiency is being treated at a phase 3 trial conducted at Eli Lilly, in Philadelphia, PA. A recombinant DNA plasmid for somatropin, also known as HGH, human growth hormone is being administered and "height velocity" of those on this treatment and those on placebo, will be measured. In this study, treatment will be continued until patients reach normal adult height. (NCT00190658).

At two locations, Dubowitz Neuromuscular Centre, Hammersmith Hospital and Clinical Trails Unit, St Mary's Hospital, London, United Kingdom, Duchenne Muscular Dystrophy (DMD) is being treated by intramuscular administration of antisense therapy with the use of antisense oligonucleotides (AON) which has the potential to restore the production of dystrophin, the defective protein, in >70 % of DMD. The intramuscular administered morpholino oligomer is directed against exon 51 (AVI-4658 PMO). (NCT00159250).

At locations in 6 European countries, phase 2 trials are underway to treat patients with severe peripheral arterial occlusive disease, Fontaine's stage IV. The pCOR plasmid, named XRP0038 (NV1FGF) was constructed by inserting the gene coding for the fibroblast growth factor (FGF). FGF plays a role in angiogenesis. (NCT00368797).

1.3.6.2.2 Naked DNA with Electroporation

In the first clinical trial to combine electroporation with free plasmid delivery, free IL-12 plasmid is injected into melanoma tumors near the surface of the skin then electroporation is applied. This phase 1 study is being carried out at the H. Lee Moffitt Cancer Center & Research Institute, in Tampa, Florida. (NCT00323206).

1.3.6.2.3 Hybrid Oligonucleotides

In phase 1 trial at Albert Einstein Comprehensive Cancer Center, in Bronx, New York, an 18-mer hybrid oligonucleotide is being used to study the effectiveness of combining docetaxel and GEM 231 in treating patients who have recurrent or refractory solid tumors. GEM-231 (a mixed backbone oligonucleotide) is a strand of synthetic DNA, which has been modified with 2'-O-methyl ribose at both ends in order to resemble RNA targeted against the RIalpha subunit of protein kinase A (PKA).[218; 219]

1.3.6.3 Lipid-Based Nucleic Acid Carriers in Clinical Trials

Cationic liposomes composed of DMRIE/DOPE, have been used to delivering pGT-1 (cystic fibrosis gene) to cells lining the nose of cystic fibrosis patients. DMIRE is a cationic lipid, an abbreviation for 1,2-dimyristyloxypropyl-3-dimethyl-hydroxy ethyl ammonium bromide, while DOPE is a neutral lipid, an abbreviation for that stands for L-alpha-dioleoyl phosphatidylethanolamine. Delivery was facilitated by syringe instillation over thirty minutes to the right inferior nasal turbinate. Studies are in phase 1 trials at the University of Alabama at Birmingham. (NCT00004471).

At the M.D. Anderson Cancer Center, Houston, Texas, DOTAP:chol liposomes were complexed with the fus1 gene to deliver i.v. in the treatment of lung cancer. (NCT00059605).

To treat patients with recurrent or refractory stage III or stage IV head and neck cancer, cationic liposomes (DOTMA/chol) were used to, delivering the interleukin-2 gene. N-(1-(2,3-dioleyloxy)propyl)-N,N,N-trimethylammonium chloride is abbreviated by DOTMA. The theory behind the treatment, reasons that by inserting IL-2 DNA into tumor cells, an immune response will be recruited to destroy the tumor. The treatment is being compared to methotrexate in phase 2 studies at the H. Lee Moffitt Cancer Center and Research Institute. (NCT00006033).

At University of Pittsburgh's Cancer Institute, in a phase 1 study, DC-chol liposomes were delivered with EGFR antisense DNA i.t. to advanced squamous cell carcinoma of the head and neck. This study was sponsored by the National Cancer Institute. (NCT00009841).

An IL-2 plasmid DNA/lipid complex is being used to treat stage II or stage III organ confined prostate cancer. Lipid portion of the vehicle is made of a mixture of DMIRE and DOPE.[220] The lipoplex is injected intraprostatically under ultrasound guidance. The phase 2 studies are underway at Jonsson Comprehensive Cancer Center, UCLA, in Los Angeles, California and the Cleveland Clinic Taussig Cancer Center, in Cleveland, Ohio. (NCT00004050). Leuvectin has also been used to treat locally recurrent prostate cancer following radiation therapy. These are phase 1 and 2 trials at the same locations as the previous study. (NCT00005072).

In an effort to make cancer cells more sensitive to radiation therapy, the experimental agent LErafAON is being tested by delivering cationic liposomes carrying antisense oligonucleotide against the Raf-1 protein. LErafAON is delivered by i.v. infusions for the treatment of solid advanced tumors. These phase 1 studies are being conducted at three locations in the U.S. (NCT00024661, NCT00024648).

Allovectin-7® is a plasmid/cationic lipid complex containing the DNA sequences encoding HLA-B7 and ß2 microglobulin, which together form a class I Major Histocompatibility Complex, or MHC-I antigen for treating stage III or stage IV metastatic melanoma.[221] The therapy is administered through an intratumoral/lesional injection. Study locations of this phase 2 trial include Mayo Clinic Cancer Center, in Rochester, Minnesota; Roswell Park Cancer Institute, in Buffalo, New York, and Physician Reliance Network, Inc., in Dallas, Texas. (NCT00003646).

1.3.6.4 Polymer-Based Nucleic Acid Carriers in Clinical Trials

To treat patients with superficial bladder cancer who have failed other therapies, DTA-H19 plasmid is complexed with PEI and delivered intravesically into the bladder. This phase 1 and 2 trial is being carried out at Meir Medical Center, Kfar Saba, Israel E. Wolfson Medical Center, in Holon, Israel. (NCT00393809).

In a phase 1 trial going on in four locations across the United States, EGEN-001 (phIL-12-005/PPC) is being administered via intra-peritoneal [61] infusion to patients with recurrent, platinum-sensitive, ovarian cancer. EGEN-001 is an IL-12 plasmid complexed by a delivery polymer to stimulate an immune response to the tumor. This polyplex delivery is being combined with Carboplatin and Docetaxel. (NCT00473954).

1.3.7 Conclusion

Chemical vectors offer many benefits to gene delivery. These vectors have less toxicity compared to viral vectors and are fairly simple to manipulate. Chemical vectors vary in shape, particle size, nucleic acid complexation ability and release rate, allowing one to choose the proper delivery system for a certain application. The variety of targeting moieties allows the delivery system to have higher affinity for the microenvironment of interest, increasing the association of the particles on the cell's surface, or the rate of endocytosis. Additionally, triggering mechanisms can be engineered into the design of the delivery system to control or facilitate the release of the DNA or RNA. Finally, the use of chemical gene delivery vectors in humans is quickly approaching reality with the progress of the field. In conclusion, the flexibility of chemical vectors to be engineered to a very specific application, with the reduced toxicity compared to viral vectors, point these delivery systems to the front of the gene delivery field.

CHAPTER 2

ENANTIOSPECIFIC ADJUVANT ACTIVITY OF CATIONIC LIPID DOTAP IN CANCER VACCINE

Commercially available DOTAP is a racemic mixture of two enantiomers. The adjuvanticity of each isomer was examined using a peptide/lipid complex as a therapeutic vaccine in an established murine cervical cancer model. This simple vaccine consists of a cationic lipid (DOTAP) and a Major Histocompatibility Complex (MHC) class I restricted epitope of the Human Papillomavirus (HPV) 16 protein E7. Dose-dependent tumor regression experiments have been completed for racemic DOTAP/E7, (R)-DOTAP/E7 and (S)-DOTAP/E7. Tumor-bearing mice treated with (R)-DOTAP/E7 complexes have shown tumor regression in a dose-dependent manner comparable to those mice treated with a racemic DOTAP with E7 peptide. This data is supported by IFN-γ production by $CD8^+$ splenocytes, in vivo cytotoxic T-lymphocytes (CTL) response, $CD8^+$ tumor infiltrating lymphocytes (TIL) and IFN-γ production by $CD8^+$ TIL in (R)-DOTAP/E7 vaccinated mice. When (S)-DOTAP/E7 is delivered, tumor progression is delayed. While IFN-γ production is absent from $CD8^+$ splenocytes in mice vaccinated with (S)-DOTAP/E7, IFN-γ production by $CD8^+$ TIL is present, supporting our hypothesis that (S)-DOTAP has limited activity. Activation of bone marrow derived dendritic cells by the enantiomeric formulations has also been evaluated, as well as cytokine production and toxicity with no considerable differences between the groups.

The results show the DOTAP enantiomers act differently as adjuvants in vivo, with (R)-DOTAP being more effective at stimulating a $CD8^+$ anti-tumor response.

2.1 INTRODUCTION

Therapeutic cancer vaccines are safe treatments that can create a potent immune response against transformed host cells. Vaccines and immunotherapy avoid the toxicity of harsh chemotherapy that includes side effects such as weight loss, hair loss, nausea and leukopenia. Instead of targeting all rapidly dividing cells, as is the case of many small molecule chemotherapeutic drugs, vaccines can train the immune system how to specifically target cancer cells only. Creating an efficacious cell-mediated response is crucial for anti-tumor effects.[222] Many different types of antigens have been used in cancer vaccines, ranging from whole tumor cell lysate to MHC class I restricted peptides specifically recognizable by CTLs.[223; 224; 225] Only the use of peptide antigens allows for ease of manufacturing, as well as precise control over the purity and specificity of the vaccine. However, peptide antigens need supplementary treatments to increase immunogenicity.

There is very little variety in the adjuvants that are clinically available. The U.S. Food and Drug Administration (FDA) has only approved two adjuvants for use in humans, both aluminum hydroxide based.[226] The first, Alum (aluminum hydroxide), has been approved since the 1920s. The second, AS04 (3-O-desacyl-4'-monophosphoryl lipid A adsorbed on to aluminum as hydroxide salt), was approved in the U.S. in 2009, is only

used in one vaccine that is currently on the market (Cervarix).[227] The scarcity of available adjuvants, particularly in the United States, demonstrates a need for new safe adjuvants allowing more options in formulation and titrating of the desired immune response via immunotherapy.

Development and subsequent approval of new adjuvants face several barriers. Encouraged by the FDA, scientists arecreating treatments that are chirally pure is a trend growing in popularity across pharmaceutics, with the increased ease of separation of enantiomers after synthesis.[228; 229] However, chiral drugs can have different efficacies *in vivo.* It is known that stereoisomers of small molecule drugs can have widely varied effects, with one being efficacious and the other showing no therapy, or worse, toxicity.[230] Biology provides an asymmetric environment, containing chiral components at its most basic molecular level, L-amino acids and D-carbohydrates. It is no surprise that highly purified antigens show stereospecificity in all types of immune reactions.[231; 232] However, it has never been shown that the stereospecificity of an adjuvant plays a vital role in its efficacy in producing an immune response.

Our basis for investigating this line of work starts with a therapeutic vaccine we have previously developed for a murine cervical cancer model. This nanoparticle complex consists of three molecules, racemic DOTAP lipid and E7 peptide, an H-2D^b restricted 9-mer from the HPV 16 E7 oncogene, able to cause regression in pre-existing tumors.[30] The MHC class I restriction of the peptide promotes a cell-mediated response rather than a humoral response against the growing tumor. We have shown that the racemic DOTAP lipid is able to activate bone marrow-derived dendritic cells (BMDC) *in vitro* to elicit a cytokine response via the ERK pathway.[32]

In this study, we investigate the impact of chirality on the efficacy of DOTAP lipid as an adjuvant. We have evaluated (R)-DOTAP and (S)-DOTAP for its interaction with E7 peptide in formulation properties, measuring peptide encapsulation, particle size and charge. Lipid alone was used to test the interaction and ability to stimulate BMDC, inducing activation through CD86 up-regulation and CCL2 production. Lipid toxicity was also compared when treating BMDC. *In vivo,* (R) and (S)-DOTAP formulations were compared in many ways, testing for effect on tumor regression, and further elucidating the affected cellular mechanisms that cause regression.

2.2 MATERIALS AND METHODS

2.2.1 Materials

Racemic DOTAP (99.9 % purity), (R)-DOTAP (100 % purity) and (S)-DOTAP (99.9 % purity) were obtained from Merck KGaA (Darmstadt, Germany). (R)-DOTAP stock used had a specific optical rotation $[\alpha]_D^{25}$ of -1.77°, while (S)-DOTAP stock used had a specific optical rotation $[\alpha]^{25}$ of +1.99°. H-2D^b restricted peptides E7 (H-RAHYNIVTF-OH, amino acids 49-57 from the E7 protein of HPV16) and NP (H-ASNENMETM-OH, amino acids 366-374 from the influenza virus strain A/PR/8/34 nucleoprotein) were obtained from the University of Pittsburgh Peptide Synthesis Facility (Pittsburgh, PA).

2.2.2 Tumor cell culture

TC-1 is a murine model of human cervical cancer. To create TC-1, lung endothelial cells from a C57BL/6 mouse were transfected oncogenes E6 and E7 from the Human Papillomavirus 16 (HPV16), as well as activated human H-ras.[233] TC-1 cells were obtained from American Type Culture Collection (Manassas, VA) and maintained in RPMI 1640 media supplemented with 10 % fetal bovine serum (Invitrogen, Carlsbad, CA), 100 U/mL penicillin (Invitrogen) and 100 μg/mL streptomycin (Invitrogen).

2.2.3 Preparation and Evaluation of Vaccine Formulations

DOTAP/E7, (R)-DOTAP/E7 and (S)-DOTAP/E7 complexes were made as described previously with few modifications.[30] Briefly, lipids dissolved in chloroform were dried in glass vials under a stream of nitrogen and stored under vacuum in a desiccator overnight. Lipid/peptide complexes were formed by thin film hydration, using a solution of E7 peptide in molecular grade water (Cellgro, Manassas, VA) and subsequent vortexing. After 2 h at room temperature, the suspensions were extruded through two 100 nm polycarbonate membranes (Fisher Healthcare, Houston, TX) to a size of roughly 120 nm. Particle size and zeta potential was measured with a Malvern Zetasizer Nano ZS in water (Malvern, Worcestershire United Kingdom). E7 encapsulation was determined by Microcon® centrifugal filtrate device (Millipore, Bedford, MA). Unbound peptide was measured by Micro BCA™ Protein Assay Kit (Rockford, IL). Amount encapsulated calculated as (100 - % unbound peptide).

2.2.4 Bone Marrow Derived Dendritic Cells (BMDC)

Methods to culture bone marrow-derived dendritic cells have been described previously [32]. Briefly, bone marrow from the femurs and tibias of six week old C57BL/6 mice was isolated in serum free RPMI 1640 media. Red blood cells were lysed using ACK Lysing Buffer (Invitrogen) and cells were plated for 2 h in serum free RPMI 1640 to remove suspension cells (lymphocyte precursors). Remaining adherent cells were cultured in RPMI 1640 media containing 10 % fetal bovine serum, non-essential amino acids (Invitrogen), antibiotic/antimycotic (Sigma-Aldrich, St. Louis, MO) with 1000 U/mL granulocyte-macrophage colony-stimulating factor (GM-CSF) and 1000 U/mL interleukin-4 (IL-4) (R&D Systems, Minneapolis, MN) for 6 days changing the media every 2 days. BMDCs were used in experiments on day 6.

2.2.5 Interaction of Formulations with BMDC *in vitro*

To measure CD86 expression, a sign of activation, BMDC were treated with different concentrations of liposomes (free of peptide) for 18 h. Cells were stained with anti-CD86 (GL1) and anti-CD11c (HL3) antibodies (BD Biosciences, San Jose, CA) and analyzed using a FACS Canto II flow cytometer (BD Biosciences). One hundred ng/mL LPS served as a control. Isotype controls were used. To measure toxicity, BMDC were treated with different concentrations of liposomes (free of peptide) for 18 h and stained with propidium iodide (PI) (Sigma-Aldrich) and evaluated using flow cytometry. To measure production of chemokine C-C motif ligand 2 (CCL2) in a dose-dependent manner, BMDC were treated with varying doses of (R)-DOTAP and (S)-DOTAP liposomes (free

of peptide). After 24 h, cell supernatants were collected and analyzed by ELISA (BD Biosciences).

2.2.6 Mice and Immunizations

Six week old female C57BL/6 mice were used in all studies. On day 0, 10^5 TC-1 cells were injected subcutaneously into the hair-trimmed abdomen. On day 6, formulations (100 μL) were subcutaneously injected into the contralateral side of the abdomen in a 5 % dextrose solution. In the initial tumor growth delay experiment, 100 nmol of lipid, and 20 μg of E7 peptide was used. After this initial experiment, an optimal dose was determined by delivering lipid in concentrations ranging from 3 to 600 nmol, with a constant dose of 20 nmol of peptide. In all future *in vivo* experiments, lipid formulations contained 300 nmol lipid and 20 nmol of E7 peptide. Unencapsulated peptide was not removed. Tumors were measured every 2-3 days with calipers, calculating area as (length) x (width). Humane sacrifice of mice was performed after tumors reached 20 mm in one dimension. All animal protocols were approved by the University of North Carolina at Chapel Hill's Institutional Animal Care and Use Committee.

2.2.7 Interferon gamma (IFN-γ) production by $CD8^+$ T cells

Mice were injected with 10^5 TC-1 cells on day 0. On day 6, mice were vaccinated with either (R)-DOTAP/E7 or (S)-DOTAP/E7 with lipid and peptide concentration of 300 nmol and 20 nmol, respectively. On day 14, mice were sacrificed, spleens sterilely removed and processed to a single cell suspension by crushing the spleen through a 70

μm filter (BD Biosciences). After removal, cells were incubated in RPMI 1640 media supplemented with NEAA and antibiotic/antimycotic, 1 μL/mL GolgiStop™ (BD Biosciences) and 5 μM E7 or NP peptide for 6 h at 37 °C. Cells were removed, washed with staining buffer (BD Pharmingen, San Diego, CA) and stained with anti-CD8 antibody (53-6.7). Cells were then treated with Cytofix/Cytoperm™ kit and stained intracellularly for IFN-γ (XMG1.2), washed and analyzed by flow cytometry. Percents represent IFN-γ^+ $CD8^+$ T cells out of the total $CD8^+$ T cell population.

2.2.8 *In vivo* Cytotoxic T Lymphocyte (CTL) Assay

The *in vivo* CTL assay has been described previously and was performed here with slight modifications.[234] Briefly, mice were injected with 10^5 TC-1 cells on day 0. On day 6, mice were vaccinated with either (R)-DOTAP/E7 or (S)-DOTAP/E7 with lipid and peptide concentration of 300 nmol and 20 nmol, respectively. Eight days later, naïve mice were sacrificed and splenocytes removed. Splenocytes were pulsed with either 10 μM E7 or NP peptide for 1-2 h in complete media at 37 °C. Cells were stained with carboxyfluorescein succinimidyl ester (CFSE) (Sigma-Aldrich, St. Louis, MO) , with NP peptide-pulsed and E7 peptide-pulsed cells stained with 0.4 and 4 μM, respectively in serum free media for 15 min. Cells were then washed with complete media and counted. Equal numbers of $CFSE^{high}$ (E7 pulsed cells) and $CFSE^{low}$ (NP pulsed cells) were mixed together and stained with 8 μM PKH-26 (Sigma-Aldrich) according to manufacturer's instructions. Vaccinated mice were injected with 10^7 labeled cells and *in vivo* killing of the targets was allowed for 16-20 h. After that time, spleens from treated mice were removed and made into a single cell suspension, red blood cells lysed, washed and

resuspended in phosphate buffered saline (Sigma-Aldrich). The cells were analyzed by flow cytometry, first gating for the lymphocyte population, then for the PKH-26 positive cells, to determine the amount of specific lysis of the E7 labeled cells. The following equation from Byers et al. shows this, with NP and E7 representing the number of cells pulsed with E7 or NP peptide present after *in vivo* killing.[234]

$$\text{\% specific lysis} = \frac{(NP^{*}x - E7)}{(NP^{*}x)} * 100\%$$

$$\text{where, } x = \frac{NP}{E7} \text{ from naïve mice}$$

2.2.9 Tumor Infiltrating Lymphocyte Analysis

TC-1 tumors from mice vaccinated on day 6 were removed on day 14 in a sterile environment. Tumors were minced and incubated in RPMI 1640 containing 1 mg/mL collagenase type 1 (Worthington, Lakewood, NJ) for 30 min at 37 °C. Tumors were put through a 70 µm strainer and formed a single cell suspension. Cells were blocked with Fc block (anti CD16/CD32 (2.4G2)) for 15 min, then stained with anti-CD8 (53-6.7) and anti-CD4 (RM4-5) and analyzed by flow cytometry.

Alternately, lymphocytes were isolated from the tumors. Tumors were prepared as described above to a single cell suspension. The cells were washed and resuspended in complete media. Tumor infiltrating lymphocytes (TIL) were separated from the tumor using Ficoll-Paque™ PLUS (GE Healthcare, Uppsala, Sweden), a density gradient method. These tumor infiltrating lymphocytes were plated at a concentration of 2 x 10^6 and stimulated with 5 µM E7 or NP peptide for 6 h at 37 °C. The TIL were incubated

with Fc Block, antibodies for CD8, stained intracellularly for IFN-γ and analyzed by flow cytometry.

2.2.10 Statistical Analysis:

Statistical analysis was completed by using a two-tailed Student's t-test. Data was statistically significant if the P value was less than 0.05.

2.3 RESULTS

2.3.1 Tumor Regression by Therapeutic Vaccination

One injection of racemic DOTAP/E7 (100 nmol / 20 μg) six days after TC-1 tumor inoculation caused regression of preformed tumors (**Figure 2.1a**), statistically different than untreated mice ($P<0.0001$). (R)-DOTAP/E7 complexes showed the same response, indicating that (R)-DOTAP is the active enantiomer in racemic DOTAP ($P=0.63$). (S)-DOTAP/E7 showed a partial response, statistically significant from racemic DOTAP/E7 and (R)-DOTAP/E7 treated mice ($P<0.05$). The (S)-DOTAP/E7 treated mice also had tumor growth that was statistically significant from the untreated control group and the control mice treated with E7 alone ($P<0.01$).

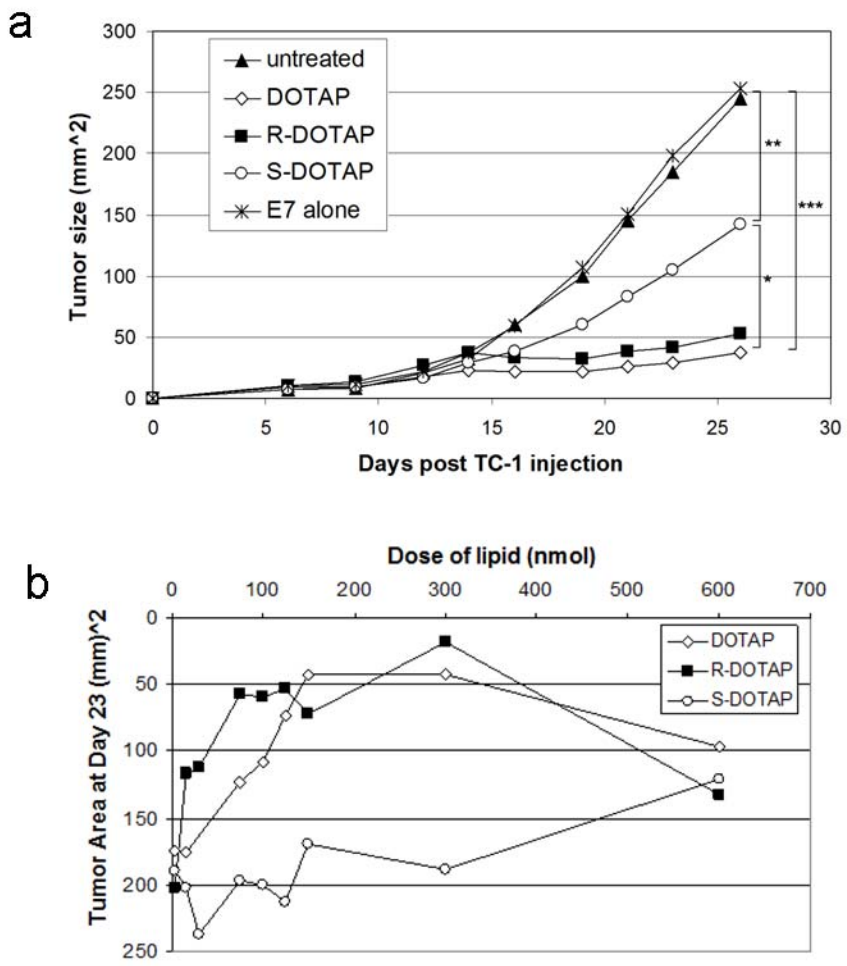

Figure 2.1 TC-1 tumor growth inhibition by vaccine delivery *in vivo*.
(a) TC-1 tumor growth inhibition in mice by lipid/E7 complexes. Six week old female C57BL/6 mice were inoculated with 10,000 TC-1 cells s.c. in the abdomen on day zero. On day 6, treatments were s.c. injected into the opposite side of the abdomen. Lipid formulations delivered contained 100 nmol lipid and 20 μg of E7 peptide. Sample size and statistics are as follows: n=5-6, *: P<0.05, **: P<0.01, ***: P<0.0001. (b) Dose-dependent antitumor activity of racemic DOTAP/E7, (R)-DOTAP/E7 or (S)-DOTAP/E7 complexes. Six week old female C57BL/6 mice were injected with 10,000 TC-1 cells s.c. as in previous studies. On day 6, treatments were s.c. injected into the opposite side of the abdomen. The dose of lipid was varied while the dose of E7 peptide was kept constant at 20 nmol. n=5-6 per dose

(R)-DOTAP/E7 complexes also showed a dose-dependent response comparable to that of racemic DOTAP/E7 when evaluating tumor size at day 23 (**Figure 2.1b**). (S)-DOTAP/E7 never achieved an optimal dose, even at very high concentrations of lipid (600 nmol). The optimal dose assessed from these studies was 300 nmol of lipid, not only because it had the greatest response in terms of tumor regression (for (R)-DOTAP /E7 and racemic DOTAP/E7 treated mice), but it also had the greatest difference between (R) and (S)-DOTAP/E7 treated groups.

2.3.2 Formulation Characterization

As shown in **Table 2.1**, the average size of (R)-DOTAP/E7 complexes was 126.8 ± 5.1 nm and (S)-DOTAP/E7 complexes were of comparable size at 125.6 ± 7.8 nm (P=0.69). Zeta potentials of the (R) and (S)-DOTAP/E7 complexes also did not vary significantly with values of 54.3 ± 4.0 mV and 55.8 ± 1.9 mV, respectively (P=0.37). Encapsulation efficiency of E7 peptide with (R)-DOTAP and (S)-DOTAP also did not differ significantly, with values of 31.3 ± 16.6 % and 32.1 ± 8.9 % at a dose of 300 nmol lipid, and 20 nmol E7 peptide (P=0.87).

Table 2.1 Physical properties of the vaccine formulations[a].

Formulation	Particle Size (nm) [*]	Zeta Potential (mV) [**]	Encapsulation Efficiency (%) [***]
R-DOTAP/E7	126.8 ± 5.1	54.3 ± 4.0	31.3 ± 16.6
S-DOTAP/E7	125.6 ± 7.8	55.8 ± 1.9	32.1 ± 8.9

[a] Lipid concentration used in these studies was 6mM, equivalent to 300 nmol of lipid per mouse

[*]. P=0.69, n=8-10.

[**] P=0.37, n=8-10.

[***] P=0.87, n=13-14. Encapsulation efficiency includes peptide capture on the surface of the liposomes, any trapped within the bilayer, or within an aqueous compartment.

2.3.3 Evaluation of (R)-DOTAP and (S)-DOTAP *in vitro*

BMDC treated with (R)-DOTAP and (S)-DOTAP for 18 h both showed similar dose-dependent effects. Activation of BMDC was increased with increasing doses of both (R) and (S)-DOTAP (**Figure 2.2a**). (S)-DOTAP increased CD86 expression more at lower doses (45 μM) and the peak of (R)-DOTAP-induced CD86 expression came at higher doses (150 μM), however, the difference was not significant. Expression of chemokine CCL2 was increased in (R)-DOTAP treated BMDC at doses of 45, 75 and 100 μM compared to (S)-DOTAP, however the difference was not significant (**Figure 2.2b**). After an 18 h treatment with either lipid, toxicity to BMDC was similar shown by the increased signal from PI (**Figure 2.2c**). Dose-dependent effects were observed with greater toxicity at higher doses, showing an increase in toxicity in 75 μM up through the highest dose tested. All toxicity levels were much higher than the LPS treated BMDC. We believe the BMDC model is not sufficient to explain the profound difference in (R) and (S)-DOTAP activity, thus moved to whole-body experiments to examine the immune response in the complete mouse.

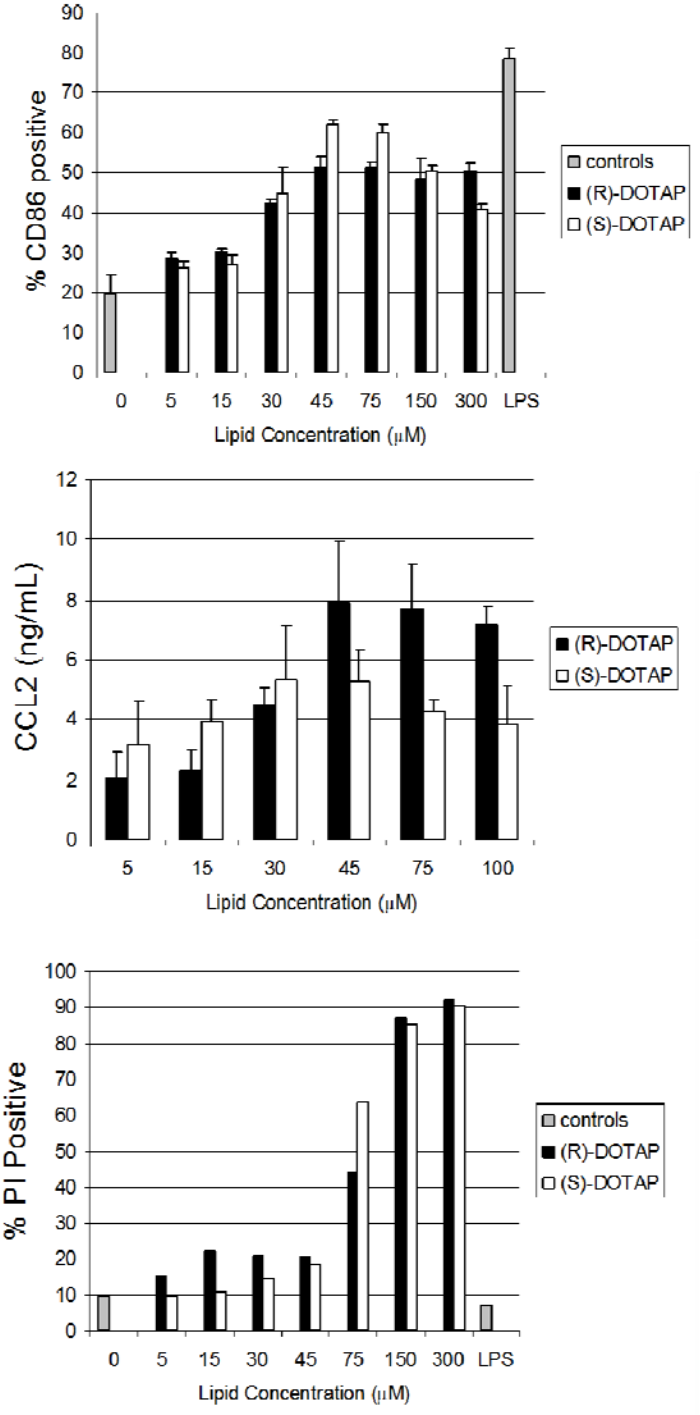

Figure 2.2 Chiral Lipid Interaction with BMDC.
BMDC were treated with (R)-DOTAP or (S)-DOTAP liposomes (free of peptide) for 18 h and (a) dose-dependent activation of CD86 was evaluated (n=3), as well as (b) dose-dependent CCL2 secretion after 24 h treatment (n=3). (c) BMDCs were also evaluated for toxicity by PI staining of cells after 18 h treatment (one representative experiment shown, repeated in triplicate).

2.3.4 IFN-γ Production by $CD8^+$ T cells from Vaccinated Mice

When comparing naïve, tumor-bearing, (R)-DOTAP/E7 treated tumor-bearing mice, and (S)-DOTAP/E7 treated tumor-bearing mice for IFN-γ production by $CD8^+$ T cells, (R)-DOTAP/E7 treated mice showed an antigen specific response (**Figure 2.3a**). Splenocytes isolated from (R)-DOTAP/E7 treated tumor-bearing mice that had been pulsed with E7 peptide for 6 h produced IFN-γ at a magnitude of 0.8 % of the $CD8^+$ T cells present, while the NP peptide pulsed control splenocytes produced 0.0 %. Splenocytes isolated from naïve mice, tumor-bearing mice, and (S)-DOTAP/E7 treated mice, whether pulsed with NP or E7 peptide, produced 0.0 % $CD8^+$ T cells. The difference between IFN-γ secreting $CD8^+$ cells per 10^4 $CD8^+$ T cells for the two groups was statistically significant ($P<0.01$) (**Figure 2.3b**).

As no groups but (R)-DOTAP/E7 treated mice pulsed with E7 produced IFN-γ, we incubated the cells with NP or E7 peptide for 12 h to evaluate if a longer incubation would show IFN-γ production in any other group (**Figure 2.3c**). However, while all the NP peptide pulsed samples remained at 0.0 %, as expected, (R)-DOTAP/E7 samples pulsed with E7 increased to 1.2 % IFN-γ producing cells out of all $CD8^+$ cells. (S)-DOTAP/E7 treated samples increased from 0.0 % at 6 h to 0.1 % at 12 h. Even with this increase, the difference between the (R) and (S)-DOTAP/E7 groups was still significant ($P<0.02$) for the number of IFN-γ secreting $CD8^+$ cells per 10^4 $CD8^+$ T cells (**Figure 2.3d**).

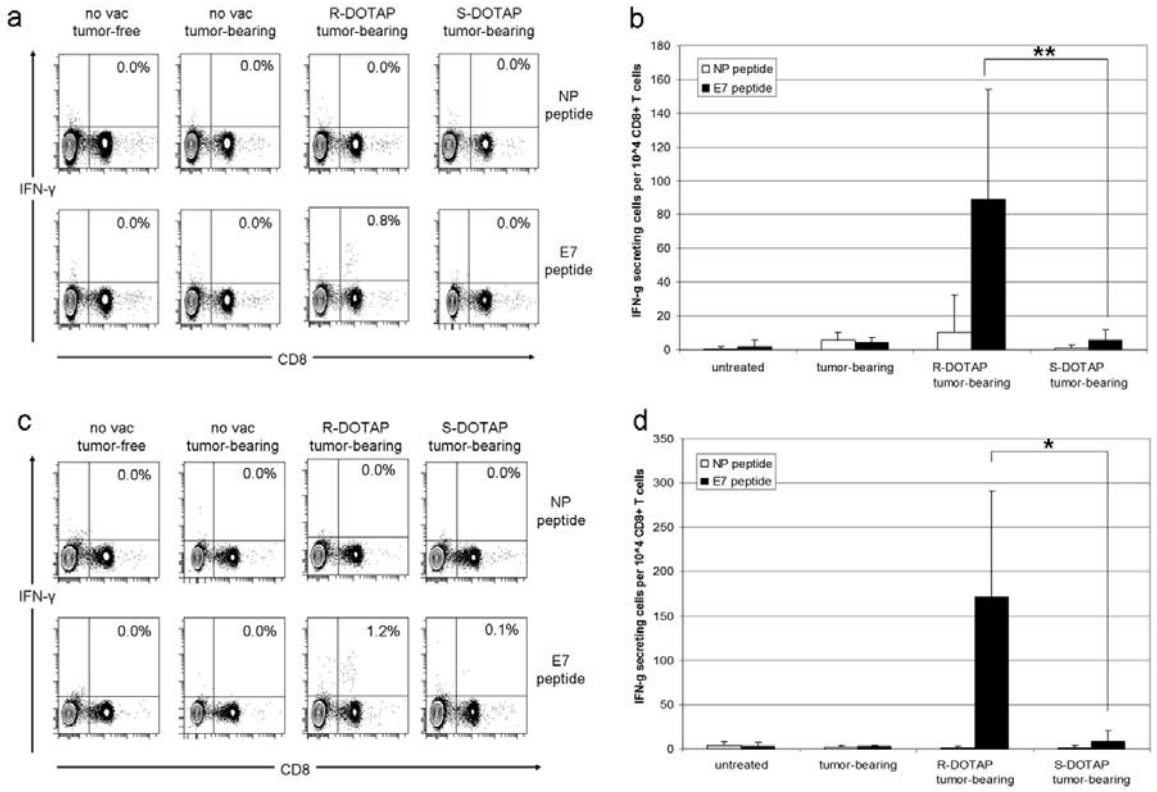

Figure 2.3 IFN-γ production from splenocytes of (R)-DOTAP/E7 or (S)-DOTAP/E7 treated mice.
(a) Splenocytes isolated (on day 14) from tumor-bearing mice treated with (R) or (S)-DOTAP/E7 at 300 nmol / 20 nmol (on day 6). Splenocytes were pulsed with E7 or an irrelevant peptide (NP) for 6 h, washed, and stained for CD8 and IFN-γ. The numbers on the contour plots indicate percentage of IFN-γ^+ $CD8^+$ T cells out of all $CD8^+$ T cells. One representative experiment is shown. (b) IFN-γ secreting $CD8^+$ cells per 10^4 $CD8^+$ T cells after 6 h pulse with peptide. n=6-8. **: $P<0.01$ (c) IFN-γ production after 12 h pulse with either NP or E7 peptide. (d) IFN-γ secreting $CD8^+$ cells per 10^4 $CD8^+$ T cells after 12 h pulse with peptide. n=6-8. *: $P<0.02$

2.3.5 *In vivo* Cytotoxic T Lymphocyte Assay

As expected, tumor-bearing mice injected with NP ($CFSE_{low}$) and E7 ($CFSE_{high}$) pulsed cells, showed no specific killing of either population (**Figure 2.4a**) with the two peaks being of equal height, and indeed containing similar numbers of cells. Shown in **Figure 2.4b**, (R)-DOTAP/E7 vaccinated mice either with or without a tumor showed similar levels of specific killing of E7 labeled targets that was statistically significant compared to tumor-bearing mice ($P<0.001$). (S)-DOTAP/E7 treated mice, even without a tumor, still were statistically different than either (R)-DOTAP/E7 treated group ($P<0.05$). Tumor bearing mice treated with (S)-DOTAP/E7 had specific killing of E7 labeled targets that was not different from tumor-bearing mice that had not been vaccinated ($P=0.20$). These results led us to conclude the tumor responds to how the formulation is affecting the immune response, thus we examined the tumor.

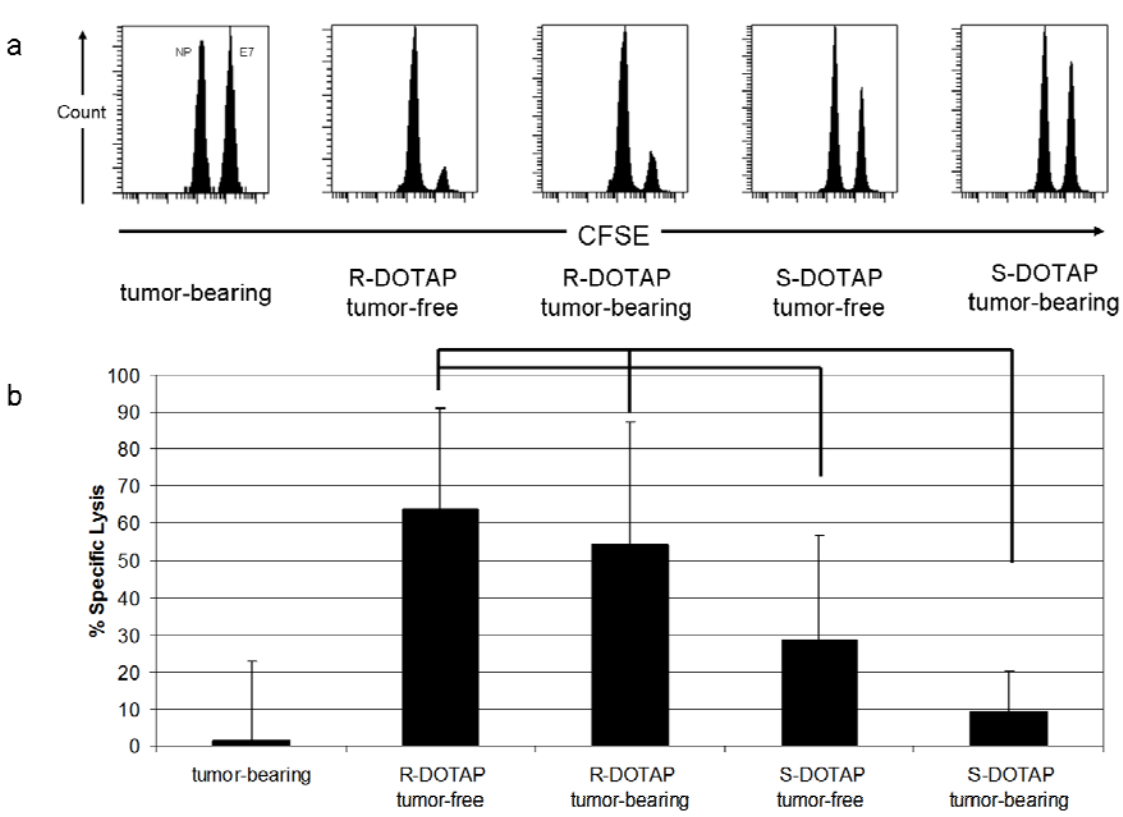

Figure 2.4 *In vivo* Cytotoxic T Lymphocyte (CTL) Assay.
(a) Targets pulsed with E7 or an irrelevant peptide (NP) were stained with high (E7) or low (NP) concentrations of CFSE, injected into treated mice and *in vivo* killing was allowed for 16-20 h, then spleens removed and analyzed by flow cytometry. (b) Percent specific lysis, $\boldsymbol{P}<0.05$ between (R)-DOTAP and (S)-DOTAP groups. No statistical difference exists between the two (R)-DOTAP treated groups, or the (S)-DOTAP tumor-bearing group and tumor-bearing untreated group. n=15-18

2.3.6 Tumor Infiltrating Lymphocytes and Their Actions

Whole tumors from mice were broken down to determine the concentration of infiltrating lymphocytes caused by each treatment (**Figure 2.5a**). Tumor-bearing mice that had not been treated with either formulation, had 0.7 % $CD4^+$ and 0.2 % $CD8^+$ cells out of all cells in the solid tumor. (R)-DOTAP/E7 treated mice had much higher levels of $CD8^+$ cells in their tumors compared to (S)-DOTAP/E7 treated mice, 0.9 % versus 0.1 %, respectively. However, the differences in levels of $CD4^+$ cells in the three groups was less dramatic, 0.5 % in (R)-DOTAP/E7 treated mice, compared to 0.2 % in (S)-DOTAP/E7 treated mice. (R)-DOTAP/E7 treated mice had greater numbers of $CD4^+$ and $CD8^+$ cells found in the tumor tissue compared to (S)-DOTAP/E7 treated mice (**Figure 2.5b**). The high levels of $CD4^+$ cells in tumor-bearing mice, similar to (R)-DOTAP/E7 treated mice, prompt further study to determine the phenotype of these cells.

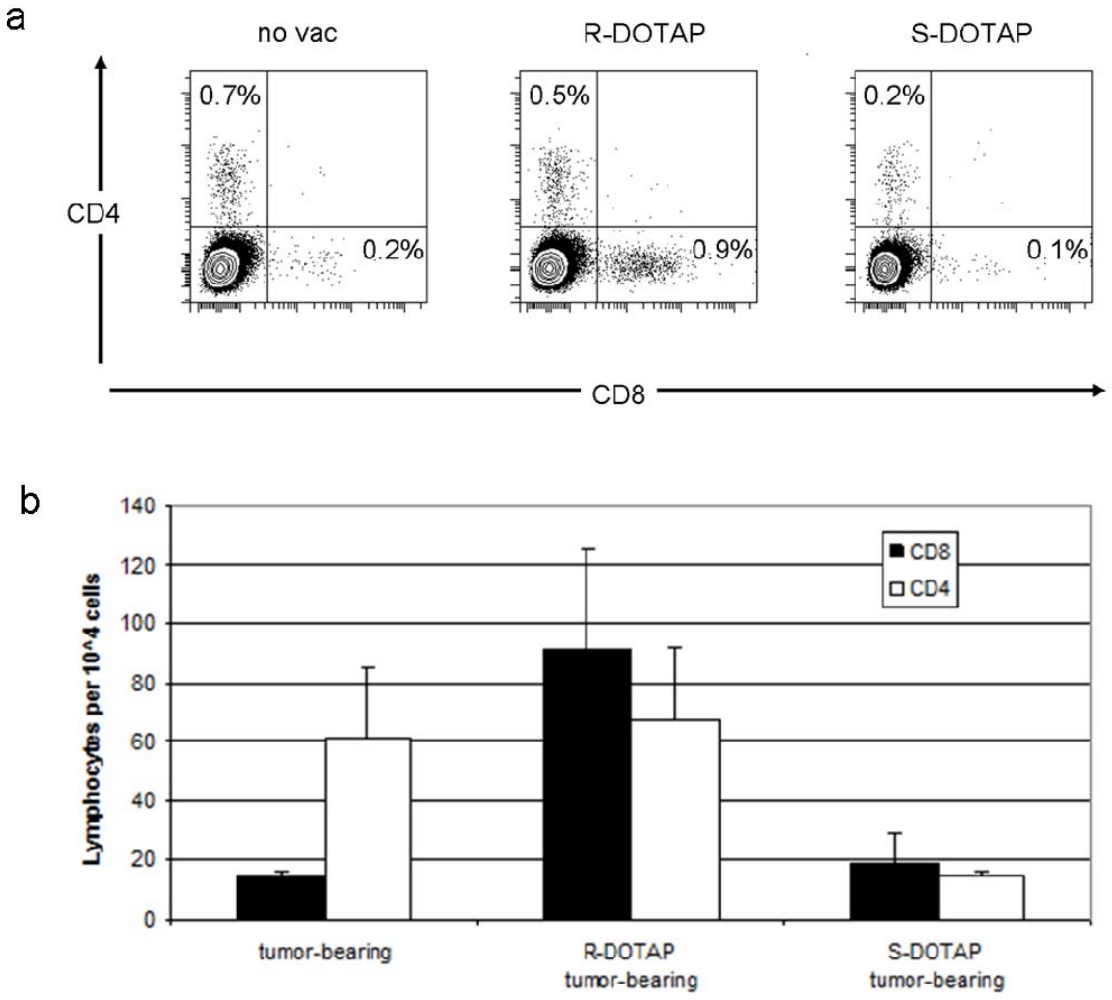

Figure 2.5 Tumor Infiltrating Lymphocytes.
Tumor infiltrating lymphocytes assayed from tumors of mice treated with (R) or (S)-DOTAP/E7 (a) $CD4^+$ and $CD8^+$ cells (b) $CD4^+$ or $CD8^+$ cells per 10,000 cells in the solid tumor. n=3-4. When comparing (R)-DOTAP to (S)-DOTAP or tumor only, $P<0.01$ for $CD8^+$ cells, however (S)-DOTAP compared to tumor alone $P=0.57$. Looking at the groups with regard to $CD4^+$ cells, all comparisons yield *P* values greater than 0.3.

Lymphocytes isolated from tumors using a density gradient protocol were stimulated with NP or E7 peptides for 6 h and assayed for IFN-γ production (**Figure 2.6a**). All samples showed some IFN-γ activity in their $CD8^+$ cells in both NP and E7 pulsed treatments. Background levels of IFN-γ production were determined to be the signal from $CD8^+$ NP pulsed cells. These levels in tumor only, (R)-DOTAP/E7 and (S)-DOTAP/E7 treated mice were 1.2 %, 10.3 % and 3.9 %, respectively. $CD8^+$ T cells from (S)-DOTAP/E7 treated mice showed some non-specific activity above control, yet not to the level of cells from (R)-DOTAP/E7 treated mice. However, 32.6 % of $CD8^+$ E7 pulsed cells produced IFN-γ when isolated from a (R)-DOTAP/E7 treated mouse. This is compared to 12.0 % in an (S)-DOTAP/E7 treated mouse, a significant difference in IFN-γ secreting $CD8^+$ T cells (**Figure 2.6b**) ($P<0.05$). With the E7 pulse, the tumor-bearing mouse had some activity above background, showing some $CD8^+$ T cells had been activated against the tumor by the process of a natural immune response. This experiment showed that although (S)-DOTAP/E7 does not have activity as great as (R)-DOTAP/E7, the treatment does have some ability to recruit E7 reactive lymphocytes to the tumor.

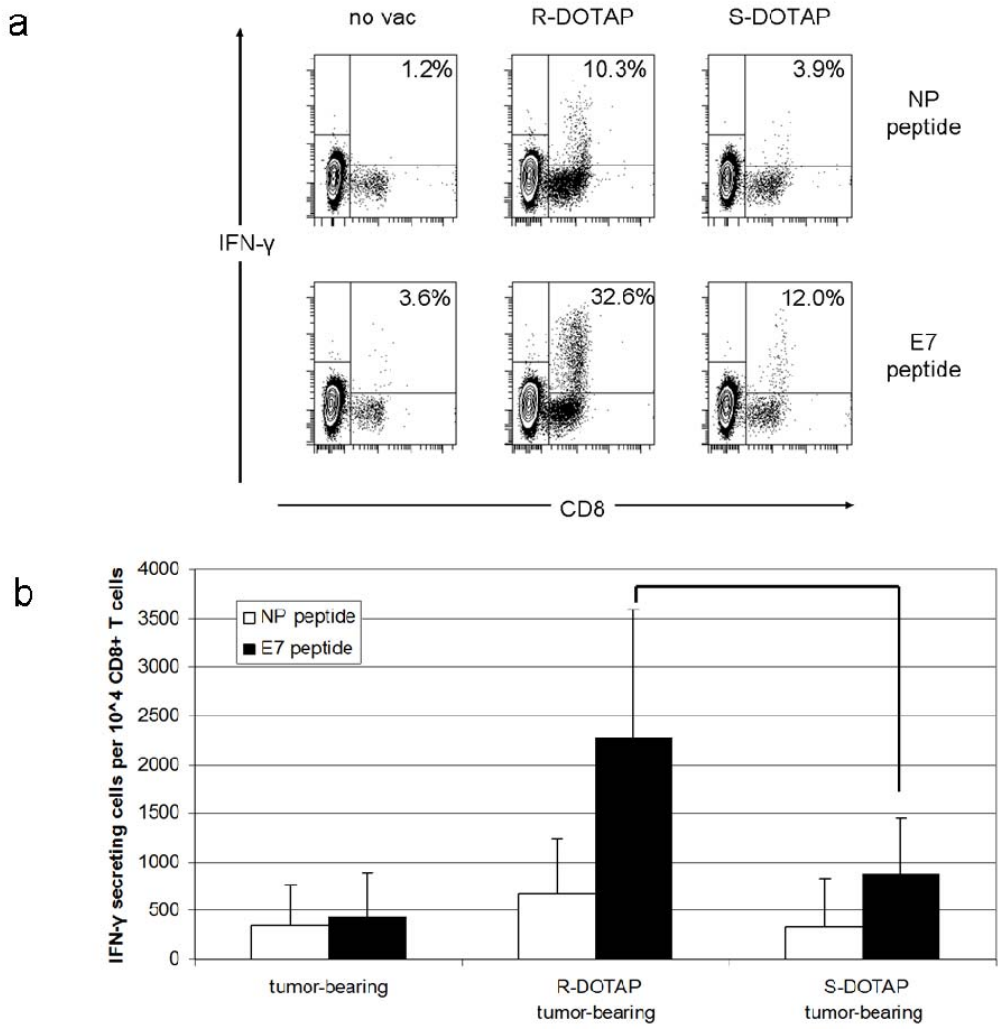

Figure 2.6 IFN-γ production by Tumor Infiltrating Lymphocytes.
TIL were isolated from tumors of mice vaccinated with (R)-DOTAP/E7 or (S)-DOTAP/E7 and pulsed for 6 h with E7 or an irrelevant peptide (NP). (a) Percentages are IFN-γ^+CD8$^+$ cells out of all CD8$^+$ cells. One dot plot is shown for each group that is representative of three experiments. (b) IFN-γ^+ producing cells per 10,000 CD8$^+$ cells, P<0.05. n=6-7

2.4 DISCUSSION

With the advancements of chiral separation technology, stereospecific drugs are not solely for academic investigation. The pharmaceutical industry has developed an interest in delivering enantiomerically pure formulations, understanding that the chirality of a drug can affect how the molecule acts in the biological milieu.

By simplifying our formulation to one enantiomer of DOTAP and the E7 peptide, we were able to further investigate the immunological action of the DOTAP lipid in formulation; both *in vitro* and *in vivo*. Our results demonstrate (R)-DOTAP is the active component in the DOTAP racemic mixture used by our group in previous vaccine studies. This is evident in dose-dependent tumor growth delay studies (**Figure 2.1**).

(R)-DOTAP and (S)-DOTAP have similar formulation characteristics of size, charge and encapsulation (**Table 2.1**). E7 peptide has two positively charged amino acids (arginine and histidine (only partial)), and a charge-charge association with cationic DOTAP is unanticipated. Previously, our group correlated increased antigen encapsulation with increased vaccine efficiency when studying an acylated version of E7 peptide, using racemic DOTAP.[235] Thus, even in the presence of (S)-DOTAP (in the racemic mixture), a high amount of E7 lipopeptide loading into the liposomes caused regression of TC-1 tumors both when delivered on 6 and 10 days after tumor inoculation. DOTAP has been hypothesized to facilitate endosomal escape through association with anionic lipids (phosphatidylserine) in the interior of the endosome causing destabilization

[236]. Thus, as APC endocytose the vaccine, E7 peptide will be released into the cytosol available to be presented by MHC Class I. As the two lipids have similar encapsulation efficiencies, shown in **Table 2.1**, no more antigen could be delivered by the (R)-DOTAP than the (S)-DOTAP formulation into the APC.

DOTAP has previously been shown to induce a tunable amount of ROS which was required for anti-tumor efficacy and correlated with activation, CCL2, and toxicity.[31] In our *in vitro* studies, (R) and (S)-DOTAP produce similar levels of activation and toxicity (**Figure 2.2a, c**) when dosed to BMDC, therefore we do not expect that ROS induction is the mechanism with which (R) and (S)-DOTAP differ. While ROS levels induced could be the same, the difference in antigen loading does not clearly explain the stark differences in cytokine levels produced by the splenocytes and TIL in an (R)-DOTAP/E7 vaccinated mouse (**Figure 2.3. Figure 2.6**).

We hypothesize the presence of the tumor during vaccine administration amplifies the difference between (R) and (S)-DOTAP, while the amplification mechanism is not known (**Figure 2.7**). *In vitro,* the enantiomeric lipids behave similarly to one another in regards to BMDC activation, cytokine production and toxicity (**Figure 2.2**). However, the difference between the two molecules in eliciting *in vivo* CTL response (**Figure 2.4**) is most profound and statistically significant when a tumor is present. Strong differences can be seen in splenocyte production of IFN-γ in tumor-bearing vaccinated mice, (**Figure 2.3**), and most obviously, in the tumor growth delay data (**Figure 2.1**). The large numbers of TIL that are immunologically active (**Figure 2.6**) support the tumor growth delay data and our hypothesis. The phenotype of the $CD4^+$ cells in the tumors of (R)-DOTAP/E7

treated mice should be investigated as their function could indicate the exact contribution of the tumor.

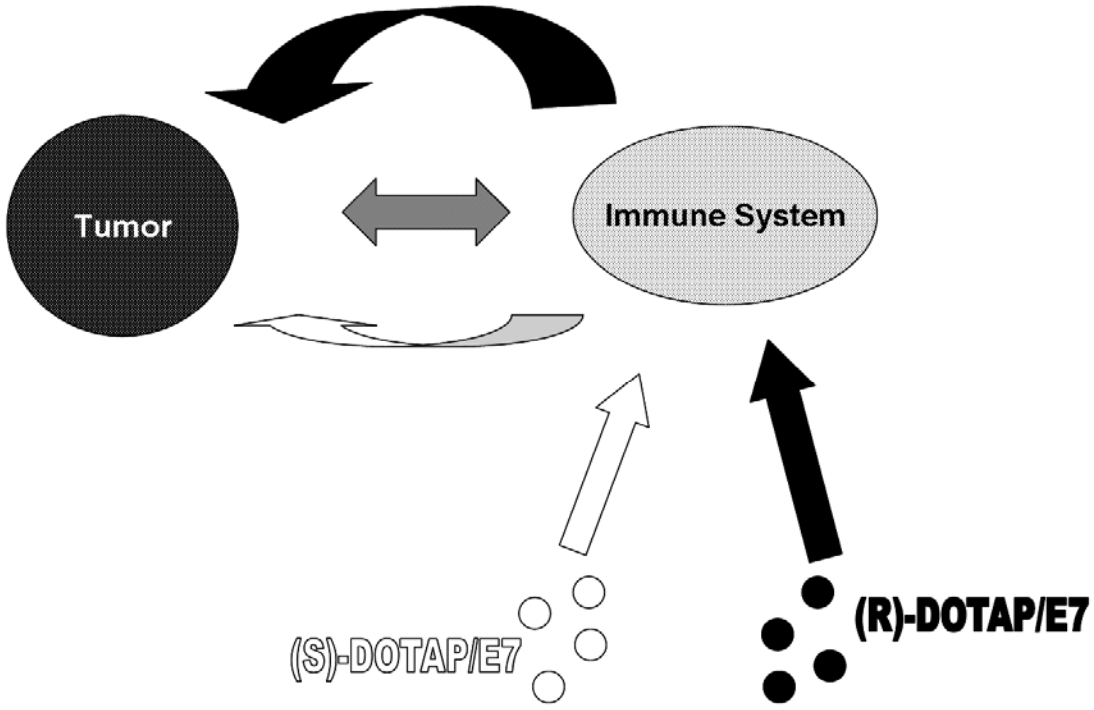

Figure 2.7 Proposed tumor interaction with DOTAP enantiomers.
In vitro (R) and (S)-DOTAP show little difference in stimulating BMDC, shown by the size of the straight arrows. Due to an unknown interaction between the immune system and the tumor, the presence of a tumor in the *in vivo* system amplified the difference between (R) and (S)-DOTAP reflected by the size of the ribbon arrows. The distinction between the two formulations is further amplified via talk back from the tumor to the immune system.

There are three requirements for a peptide vaccine to be effective: an antigen specific for the target (tumor), an efficacious adjuvant that can magnify the second signals needed for dendritic cells to produce a strong T cell response, and a delivery mechanism. (R)-DOTAP/E7 complexes provide all three to cause regression in this cervical cancer model. Future studies will expand the application of this adjuvant to other tumor models and investigate the mechanism of action that lies behind the enantiospecific activity.

CHAPTER 3

TRP2 PEPTIDE VACCINE ADJUVANTED WITH (R)-DOTAP INHIBITS TUMOR GROWTH IN AN ADVANCED MELANOMA MODEL

Previously we have shown cationic lipid (R)-DOTAP as the immunologically active enantiomer of the DOTAP racemic mixture, initiating complete tumor regression in an exogenous antigen model (murine cervical cancer model). Here, we investigate the use of (R)-DOTAP as an efficacious adjuvant delivering an *endogenous* antigen in an aggressive murine solid tumor melanoma model. (R)-DOTAP/Trp2 peptide complexes showed decreasing size and charge with increasing peptide concentration, taking a rod-shape at highest concentrations. The particles were stable for at 2 weeks at 4°C. A dose of 75nmol Trp2 (formulated in (R)-DOTAP) was able to show statistically significant tumor growth delay compared to lower doses of 5 and 25nmol which were no different than untreated tumors. (R)-DOTAP/Trp2 (75nmol) treated mice also showed increased T cell IFN-γ secretion after restimulation with Trp2, as well as CTL activity *in vivo.* This vaccination group also showed the highest population of functionally active tumor-infiltrating lymphocytes, indicated by IFN-γ secretion after restimulation with Trp2. Thus, (R)-DOTAP has shown the ability to break tolerance as an adjuvant. Its activity to enhance immunogenicity of other tumor associated antigens should be studied further.

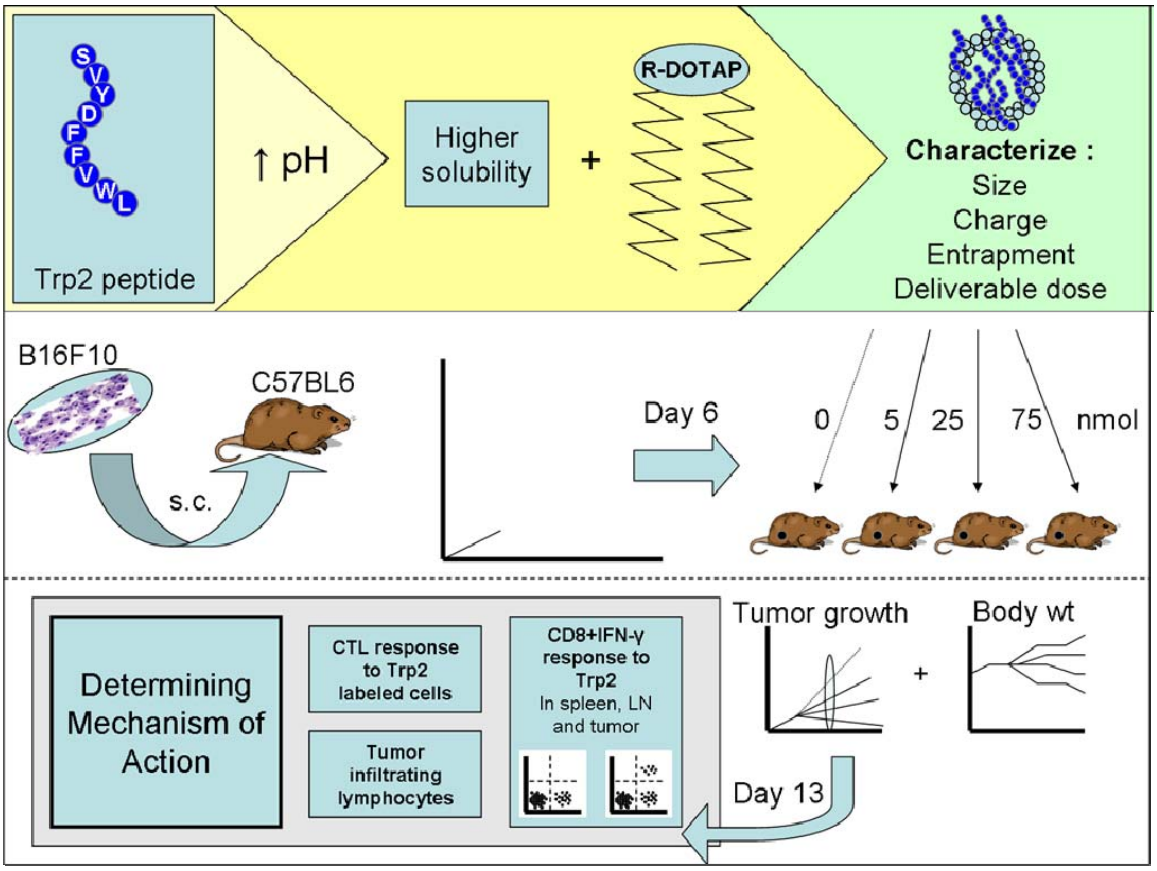

Figure 3.1 Abstract summary

3.1 INTRODUCTION

Recent clinical advances for the treatment of melanoma have great potential to revolutionalize the field, however not without associated toxicity. The recent FDA approval of the anti-CTLA4 antibody ipilimumab for unresectable and metastatic melanoma shows a step forward for biological drugs and immunotherapy for melanoma However, the approval also came with a boxed warning for immue-related adverse events (irAE) which can range from mild to severe.[237] Interestingly, the severity of irAE seemed to correlate with a positive response to therapy.[238]

Intensive research on the genetics of melanoma have led to advances in small molecule inhibitors as well.[239] Several companies are investigating drugs for melanomas with oncogene mutations, most notably, BRAF V600E which occurs in almost 50 % of melanoma cases.[240] The recent approval of vemurafenib showed up to an 81 % response rates in trials.[241] Other small molecule BRAF inhibitors are still in the clinical trials and include RAF-265, XL281, and GSK2118436. However, even with promising BRAF inhibitors selective for patients with the V600E mutation, side effects are seen, such as resectable cutaenous carcinoma, and more importantly, induction of resistance.[242; 237; 241] With side effects produced by the new frontier of both biological and small molecule drugs for melanoma, there is still space to innovate a treatment that is able to treat aggressive tumors with fewer off-target effects.

As a treatment option, peptide vaccines offer the safety and specificity of a restricted epitope. Specific antigen in the form of peptide sequences (8-10 amino acids long) can be delivered to antigen presenting cells (APCs). Restricting the sequence choice to bind to major histocompatibility complex (MHC) class I ensures $CD8^+$ T cell engagement. Activation of APCs and presentation of the peptide can stimulate a corresponding cytotoxic T lymphocyte (CTL) response against the epitope. As an antigen, peptides are easy to manufacture and specific, however, they are rarely immunostimulatory alone. Dendritic cells pulsed with melanoma tumor-specific peptide were unable to stimulate a therapeutic response when injected on the same day as the tumor.[243] Delivery of a peptide antigen with an adjuvant is required for potent activation of APCs, and associated CTL activity.

In the case of melanoma, sensitizing CTLs against the corresponding endogenous, or self-antigen poses yet another challenge. As T cells develop in the thymus, self-reactive T cells are deleted, and regulatory T cells develop in circulation and particularly in the presence of tumors. Some have taken the approach to genetically modify T cell receptors to be specific for tumors, instead of efforts to vaccinate and allow a response to develop in an aided fashion.[244] A strong adjuvant would be required to break through this tolerance and stimulate a powerful anti-tumor response.

While many melanoma peptide antigens are well characterized, tyrosinase-related protein 2 (Trp2) is particularly attractive as an antigen. Trp2 peptide (amino acids 180-188 of the Trp2 protein, sequence: SVYDFFVWL) is MHC class I H-$2K^b$ restricted in mouse, allowing for examination of a $CD8^+$ CTL response. The sequence is also HLA-A2 restricted, thus the potential exists for the same formulation to be tested both in mouse

and in humans. Additionally, since melanoma and glioma cells are both neuroectodermal in origin, Trp2 is also expressed in this additional cancer line, allowing for a natural secondary application of any developed formulation.[245; 243] However, as delivery cargo, Trp2 peptide is hydrophobic and difficult to formulate in an aqueous solution or delivery vehicle. The most successful work with Trp2 peptide as an antigen has been with preventative models.[246; 247; 248; 249] Few studies examine the treatment of established tumors, and none to date have shown any effect in aggressive solid tumor models.[250; 251; 252]

Previously, our group has studied DOTAP lipid as an adjuvant in peptide and protein vaccine formulations. A DOTAP/peptide vaccine has shown complete tumor regression in an exogenous antigen model.[30; 253] Further investigation of the DOTAP lipid, showed chiral specificity of the adjuvant activity.[253] These studies led us to discover (R)-DOTAP as the active immune-stimulating enantiomer. (R)-DOTAP (or even the DOTAP racemic mixture) has never been tested as an adjuvant in an endogenous tumor model, and indeed the challenges of breaking tolerance are not slight. Particularly, treating an established tumor model in melanoma is rarely tested due to the difficulty of generating an adequate immune response to cause tumor growth delay due to the suppressive effects of an established tumor. In work presented in Section 3, we address the formulation challenges of delivering an adequate dose of the innately hydrophobic Trp2 peptide and utilize (R)-DOTAP/Trp2 complexes in an advanced melanoma model to break tolerance and show statistically significant tumor growth delay.

3.2 MATERIALS AND METHODS

3.2.1 Materials

(R)-DOTAP, (R)-1,2-dioleoyl-3-trimethylammonium-propane, was obtained from Merck KGaA (Darmstadt, Germany). H-2K^b restricted peptides Trp2 (H-SVYDFFVWL-OH, amino acids 180-188 from the tyrosinase-related protein 2 over-expressed in human and murine melanoma, MW 1175) and Ova (H-SIINFEKL-OH, amino acids 257-264 from the ovalbumin, MW 1773) were obtained from Peptide 2.0 (Chantilly, VA), supplied as trifluoracetate salts. Molecular biology grade water was obtained from Cellgro (Manassas, VA). Sodium methoxide, pure titrant (0.5M in methanol) and HPLC grade methanol were obtained from Fisher Scientific (Pittsburgh, PA). Absolute ethanol was obtained from Decon Labs, Inc. (King of Prussia, PA).

3.2.2 Trp2 peptide preparation

Specific weights of Trp2 peptide were dissolved in a 1:1 solution of methanol:ethanol. Serial dilution of Trp2 peptide was measured on a Shimadzu UV-Vis spectrophotometer (model UV-2501 PC, Columbia, MD), and absorbance recorded. The measurements were made in triplicate, and standard curve created utilizing the Beer-Lambert law. The extinction coefficient, $\varepsilon = 5{,}367.7$ ($M^{-1}cm^{-1}$), was found with the measured absorbance at 280nm wavelength to estimate Trp2 peptide concentration and encapsulation.

Trp2 peptide was formulated as a disodium salt for delivery. Peptide arrived as a trifluoroacetate salt and was dissolved in HPLC grade methanol in a glass vial and a

magnetic stir bar added. The peptide was stirred in an ice bath, as two equivalents of sodium methoxide were added drop wise. Titrated peptide was allowed to stir for 10min as the solution became clear. Aliquots of the peptide solution were added to water and pH measured (pH 9). Methanol was dried off using a rotoevaporator, and peptide was resuspended as a 1.5mM working concentration in molecular biology grade water.

3.2.3 Preparation and Evaluation of Vaccine Formulations

Briefly, 6,000 nmol of (R)-DOTAP dissolved in chloroform was dried in a glass vial under a stream of nitrogen and stored under vacuum in a desiccator overnight to ensure removal of any remaining chloroform. Lipid/peptide complexes were formed by thin film hydration, using a 1mL solution of Trp2 peptide at different concentrations in molecular grade water (Cellgro, Manassas, VA) and subsequent vortexing. After 1 h at room temperature, the suspensions were extruded ten times through two 100 nm polycarbonate membranes (Fisher Healthcare, Houston, TX).

Particle size and zeta potential were measured with a Malvern Zetasizer Nano ZS (Worcestershire, United Kingdom). Samples were prepared for size and charge characterization by adding 10 μL 6 mM (R)-DOTAP/(1.5 to 0 mM) Trp2 complexes to 990 μL of molecular biology grade water. Trp2 peptide encapsulation efficiency was measured by adding 50 μL of extruded lipid/peptide complexes to a Microcon 100kDa molecular weight cut off centrifugal filtrate device (Millipore, Bedford, MA). The column was centrifuged at 10,000 g for 10 min at 25 °C. Flow-through was analyzed using 2 μL of sample on a Nanodrop Spectrophotometer, ND-1000 (Thermo Scientific, Wilmington, DE), measuring the absorbance at 280 nm wavelength. Concentration of

peptide in flow-through (unencapsulated) was calculated using Beer-Lambert law (A_{280} = ε*b*c), with ε = 5,367.7 ($M^{-1}cm^{-1}$), calculated from a standard curve of Trp2 peptide. Final encapsulated concentration was calculated by subtracting the concentration in flow-through from the known concentration used for hydration. Trp2 peptide loss in the column was < 5 %.

Transmission electron microscope (TEM) images of the (R)-DOTAP/Trp2 complexes were acquired by the use of a JEOL 100CX II TEM (Tokyo, Japan). Briefly, 4 µl of nanoparticle solution was dropped on to a 300 mesh carbon coated copper grid (Ted Pella, Inc., Redding, CA) for 2 min. Excess fluid was removed with filter paper, and copper grid was dried before the observation with TEM. A total of 210 particles from 3 different fields were measured. Particle dimensions were calculated by measuring the longest dimension and the perpendicular diameter.

3.2.4 Tumor cell culture

B16F10 cells, a murine melanoma model (syngeneic with C57BL/6) were originally obtained from American Type Culture Collection (ATCC) (Manassas, VA). Previously, in collaboration with Dr. Pilar Blancafort at the University of North Carolina at Chapel Hill (UNC), B16F10 was stably transfected with GL3 firefly luciferase gene using a retroviral vector to create B16F10-luc.[254; 255] B16F10-luc cells were used in all studies presented here and maintained in Dulbecco's Modified Eagle Medium (Gibco (Invitrogen), Carlsbad, CA) supplemented with 10 % fetal bovine serum (FBS) (Invitrogen, Carlsbad, CA), 100 U/mL penicillin (Invitrogen) and 100 µg/mL streptomycin (Invitrogen).

3.2.5 Mice and Immunizations

Six week old female C57BL/6 mice obtained from the National Cancer Institute, were used in all studies. On day 0, $3x10^5$ B16F10-luc cells in 50 μL of PBS were injected subcutaneously into the hair-trimmed abdomen. On day 6, formulations were subcutaneously injected into the contralateral side of the abdomen in 100 μL of 5 % dextrose solution. In all experiments, 300nmol (R)-DOTAP per mouse was the therapeutic dose of adjuvant used, as shown by our lab previously.[253] Tumors were measured every 2-3 days with calipers, recording the longest diameter as length and the perpendicular dimension as width. Area was calculated as (length) x (width). Humane sacrifice of mice was performed after tumors reached 20 mm in one dimension. All animal protocols were approved by the University of North Carolina at Chapel Hill's Institutional Animal Care and Use Committee.

3.2.6 Multi-organ interferon gamma (IFN-γ) production by $CD8^+$ T cells

Mice were inoculated with $3x10^5$ B16F10-luc cells on day 0. On day 6, mice were vaccinated with varying doses of (R)-DOTAP/Trp2 (with R-DOTAP at a constant dose of 300 nmol/mouse). On day 13, mice were sacrificed and spleen, vaccine draining lymph node (right inguinal) and tumor draining lymph node (left inguinal) were removed from each mouse in a sterile hood. Organs were processed into a single cell suspension by crushing through a 70 μm filter (BD Biosciences, San Jose, CA). After removal, cells were incubated in Roswell Park Memorial Institute (RPMI) 1640 media supplemented

with FBS, non-essential amino acids (NEAA) (Cellgro), antibiotic/antimycotic (Cellgro), 1 μL/mL GolgiStop™ (BD Biosciences) and 5 μM Trp2 or Ova peptide for 6 h at 37 °C. Cells were removed, washed with staining buffer (BD Pharmingen, San Diego, CA) and stained with anti-CD8 (clone 53-6.7). Cells were then treated with Cytofix/Cytoperm™ according to kit instructions (BD Pharmingen) and stained intracellularly with anti-IFN-γ (clone XMG1.2), washed and analyzed with a FACS Canto flow cytometer (BD Biosciences) and analyzed with FACS Diva software (BD Biosciences).

3.2.7 *In vivo* Cytotoxic T Lymphocyte (CTL) Assay

The *in vivo* CTL assay has been described previously and was performed here with slight modifications.[234; 253] Briefly, mice were inoculated with $3x10^5$ B16F10-luc cells on day 0 and vaccinated with (R)-DOTAP/Trp2 formulations on day 6. Seven days later, naïve mice were sacrificed and splenocytes removed. Splenocytes were pulsed with either 10 μM Trp2 or Ova peptide for 1-2 h in complete media at 37 °C. Cells were stained with carboxyfluorescein succinimidyl ester (CFSE) (Sigma-Aldrich, St. Louis, MO), with Ova peptide-pulsed and Trp2 peptide-pulsed cells stained with 0.4 and 4μM, respectively in serum free RMPI 1640 media for 15 min. Cells were then washed with complete media (RMPI 1640 with FBS, NEAA and antibiotic/antimycotic) and counted. Equal numbers of $CFSE^{high}$ (Trp2-pulsed cells) and $CFSE^{low}$ (Ova-pulsed cells) were mixed together and stained with 8 μM PKH-26 (Sigma-Aldrich) according to manufacturer's instructions. Vaccinated mice were injected with 10^7 labeled cells and *in vivo* killing of the targets was allowed to take place for 22 h. After that time, spleens from treated mice were removed and processed into a single cell suspension and red blood cells lysed with ACK lysing

buffer (Invitrogen). Cells were washed in complete media and resuspended in phosphate buffered saline (Sigma-Aldrich). The cells were analyzed with a FACS Canto flow cytometer (BD Biosciences) and FACS Diva software (BD Biosciences), first gating for the lymphocyte population, then for the PKH-26 positive cells, to determine the amount of specific lysis of the $CFSE^{high}$ Trp2-pulsed cells. The following equation from Byers et al., describes *Ova* and *Trp2* representing the number of peptide-pulsed cells present after the *in vivo* killing time allotment.[234]

$$\%\ \text{specific lysis} = \frac{(Ova * x - Trp2)}{(Ova * x)} * 100\%$$

$$\text{where } x = \frac{Trp2}{Ova} \text{ from naïve mice}$$

3.2.8 Tumor Infiltrating Lymphocyte Analysis

B16F10-luc tumors from mice vaccinated on day 6 were removed on day 13 in a sterile environment. Tumors were minced and processed through a 70 μm strainer to form a single cell suspension. Cells were blocked with Fc block (anti CD16/CD32 (clone 2.4G2)) for 15 min, then stained with anti-CD3 (clone 145-2C11), anti-CD8 (clone 53-6.7) and anti-CD4 (clone RM4-5) and analyzed by flow cytometry.

3.2.9 Functionality of Tumor Infiltrating Lymphocytes

Alternately, lymphocytes were isolated from the tumors. Tumors were prepared as a single cell suspension (described above). The cells were washed and resuspended in complete media. Tumor infiltrating lymphocytes (TIL) were separated from the tumor

using Ficoll-Paque^{TM} PLUS (GE Healthcare, Uppsala, Sweden), a density gradient method. Briefly, the single cell suspension of tumor cells were resuspended in 8mL of complete media (RPMI 1640 with 10 % FBS, NEAA and antibiotic/antimycotic). This volume was layered over 4 mL of Ficoll-Paque^{TM} PLUS in a 15 mL conical centrifuge tube and centrifuged at 2,500 rpm for 30 min at 25 °C. After centrifugation, the cells at the density interface were removed, and washed with complete media. To assay for $CD8^+$ cell activity, tumor infiltrating lymphocytes were plated at a concentration of $2x10^6$ cells/mL and stimulated with 5 μM Trp2 or Ova peptide for 6 h at 37 °C. The TIL were incubated with Fc Block, anti-CD8, stained intracellularly for IFN-γ and analyzed by flow cytometry as described above.

3.2.10 Statistical Analysis

Statistical analysis was completed by using a two-tailed Student's t-test. Data was qualified as statistically significant if the *P* value was less than 0.05.

3.3 RESULTS

3.3.1 Formulation Characterization

Maximum solubility of Trp2 peptide in water was measured at 1.825 mM after conversion to a disodium salt, compared to 0.06 mM of the trifluoracetate salt in water, an increase of 30.4 fold.

Our method of preparing (R)-DOTAP/Trp2 complexes by thin film hydration and extrusion formed stable nano-sized complexes. We observed decreasing size with increasing concentration of Trp2 incorporated, ranging from 120 to 87 nm, for 0 to 1.5 mM Trp2 used for hydration, respectively (**Figure 3.2A**). All particles had a polydispersity index measurement less than 0.1 (data not shown). Likewise, we observed a decrease in zeta potential with increasing Trp2 dose incorporated, as the Trp2 peptide formulated as a disodium salt, contains two exposed negative charges (on the aspartic acid and C terminus) after conversion from a trifluoroacetate salt (pH 4) to a disodium salt (pH 9). Percent entrapment was consistently high over a range of Trp2 doses (**Figure 3.2B**). Stability of the complexes was measured over two weeks at 4 °C, showing consistent size (no aggregation or flocculation) (**Figure 3.2C**). TEM images of (R)-DOTAP/Trp2 (75nmol) show rod-like particles with an average length and width of 78.8 ± 29.8 and 32.9 ± 6.8 nm, respectively (**Figure 3.2D**).

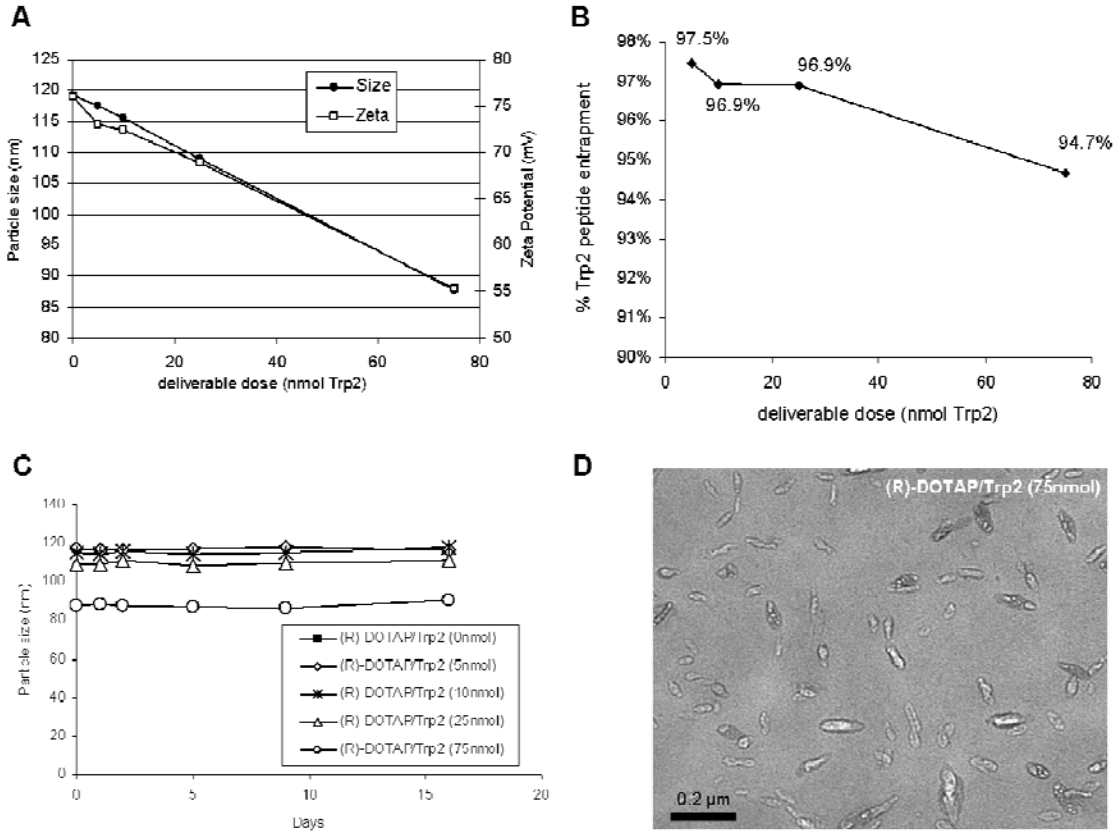

Figure 3.2 R-DOTAP/Trp2 characterization and stability.
(A) Size, charge and (B) entrapment of Trp2 was evaluated on (R)-DOTAP/Trp2 complexes with varying concentrations of Trp2, n=3. (R)-DOTAP/Trp2 nanoparticles were stored at 4°C and (C) size measured over a period of two weeks, n=3. Experiment was repeated twice. In (C), the size measured from 0nmol Trp2 was the same as that with 5nmol Trp2, overlaying completely at every time point. (D) TEM image of (R)-DOTAP/Trp2 (75nmol) complexes. A total of 210 particles from 3 different fields were measured. Particle dimensions were calculated by measuring the longest dimension and the perpendicular diameter.\

3.3.2 Tumor Growth Delay by Therapeutic Vaccination

Mice were inoculated with tumors on day 0, treated with (R)-DOTAP/Trp2 vaccines on day 6 with varying concentrations of Trp2 peptide, and tumor growth was followed for 20 days (**Figure 3.3**). While (R)-DOTAP/Trp2 nanoparticles delivering 5nmol and 25 nmol Trp2 had no effect on tumor growth delay, delivery of 75 nmol Trp2 adjuvanted by (R)-DOTAP was able to show statistically significant tumor growth delay, with $P<0.005$ compared to control mice. Shown in the **Figure 3.3** inset, body weight of these tumor-bearing mice was also monitored, and while no statistical difference exists, there was observable weight gain (due to tumor size) in control, (R)-DOTAP/Trp2 (5nmol), and (R)-DOTAP/Trp2 (25nmol) groups, that was not seen in the (R)-DOTAP/Trp2 (75nmol) group.

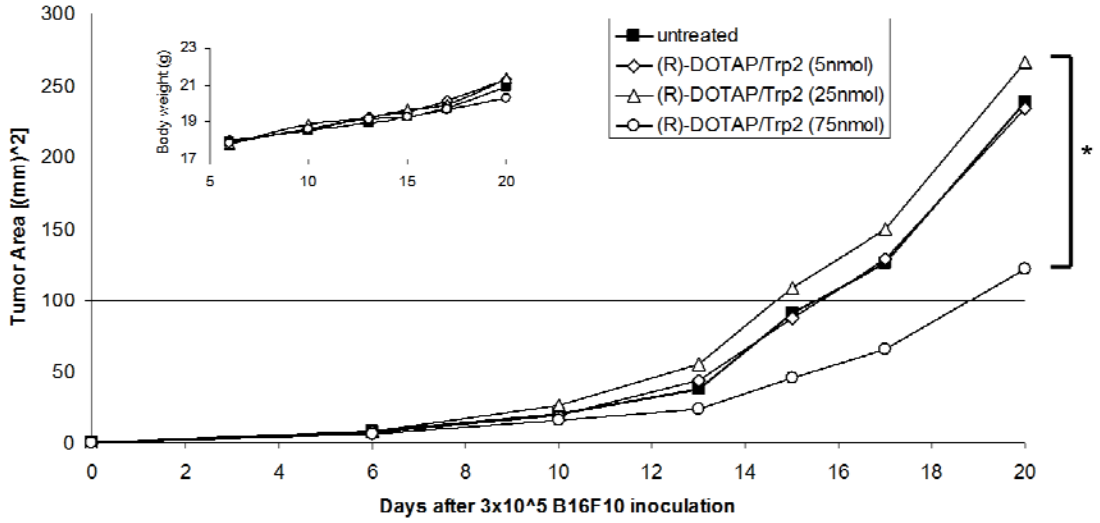

Figure 3.3 B16F10-luc tumor growth inhibition by (R)-DOTAP/Trp2 complexes *in vivo*.
Six week old female C57BL/6 mice were inoculated with $3x10^5$ B16F10-luc cells s.c. in the abdomen on day 0. On day 6, treatments were s.c. injected into the opposite side of the abdomen. Lipid formulations delivered contained 300nmol (R)-DOTAP and varying doses of Trp2 peptide. Tumors were measured with calipers with area calculated as length times width. The inset represents body weight tracked over time. Seven mice were used per group. Experiment was repeated twice. *: $P<0.005$.

3.3.3 Multi-Organ IFN-γ Production by $CD8^+$ T cells from Vaccinated Mice

Seven days after vaccination with various (R)-DOTAP/Trp2 nanoparticles, mice were sacrificed and lymph organs of interest extracted and processed to single cell suspensions to analyze Trp2 responsiveness in $CD8^+$ populations. Cells from the spleen, tumor-draining lymph node and vaccine draining lymph node (inguinal for both) were treated with Trp2 or a non-specific peptide (Ova), as well as GolgiStop™ to prevent protein secretion for 6h and then stained for $CD8^+$ cells as well as intracellular IFN-γ accumulation (**Figure 3.4**). There was no background from Ova-pulsed cells secreting IFN-γ for any group in any organ. Naïve mice, tumor-bearing mice, 75 nmol Trp2 peptide alone, and the lowest dose of (R)-DOTAP/Trp2 (5 nmol) showed no response to Trp2 pulse in any lymph organ.

Of the organs examined, splenocytes showed the highest population of responding cells, with mice receiving the (R)-DOTAP/Trp2 (75 nmol) vaccination producing the greatest response at 0.3 % of $CD8^+$ cells (**Figure 3.4A**). (R)-DOTAP/Trp2 (25 nmol) also showed some response in $CD8^+$ splenocytes, but at a much lower level (0.1 %). Vaccine-draining lymph node samples, showed an increased response in 75 and 25 nmol Trp2 deliverable dose (0.1 %) (**Figure 3.4B**). Tumor-draining lymph nodes also showed the same response for 75 and 25 nmol Trp2 deliverable dose (0.1 %), which possibly indicates the contribution of the tumor close to the skin's surface, dampening the strong response of the 75 nmol formulation to the 25 nmol level at those locations (**Figure 3.4B, C**).

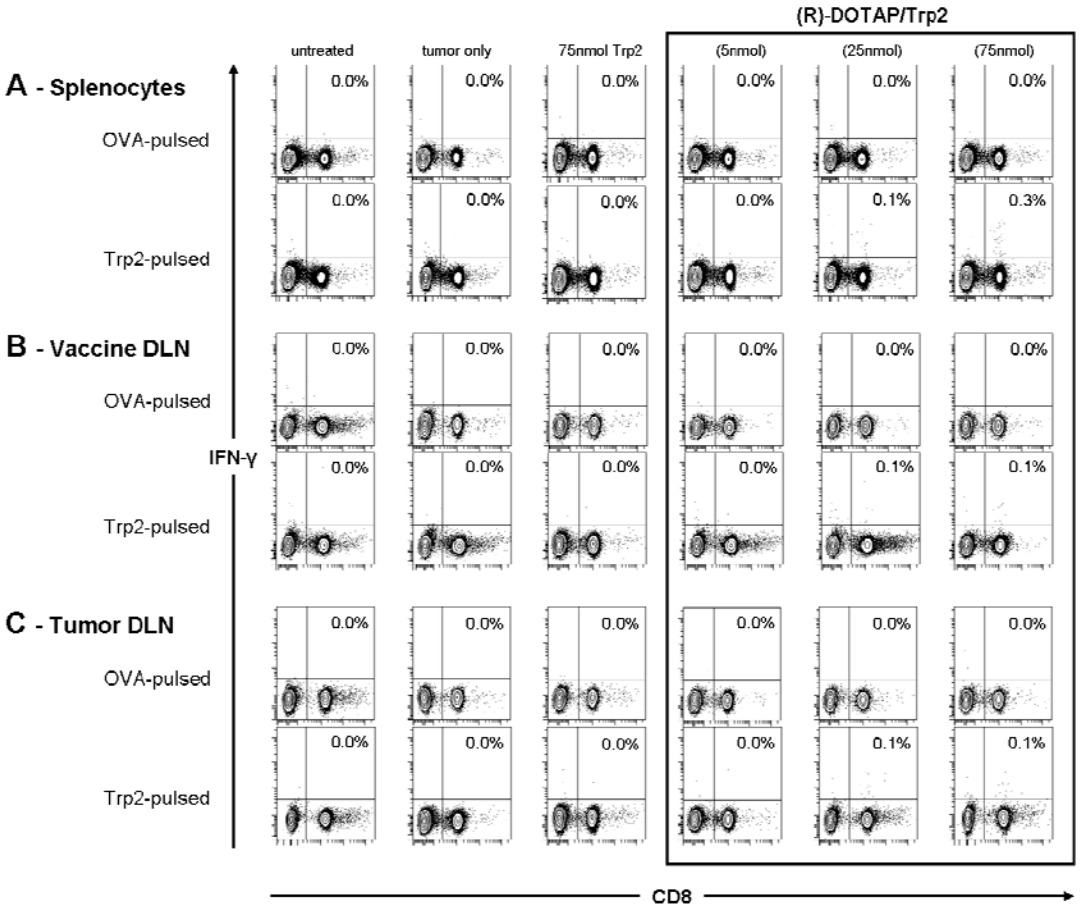

Figure 3.4 Multi-organ IFN-γ production from (R)-DOTAP/Trp2 vaccinated mice.
(A) Splenocytes, (B) vaccine draining lymph nodes, or (C) tumor draining lymph nodes were isolated (on day 13) from tumor-bearing mice treated with (R)-DOTAP/Trp2 (300nmol (R)-DOTAP/ varying Trp2 doses) (on day 6). Resulting cells were pulsed with Trp2 or an irrelevant peptide (Ova) for 6h, washed, and stained for CD8 and IFN-γ. The numbers on the contour plots indicate percentage of IFN-γ^+CD8$^+$ T cells out of all CD8$^+$ T cells. Data from one representative mouse is shown, with five to seven total animals per group. Experiment was repeated twice.

3.3.4 *In vivo* Cytotoxic T Lymphocyte Assay

Seven days after vaccination, tumor-bearing mice were injected with Trp2- and Ova-pulsed targets labeled with different levels of CFSE for 22 h before sacrificing the mice and removing the remaining cells (by processing the spleen). The purpose of this assay is to evaluate if a vaccinated mouse can show specific lysis of targets presenting the antigen from vaccination (Trp2 peptide). Unvaccinated tumor-bearing mice showed similar amounts of specific lysis as 75 nmol Trp2 peptide alone, and (R)-DOTAP/Trp2 (5 nmol) and (25 nmol) doses (**Figure 3.5**). Seventy five nmol of peptide alone (without (R)-DOTAP), also showed negligible amounts of specific lysis. However, (R)-DOTAP/Trp2 (75 nmol), showed significant specific lysis after 22 h of *in vivo* incubation of Trp2- and Ova-pulsed targets. This indicates that not only the dose of Trp2, but also the inclusion of (R)-DOTAP is crucial to elicit a CTL response.

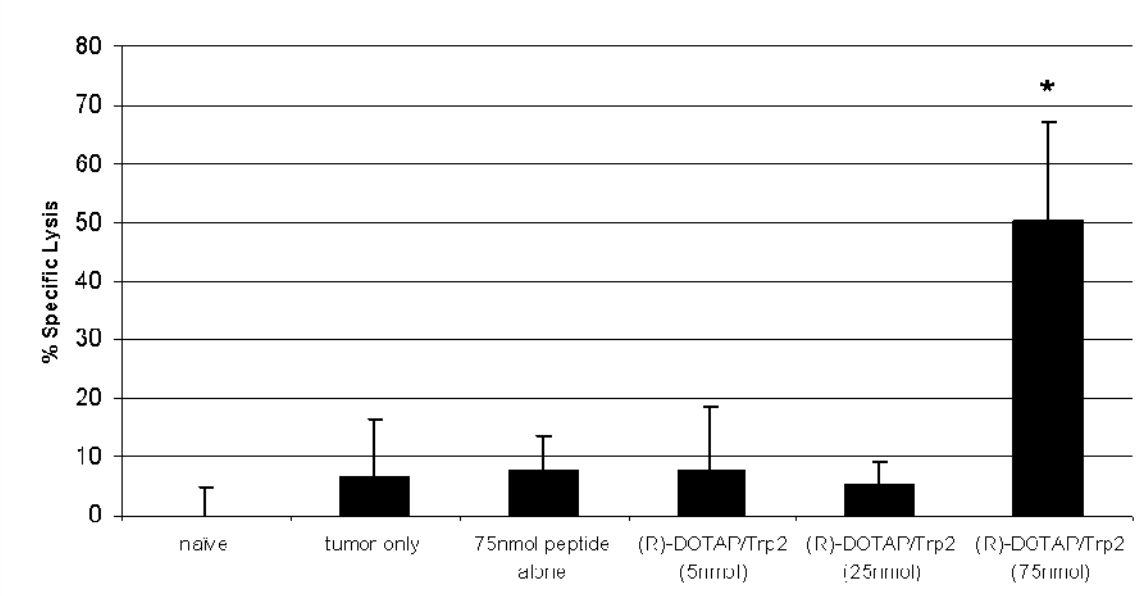

Figure 3.5 In vivo CTL shows specific lysis of Trp2-pulsed targets elicited by (R)-DOTAP/Trp2 (75nmol) vaccination.
Targets pulsed with Trp2 or an irrelevant peptide (Ova) were stained with high (Trp2) or low (Ova) concentrations of CFSE, injected into (R)-DOTAP/Trp2 vaccinated mice and *in vivo* killing was allowed for 22h, then spleens removed and analyzed by flow cytometry. Percent specific lysis, $P<0.05$ between (R)-DOTAP/Trp2 (75nmol) and other groups. Three to five mice were used per group. Experiment was repeated twice.

3.3.5 Tumor infiltrating lymphocytes

Seven days after vaccination, tumors were removed, minced and prepared as a single cell suspension to detect the infiltrating $CD3^+CD4^+$ and $CD3^+CD8^+$ lymphocytes (**Figure 3.6**). Twenty-five nmol and 75 nmol Trp2 formulated in (R)-DOTAP were able to elicit recruitment of both $CD4^+$ and $CD8^+$ T cells into the solid tumor (**Figure 3.6**). Nearly 1 % of the cells in the tumor mass of (R)-DOTAP/Trp2 (75 nmol) vaccinated mice were $CD3^+CD8^+$ cells; 0.2 % were identified as $CD3^+CD4^+$ cells. (R)-DOTAP/Trp2 (25 nmol) had a less profound effect, but quantifiable amounts of $CD8^+$ and $CD4^+$ T cells (0.3 % and 0.1 %, respectively). Other groups (untreated tumor, 75 nmol Trp2 peptide alone, and (R)-DOTAP/Trp2 (5 nmol)), showed lower than 0.1 % $CD4^+$ or $CD8^+$ T cells out of the tumor mass.

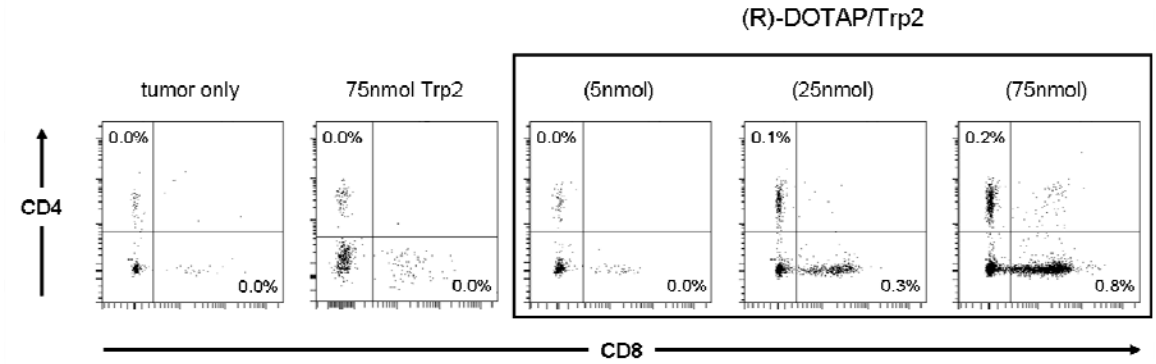

Figure 3.6 $CD3^+$ Tumor Infiltrating lymphocytes are higher numbers with higher vaccination doses. $CD4^+$ and $CD8^+$ tumor infiltrating T cells assayed from tumors of mice treated with varying doses of (R)-DOTAP/Trp2. Cells were gated on $CD3^+$, and percentages represent $CD3^+CD4^+$ or $CD3^+CD8^+$ out of total numbers of cells in the tumors. Data from one representative animal is shown, three to four mice were used per group. Experiment was repeated twice.

When lymphocytes were isolated from tumors of vaccinated mice, reactivity to Trp2 was examined. After a 6 h pulse with Trp2 or Ova peptide (and GolgiStop^{TM}), cells were examined for IFN-γ secretion (**Figure 3.7**). (R)-DOTAP/Trp2 (75 nmol) showed statistically significant response to Trp2 compared to all other groups, nearly 6 % of all $CD8^+$ TIL, with $P<0.005$. There was some background IFN-γ secretion by Ova-pulsed cells in tumors of (R)-DOTAP/Trp2 (75 nmol) treated mice. Lower deliverable doses of Trp2 (25 nmol and 5 nmol), and unvaccinated mice showed Trp2 reactivity by less than 1 % of $CD8^+$ TIL.

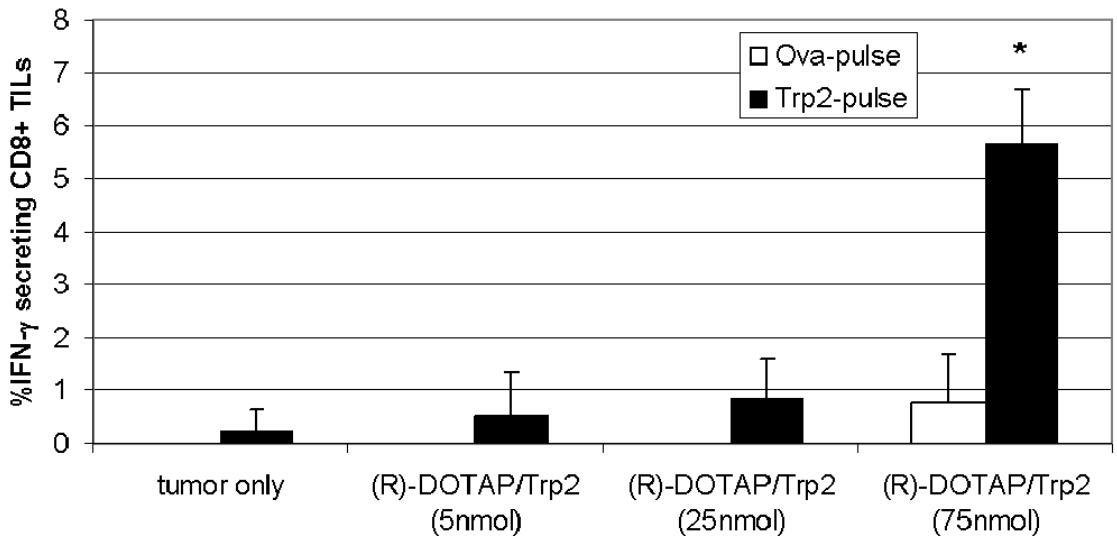

Figure 3.7 Tumor infiltrating lymphocytes respond to Trp2 after a high vaccination dose.
TIL were isolated from tumors of mice vaccinated with varying doses of (R)-DOTAP/Trp2, pulsed for 6h with Trp2 or an irrelevant peptide (Ova) and analyzed for intracellular IFN-γ in $CD8^+$ cells. Percentages are IFN-γ^+CD8^+ cells out of all $CD8^+$ cells., *: $P<0.005$. Three mice were used per group. Experiment was repeated twice.

3.4 DISCUSSION

Even with current advances in melanoma therapy (anti-CTLA4 mAb and small molecule BRAF inhibitors), there still exists an opportunity to innovate and further refine therapeutic treatment for aggressive melanoma decreasing side effects and honing specificity. Data presented here has shown that peptide-based vaccines offer a safe and significant advancement against an aggressive murine melanoma solid tumor model.

3.4.1 Overcoming formulation difficulty of the Trp2 peptide

Others have made efforts to combat the difficulty in formulating Trp2 peptide in an aqueous solution, ranging from looking at modifying the epitope to conjugation to larger proteins to enhance delivery.

Tang et. al. investigated increasing Trp2 binding efficacy to HLA-A201 by modifying the anchor residues.[249] Modifying SVYDFFVWL to S**M**YDFFVWL (or a Trp2 2M modification) was delivered in comparable doses to what we've shown in this study. When 100 μg (63.8 nmol) was delivered with 50 μg of the PADRE T helper epitope (AKFVAAWTLKAAA) in incomplete Freund's adjuvant (IFA) to a transgenic HLA-A2.1/K^b model, higher amounts of IFN-γ was elicited compared to vaccination with wild type peptide. Trp2 has also been modified into (S**I**YDFFVWL), called "deltaV" which showed increased T cell responsiveness to Trp2 by intracellular IFN-γ staining.

However, when deltaV was delivered with poly(I:C) and anti-CD40 and later boosted with these two adjuvants, no increased growth delay was seen with in a prophylactic B16F10 model compared to wild type peptide.[247] Other inventive ways to deliver Trp2 to APCs have been published. Kou et. al. developed a ScFv-peptide conjugate to target Trp2 to $CD11c^+$ dendritic cells *in vitro*.[248] This conjugate has shown stimulation of T cell proliferation, but Trp2 peptide alone showed comparable levels in the study. As a self-antigen, suppression mechanisms also exist to prevent the expansion of T cells in a tumor environment, thus the difficulty of low doses of Trp2 in (R)-DOTAP/Trp2 (5nmol) and (25nmol) in eliciting an IFN-γ response (**Figure 3.4A**).

3.4.2 Common models for murine melanoma rarely include therapeutic treatments in advanced solid tumors

An advanced solid tumor model is rarely investigated in Trp2 peptide-based vaccines; more often, a prophylactic model or CTL characterization is tested.[246; 247; 248; 249] However, it is unlikely that a prophylactic melanoma vaccine would ever be commercially developed. The potential side effect of vitiligo is not likely to be traded for the possibility of protection, particularly as Trp2 peptide reactivity has been tied to this autoimmune depigmentation.[256]

Trp2 peptide encapsulated in liposomes with p53 peptide, PADRE T helper peptide, CpG oligos together to was able to prevent tumor establishment when delivered six days after inoculation of $1x10^4$ B16F10 cells.[251] However, as a measure of tumor challenge, only two-thirds of the control group ever established tumors. Another liposomal treatment required CpG to show a therapeutic response, with two doses of

liposomal Trp2 and a separate formulation of liposomal CpG delivered in a $1x10^5$ B16F10 subcutaneous model.[250] However it is not clear from the data published from either study, that tumors were palpable or even visible when treated. Our choice of an advanced tumor model, $3x10^5$ B16F10-luc cells for subcutaneous inoculation, was based on all mice having measurable tumors on day 6, compared to inoculation with fewer cells (data not shown). Also, while CpG is a well characterized TLR9 agonist, the elegance of liposomal (non-viral) delivery is not aptly executed by the above two studies, with multiple adjuvants and multiple delivery devices needed. Our adjuvant, (R)-DOTAP also acts as the carrier for Trp2 peptide, simplifying the vaccine to active ingredients only, one stable and versatile particle that can show response against an established tumor (**Figure 3.2, Figure 3.3**).

Viral delivery of Trp2 peptide or protein has shown non-robust immunity compared to the statistically significant tumor growth delay we see with (R)-DOTAP/Trp2 nanoparticles delivering 75 nmol of antigen (**Figure 3.3**) in an aggressive solid tumor model. Recombinant adeno-associated virus (rAAV) carrying Trp2 cDNA delivered 22 days before tumor challenge was unable to induce tumor growth delay.[252] Delivered at a dose of 10^{10} or 10^{11} rAAV viral particles were unable to protect against a tumor challenge of $3x10^5$ B16F10, even with the addition of other adjuvants, including CpG oligonucleotides and imiquimod. Interestingly, like (R)-DOTAP/Trp2 (25nmol), the rAAV-Trp2+CpG treatment showed an IFN-γ response from splenocytes, however, was not able to break tolerance and show any tumor growth delay. Multiple doses of Trp2 peptide conjugated to exposed lysines on the tobacco mosaic virus (TMV) was delivered with CpG oligonucleotides prior to inoculation with $5x10^4$ B16F1, showing no statistical

difference compared to control or TMV with a different melanoma antigen p15e.[246] Additionally, in this challenge model, tumor penetration was 11 out of 12.

Dendritic cells pulsed with Trp2 peptide have also shown ineffective responses in both prophylactic and simultaneous tumor models.[243] However, when the HIV TAT protein transduction domain was ligated to a 472 amino acid sequence from the Trp2 protein or to the Trp2 peptide (180-188 amino acids); both showed better tumor prevention compared to dendritic cells pulsed with Trp2 peptide only.[257; 258] This supports the need for an intracellular delivery mechanism like (R)-DOTAP/Trp2 formulations to ensure Trp2 peptide is presented on MHC class I. An interesting result of the above mentioned study showed *in vitro* CTL reactivity to B16 cells correlated with tumor size. Our *in vivo* CTL results on day 13, when all groups had statistically indistinguishable tumors, is an early indicator of the ability of a formulation to cause statistically significant tumor growth delay (**Figure 3.5, Figure 3.3**).

Our choice to use an aggressive subcutaneous model versus a lung metastatic model was to utilize the existence of a suppressive tumor microenvironment. Many types of suppressive immune cell exist in the tumor that tolerize the immune system to the tumor's presence, and combating these cell types with possible therapies should be the next frontier of immunotherapy.[259] With a larger tumor mass existing in the solid tumor model versus the metastatic model, the bar is higher for a vaccine to break this tolerance. In a model of transgenic Trp2 peptide specific T cells, the adoptive therapy of T cell transfer was able to cause statistically significant decrease in lung nodules (P>0.0001), however, had no effect whatsoever on any tumor growth delay in a solid tumor model.[260] The adoptive cell transfer was able to show nearly 98 % specific lysis of Trp2 pulsed

targets in an *in vivo* CTL assay, however, not able to reject the $2x10^5$ B16F10 solid tumor inoculation. Even with the addition of a Trp2-pulsed dendritic cell vaccine, no significant tumor growth delay was observed in the solid tumor model. While Trp2 specific T cells were detected in the solid tumor, they did not affect tumor growth, unlike our detection of infiltrating T cells that correlated with tumor growth delay (**Figure 3.6, Figure 3.7**).

Future directions in melanoma immunotherapies should tackle established tumors with an existing suppressive microenvironment. As shown by the ipilimumab approval and increasing numbers of biologic drugs; targeting suppressive mechanisms in and around the tumor, shutting down this protective barrier could empower immunotherapy to become the standard of care over conventional chemotherapy. Anti-CTLA4 antibodies are already being tested in a wide range of tumors, expanding the application beyond melanoma.[261] The ability and strength of (R)-DOTAP to break tolerance in this model after one immunization and the flexibility of the adjuvant to deliver an adequate dose of antigen in a stable formulation pushes it forward to be tested in other aggressive tumor models and possibly into clinical development.

CHAPTER 4

DELIVERY OF PD-L1 siRNA, MELANOMA PEPTIDE ANTIGEN, AND (R)-DOTAP AS A THERAPEUTIC VACCINE FOR MELANOMA

4.1 INTRODUCTION

The immune system is a complex network of stimulation and suppression, allowing for activation against invading pathogens, and prevention of autoimmunity. However, as a cell begins to mutate and become cancerous, often, the immune system reacts by trying to promote angiogenesis and release growth factors, rather than attack and clear tumor cells. There are several cell types and tumor-expressed ligands that may play a role in promoting the suppressive tumor microenvironment.[262; 263] Cell mediated immunity is required for tumor cell rejection, thus pathways that cripple T cells should be disabled to restore proper immune function. The FDA approval of ipilumumab, a fully human antibody against CTLA4, helps block the receptor on cytotoxic T lymphocytes, preventing anergy and inactivation.[264; 265] The therapy has shown a 10.9 % response rate in melanoma patients and 34 % reduction of risk of death, a significant benefit compared

to the previous standard of care in these patients (treatment with the chemotherapy darcarbazine).[266]

To re-energize T cells, other pathways that limit their function should be considered. Dendritic cells upregulate certain receptors to inhibit chronic activation (and thus exhaust and anergy) of T cells.[267; 268; 269; 270; 271] Tumors employ a similar pathway, and often have upregulated levels of surface receptors such as DC-HIL, and PD-L1, which prevent recognition by T cells.[272; 273] Researchers have delivered siRNA against this immune inactivation to tumors, DCs or T cells (the corresponding receptor to PD-L1; PD-1), and shown the silencing of these suppressive signals allow for the rebound of T cell activity and corresponding tumor growth delay.[274; 275; 276; 273] However, as stated previously, the immune system is a balance of both activation and suppression. If both could be accomplished with a single injection; suppression of inhibition and activation of T cell, it may be possible to unleash an even stronger pulse of anti-tumor activity.

Cancer vaccines have been well established preclinically, and although the FDA-approved prostate cancer vaccine Sipuleucel-T has not gained mainstream use as quickly as expected, the approval is a solid proof-of-concept. In the case of Sipuleucel-T, a fusion protein of prostate cancer tumor associated antigen (TAA) prostatic acid phosphatase (PAP) and GM-CSF are delivered to APCs *ex vivo*, and the reinjected into the patient, showed a 22 % reduction in the risk of death in its pivotal trial.[277] Other peptide vaccines have been developed, particularly in melanoma, to invigorate a specific CTL population, break tolerance and cause tumor growth delay of even prevention (if dosed in a prophylactic manner).[278; 279; 280; 281; 282] Cases of spontaneous regression have been

observed in melanoma, often in tandem with vitiligo, thus the development of immunotherapies is an exciting opportunity for enhanced immune activation.[283; 284; 285; 286]

Our laboratory has developed a Trp2 peptide/(R)-DOTAP therapeutic vaccine which statistically improves tumor growth delay in a B16F10 melanoma model after subcutaneous delivery.[287] Trp2 (Tyrosinase-related protein 2) is a protein overexpressed in many melanomas and also in glioma cells based on the shared neuroectodermal origins of these tumors.[245] Additionally, the Trp2 peptide used (SVYDFFVWL) is H-2K^{b} restricted, to ensure CD8^{+} T cell engagement.[288] The antigen/adjuvant combination creates rod-shaped particles, rather than traditional liposomes that are formed most often in peptide/lipid combinations.[289; 290; 291] In contrast to our work with Trp2 peptide, traditionally, only very soluble antigen peptides are even considered for investigation. The unique rod shaped particles led us to hypothesize a specific interaction between the hydrophobic residues of the peptide and the fatty acid chains of the (R)-DOTAP. Admittedly, this unique formulation has limited application, only towards tumors in which Trp2 peptide is expressed, however, it widens the opportunity for investigation of poorly soluble peptides with the lipid adjuvant, (R)-DOTAP, whose enantiomeric adjuvant specificity was discovered by our group.[33]

Uniting the opportunity to deliver both peptide and nucleic acids is a look to the past for the Huang group, as our peptide antigen delivery with lipid adjuvant grew from a non-viral nanoparticle primarily developed for gene delivery. Soluble peptides were easily incorporated into a DNA core and lipid coated particle. Gao and Huang developed LPD, a carrier that delivered lipid, polycation and DNA, which has subsequently been investigated further as a gene delivery system.[292; 293; 294; 295; 296] When a water soluble

antigen (E7 peptide, RAHYNIVTF), was incorporated, the nanoparticle was found to have efficacy against a tumor expressing E7 protein (TC-1, a murine model of HPV16-induced cervical cancer). This formulation was thoroughly tested in our laboratory, delivering even proteins (vs. peptides) and correspondingly evaluated as a vaccine formulation.[35; 36; 37; 42]

Studies by Vangasseri et al and Chen et al increased our understanding and discovered that DOTAP was the efficacious adjuvant.[39; 30] The CpG motifs on the plasmid DNA were attributed to an increased TNF-α response and had no effect on the tumor regression data. As an adjuvant, (R)-DOTAP has shown efficacy in two tumor models; one with exogenous tumor antigens (HPV16 E7 protein in the TC-1 model),[33] and endogenous tumor antigens (Trp2 protein in the B16F10 model),[287] showing a safe and efficacious response.

Our studies with (R)-DOTAP/Trp2 as well as observance of the need to quench the suppressive immune response in tumor therapy, led us to develop a tri-modal delivery vehicle. Our (R)-DOTAP acts as adjuvant, Trp2 peptide as antigen and simultaneously, PD-L1 siRNA to release the breaks APCs use to temper or slow cytotoxic T lymphocytes from being active against Trp2-presenting B16F10 established tumors in a C57BL/6 model. By delivering all three signals subcutaneously, we target the particles to APCs in the subcutaneous space and draining lymph nodes (as shown by Chen et al).[30] We hypothesize this tri-modal particle, which we term RTP for the three components, will show enhanced tumor growth delay, compared to control siRNA containing formulations, termed RTC.

4.2 MATERIALS AND METHODS

4.2.1 Materials

(R)-DOTAP, (R)-1,2-dioleoyl-3-trimethylammonium-propane] was obtained from Merck KGaA (Darmstadt, Germany). NBD-DOPC, 1,2-dioleoyl-sn-glycero-3-phosphoethanolamine-N-(7-nitro-2-1,3-benzoxadiazol-4-yl) (ammonium salt) was obtained by Avanti Polar Lipids (Alabaster, AL). H-2K^{b} restricted peptides Trp2 (H-SVYDFFVWL-OH, amino acids 180-188 from the Tyrosinase-related protein 2 over-expressed in human and murine melanoma, MW 1175) and Ova (H-SIINFEKL-OH, amino acids 257-264 from the ovalbumin, MW 1773) were obtained from Peptide 2.0 (Chantilly, VA), supplied as trifluoracetate salts. Molecular biology grade water was obtained from Cellgro (Manassas, VA). Sodium methoxide, pure titrant (0.5M in methanol) and HPLC grade methanol were obtained from Fisher Scientific (Pittsburgh, PA). Absolute ethanol was obtained from Decon Labs, Inc. (King of Prussia, PA). PD-L1 siRNA (5' – CCC ACA UAA AAA ACA GUU G dTdT – 3')[297] and control siRNA (5′-AAT TCT CCG AAC GTG TCA CGT-3′)[298] were obtained from Dharmacon ThermoScientific (Lafayette, CO). TexasRed labeled oligonucleotides (5'-75TexasRed-XN/CAA GGG ACT AGG CTG-3') were obtained from Integrated DNA Technologies (Coralville, IA).

Trp2 peptide was formulated as a disodium salt for delivery as described previously.[287]

4.2.2 Preparation and Evaluation of RTP Formulations

(R)-DOTAP was obtained as a powder and dissolved in chloroform. Twenty μmol of lipid was dried in a glass vial under a stream of nitrogen and stored under vacuum in a desiccator overnight to ensure removal of any remaining chloroform. The thin film of lipid was hydrated with 1 mL molecular biology grade water and subsequently vortexed. After 1 h at room temperature, the suspensions were extruded 10x through two 100 nm polycarbonate membranes, then 10x through two 50 nm membranes (Fisher Healthcare, Houston, TX). Extruded liposomes were stored at 4 °C.

The core of the particle was made by mixing 5 μL of molecular biology grade water with 12 μL of 2 mg/mL siRNA (PD-L1, control or TexasRed-labeled oligonucleotides), then 18 μL of 2 mg/mL protamine sulfate salt sourced from Salmon, Grade X (Sigma-Aldrich) in molecular biology grade water and allowed to sit at room temperature for 5 min. Then, 50 μL of 1.5 mM Trp2 disodium salt (in molecular biology grade water), was added to the core by gentle mixing and allowed to sit for an additional 5 min at room temperature. Subsequently, 15 μL of 20 mM of (R)-DOTAP liposomes was added to the core-peptide aggregates and allowed to incubate at room temperature for 20 min. RTP is used throughout the manuscript to denote (R)-DOTAP/Trp2 peptide/PD-L1 siRNA; RTC is used to denote (R)-DOTAP/Trp2 peptide/control siRNA; and RT(TxRed) is used to denote (R)-DOTAP/Trp2 peptide/TexasRed oligonucleotides.

Particle size and zeta potential were measured with a Malvern Zetasizer Nano ZS (Worcestershire, United Kingdom). Trp2 peptide encapsulation efficiency was measured using a Microcon 100 kDa MWCO centrifugal filtrate device (Millipore, Bedford, MA). Flow-through was analyzed using 2 μL of sample on a Nanodrop Spectrophotometer,

ND-1000 (Thermo Scientific, Wilmington, DE), measuring the absorbance at 280 nm wavelength. Concentration of peptide in flow-through (unencapsulated) was calculated using Beer-Lambert law ($A_{280} = \varepsilon*b*c$), with $\varepsilon = 5367.7$ ($M^{-1}cm^{-1}$), calculated from a standard curve of Trp2 peptide.[287] Final encapsulated concentration was calculated by subtracting the concentration in flow-through from the known concentration used for hydration. Trp2 peptide loss in the column was < 5 %.

Transmission electron microscope (TEM) images of the RTP complexes were acquired by the use of a JEOL 100CX II TEM (Tokyo, Japan). Briefly, 4 µl of nanoparticle solution was dropped on to a 300 mesh carbon coated copper grid (Ted Pella, Inc., Redding, CA) for 2 min. Excess fluid was removed with filter paper, and copper grid was dried before the observation with TEM. Particles from several different fields were measured. Particle dimensions were calculated by measuring the diameter in case of spherical particles, or in the case of rod-shaped or oval particles, the largest dimension and the corresponding diameter perpendicular to the first measurement. One hundred particles were examined per field and particles from three fields were compiled.

4.2.3 Bone Marrow Derived Dendritic Cells (BMDC)

Methods to culture bone marrow-derived dendritic cells have been described previously.[32] Briefly, bone marrow from the femurs and tibias of six week old C57BL/6 mice was isolated in serum free RPMI1640 media. Red blood cells were lysed using ACK Lysing Buffer (Invitrogen) and cells were plated for 2 h in serum free RPMI 1640 to remove suspension cells (lymphocyte precursors). Remaining adherent cells were cultured in RPMI 1640 media containing 10 % fetal bovine serum (FBS), non-essential

amino acids (NEAA) (Invitrogen), antibiotic/antimycotic (Sigma-Aldrich, St. Louis, MO with 1000 U/mL granulocyte-macrophage colony-stimulating factor (GM-CSF) and 1000 U/mL interleukin-4 (IL-4) (R&D Systems, Minneapolis, MN) for 6 days changing the media every 2 days. BMDCs were used in experiments on day 6.

4.2.4 *In vitro* Uptake and *in vivo* Biodistribution

To analyze particle uptake, the 20 mM (R)-DOTAP was formulated to include 1 mol % NBD-DOPC. BMDCs at a concentration of $1x10^6$ cells/mL were seeded into 5 mL BD Falcon Flow Tubes (BD Biosciences). RTC was added to each tube in a dose of 50μM (R)-DOTAP, 12.5 μM Trp2 peptide, and 250 nM siRNA, based on the known toxicity of (R)-DOTAP in doses higher than 75 μM, and keeping the same ratios of Trp2 and siRNA as in the *in vivo* formulation.[33] Uptake was analyzed at 0, 5, 15, 30, 60 and 240 min of incubation at 37°C with 95 % humidity and 5 % CO_2. Tubes were removed and placed on ice in the dark before they were analyzed via on a FACS Canto flow cytometer and FACSDiva software (both from BD Bioscience, San Jose, CA). Samples were acquired on flow, then diluted 1:1 with 0.4 % Trypan Blue (Sigma) and evaluated with flow cytometry. Trypan Blue quenches the fluorescence on the surface of the cell, allowing for detection of internalized particles.

To analyze *in vivo* uptake, C57BL/6 mice were s.c. injected 1 cm above the right inguinal lymph node with RT(Texas Red Oligos). Mice were imaged at 0, 20 min, 1 h, 2 h, and 4 h after injection using a Kodak in vivo imaging System Fx Pro (Carestream Health Products, Rochester, NY), and analyzed using Carestream Molecular Imaging

Software (Rochester, NY). Inguinal lymph nodes and spleens were removed and imaged using the Kodak camera and Carestream imaging software.

4.2.5 Interaction of Formulations with BMDC *in vitro*

To measure CD86, PD-L1 or H-2K^b expression, BMDC were seeded at 1x10^6 cells/mL into BD Falcon tubes and treated with different formulation. RTP and RTC particles were treated at concentrations of 50 μM R-DOTAP, 12.5 μM Trp2 and 250 nM PD-L1 siRNA. Likewise, RTC particles had the same amounts of R-DOTAP, Trp2 and siRNA. Controls consisted of 25 μM (R)-DOTAP, 12.5 μM Trp2 peptide, or 250 nM PD-L1 siRNA. After 48 h, cells were stained with anti-CD86-FITC (GL1), anti-CD11c-PE (HL3) anti-H-2K^b-FITC (AF6-88.5), or anti-PD-L1-PE (MIH5) antibodies (BD Biosciences, San Jose, CA) and analyzed by using flow cytometry. Control isotype antibodies were used to assess non-specific staining.

To measure toxicity, BMDC were treated with different concentrations of RTP, RTC or appropriate controls (mentioned above) for 24 h and stained with propidium iodide (PI) (Sigma-Aldrich) and evaluated using flow cytometry.

4.2.6 BMDC-splenocyte Co-culture Experiments to Evaluate T cell Reaction *in vitro*

BMDCs were incubated at a concentration of 2x10^6 cells in 2 mL of BMDC media in 6 well plates. Cells were treated with RTP particles containing 50 μM of R-DOTAP, 12.5 μM Trp2 peptide and 250 nM of PD-L1 siRNA, or 250 nM control siRNA (in the case of

RTC particles), or associated controls of lipid alone, peptide alone, PD-L1 siRNA alone (in concentrations equal to those in RTP particles).

To measure T cell proliferation, carboxyfluorescein succinimidyl ester (CFSE)-pulsed splenocytes from naïve mice were added to treated BMDC and evaluated 36 h later. In brief, spleens were removed from C57BL/6 mice, crushed through a 70 um filter and red blood cells lysed. Afterwards, cells were washed, and incubated in serum-free RPMI with 4 μM CFSE for 15 min at 37 °C. Cell were then washed in complete RPMI media made of RPMI1640 media supplemented with 10 % FBS, NEAA and antibiotic/antimycotic (Cellgro), Splenocytes were incubated with treated BMDCs in a 100:1 ratio, and 20 U IL-2/mL was added to the media to sustain T cell growth. Thirty-six h later, wells were imaged with a Vista Vision light microscope, cells were removed and wells washed with PBS. Samples were analyzed with flow cytometry to evaluate the dye-dilution due to cell division.

To measure specificity of response, splenocytes were removed, made into a single-cell suspension (as above), and incubated in a 100:1 ratio with 24 h treated BMDCs, plus 20 U/mL IL-2. Thirty-six h later, suspension cells were removed, and resuspended at $2x10^6$ cells in complete RPMI media, plus 1 μL/mL GolgiStop™ (BD Biosciences) and 5 μM Trp2 or Ova peptide for 6 h at 37 °C. Cells were removed, washed with staining buffer (BD Pharmingen, San Diego, CA) and stained with anti-CD8-APC (53-6.7). Cells were then treated with Cytofix/Cytoperm™ according to kit instructions (BD Pharmingen) and stained intracellularly with anti-IFN-γ-FITC (XMG1.2), washed and analyzed by using flow cytometry.

4.2.7 Tumor Cell Culture

B16F10 cells, a murine melanoma model (syngenaic with C57BL/6) were originally obtained from American Type Culture Collection (ATCC) (Manassas, VA). Previously, in collaboration with Dr. Pilar Blancafort at the University of North Carolina at Chapel Hill, B16F10 was stably transfected with GL3 firefly luciferase gene using a retroviral vector to create B16F10-luc.[254; 255] B16F10-luc cells were used in all studies presented here and maintained in Dulbecco's Modified Eagle Medium (Gibco (Invitrogen), Carlsbad, CA) supplemented with 10 % fetal bovine serum (Invitrogen, Carlsbad, CA), 100 U/mL penicillin (Invitrogen) and 100 μg/mL streptomycin (Invitrogen).

4.2.8 Interferon Gamma (IFN-γ) Production by $CD8^+$ T cells

Mice were vaccinated with RTP, RTC formulations or associated controls in a dose of 300 nmol (R)-DOTAP lipid, 75 nmol Trp2 peptide or 24 μg siRNA. Seven days later, mice were sacrificed and spleens sterilely removed from each mouse. Spleens were processed into a single cell suspension by crushing through a 70 μm filter (BD Biosciences, San Jose, CA). After removal, cells were incubated in complete RPMI media, 1 μL/mL GolgiStop™ and Trp2 or Ova peptide, stained for CD8 and IFN-γ and analyzed via flow cytometry as described above.

4.2.9 Mice and Immunizations

Six week old female C57BL/6 mice obtained from the National Cancer Institute, were used in all studies. On day 0, $3x10^5$ B16F10-luc cells in 50 μL of PBS were injected subcutaneously into the hair-trimmed abdomen. On day 6, RTP or RTC were subcutaneously injected into the contralateral side of the abdomen in 100 μL of 5 % dextrose solution. In all experiments, 300 nmol (R)-DOTAP per mouse was the therapeutic dose of adjuvant used, as shown previously.[253] Tumors were measured every 2-3 days with calipers, recording the longest diameter as length and the perpendicular dimension as width. Area was calculated as (length) x (width). Humane sacrifice of mice was performed after tumors reached 20 mm in one dimension. All animal protocols were approved by the University of North Carolina at Chapel Hill's Institutional Animal Care and Use Committee.

4.2.10 Statistical Analysis:

Statistical analysis was completed by using a two-tailed Student's t-test unless otherwise specified. Tumor growth delay data was analyzed using repeated measures ANOVA. Data was qualified as statistically significant if the *P* value was less than 0.05.

4.3 RESULTS

4.3.1 Formulation of RTP particles by optimal combination of PD-L1 siRNA with Trp2 peptide and (R)-DOTAP

Protamine was mixed with siRNA to create a solid core. Afterwards, Trp2 peptide as a disodium salt was added at different Trp2:siRNA weight ratios (**Figure 1A)**. Greater than 1, the ratios created particles above 3,000 nm, indicating the possible hydrophobic interactions with increasing amounts of Trp2. Eventually, the size stabilized to slightly larger than 4,000 nm, and 3.125 was the ratio chosen for further experiments. The "core+Trp2" was then incubated with different mol/mol ratios of (R)-DOTAP to Trp2 peptide and size was measured over time (**Figure 1B**). This showed a time-dependent decrease in size for most ratios, and further investigation showed after 20 min of incubation, equilibrium had been reached. With this new optimized timeline, of 5 min for core mixing, 5 min for "core+Trp2" incubation and 20 min incubation after lipid addition; size and zeta potential of the RTP particles was measured over a range of (R)-DOTAP/Trp2 mol/mol ratios **(Figure 1C)**. The particles were stable over a range of ratios, with size around 60-80 nm and charge increasing from 40 to 60 mV as the positively charged lipid was added (**Figure 1D)**.

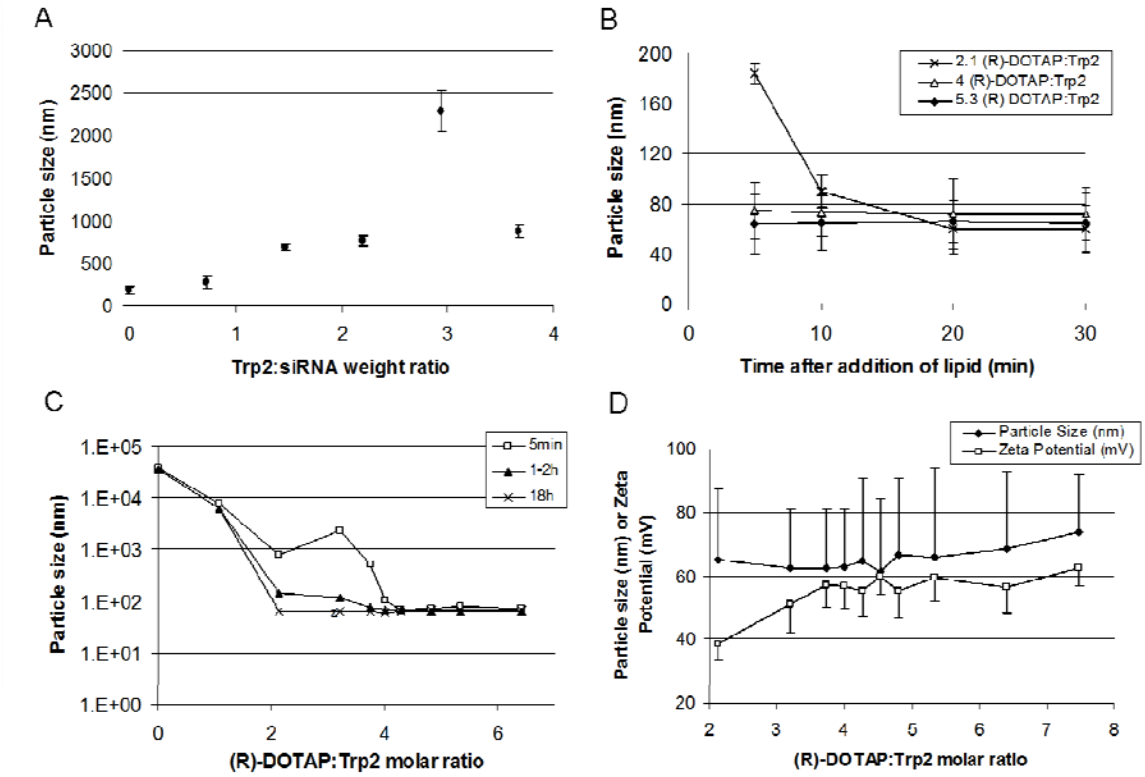

Figure 4.1 RTP Particle Optimization.
siRNA and protamine was mixed together in a weight ratio of 3:2. A) The protamine/siRNA mixture was then added to Trp2 peptide and allowed to incubate at room temperature for 5 minutes and then particle size was measured (n=3). The highest Trp2/siRNA ratio was used moving forward. B) (R)-DOTAP was added to the protamine/siRNA/Trp2 aggregates in different molar ratios and particle size measured at different time points (n=3). C) To optimize the shortest amount of time for size, particle size was measured over time after addition of different (R)-DOTAP ratios (n=3). D) After 5 min mixing of protamine/siRNA, addition of Trp2 peptide and 5 minutes incubation, then 30 sec mixing with different ratios of (R)DOTAP and 20 min incubation at RT, size and zeta potential of the different formulations were measured.

After optimization and stabilization of the protocol, the final times of 5 min incubation after core components of protamine and siRNA were mixed, 5 min incubation of Trp2 peptide and core particles and 20 min incubation of core+Trp2 peptide with (R)-DOTAP lipid (**Figure 2**). TEM images were taken at each step in the process to help visualize the particles being created. After mixing of the siRNA and core, we could see small (23 ± 3 nm) particles aggregated by excess protamine (**Figure 2A**). When lowered amounts of protamine were used, particles aggregated and flocculated after the addition of lipid, in contrast to aggregating and flocculating after the addition of Trp2, indicating that the protamine stabilizes the lipid in the core (data not shown). As mentioned above, we observed aggregates much larger in size (102 ± 25 nm) from the addition of Trp2 peptide to the core particles, indicting an anchoring of the negatively charged Trp2 to the positively charged core (**Figure 2B**). To better understand the (R)-DOTAP/"core+Trp2" interaction and structure, lipid was added in 3 different (R)-DOTAP/Trp2 mol/mol ratios: 2, 4 and 6 (**Figure 2C, 2D, 2E**). With a low ratio, aggregates were observed (length 204 ± 86 nm, width 120 ± 45 nm), due to incomplete fusion of liposomes to "core+Trp2" particles. With a ratio of 4:1, small round particles (diameter 33 ± 14 nm) were mainly observed with some rod shaped particles (7 % of total particles via TEM, (length 216 ± 64 nm, width 44 ± 8 nm). The rod shaped particles are similar to particles we have observed previously with (R)-DOTAP/Trp2 lipid/peptide complexes without siRNA.[287] Finally, at a mol/mol ratio of 6, mostly small round particles were observed (diameter 31 ± 9 nm) and 7 % aggregated particles (length: 307 ± 122 nm, width: 117 ± 25 nm). This 6:1 ratio was consistent with particle sizing and some aggregates, which resemble the blobs in the 2 ratio image, possibly indicating excess liposomes added. As (R)-DOTAP

(as well as many cationic lipids), is known to be toxic to BMDCs in high doses, we chose the RTP with a ratio of 4 to be used in subsequent experiments to eliminate any unneeded lipid. The RTP ratio of 4 was utilized also to take advantage of the consistently sized particles (**Figure 2D**).

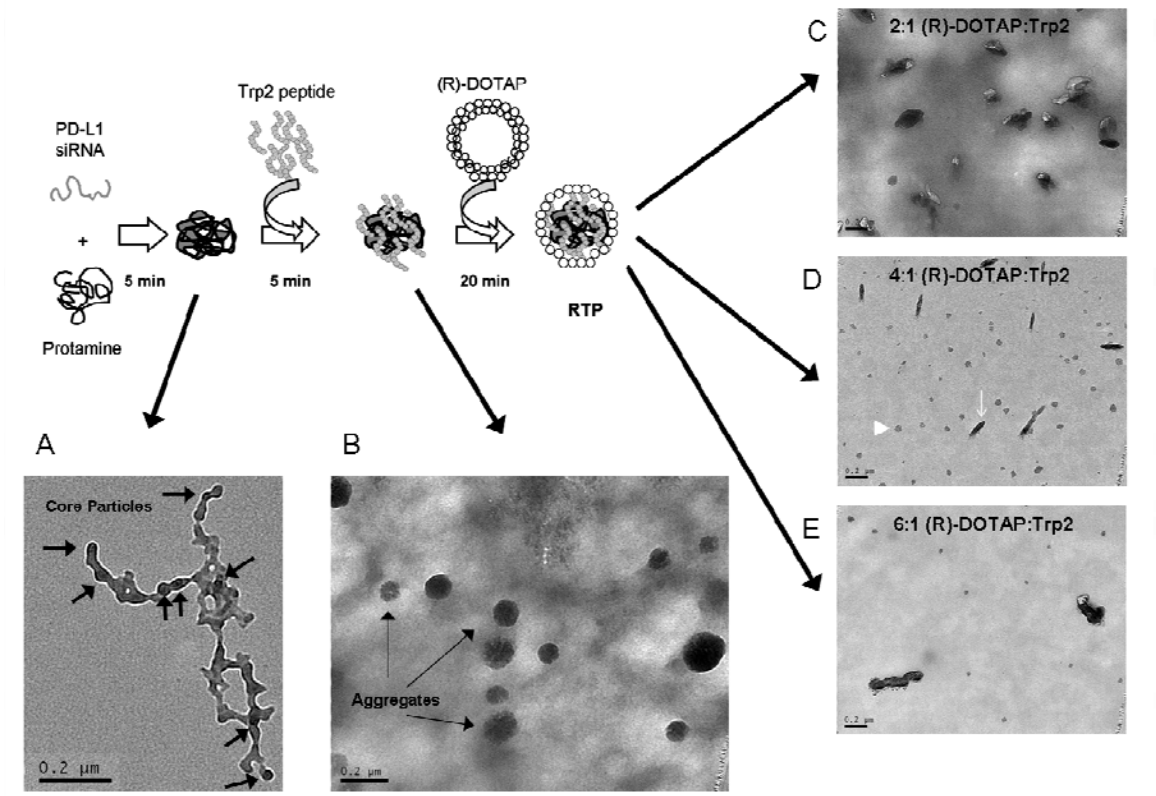

Figure 4.2 TEM images of RTP particle characterization at each step.
TEM images were taken at each step of the formulation. A) 18 µL of 2 mg/mL protamine was mixed for 10 sec with 12 µL of siRNA (and 5µL of molecular biology grade water) and allowed to incubate at room temperature for 5 min. Core particle size from TEM image was 22 ± 3 nm. B) 50µL of 1.5mM Trp2 peptide was added to the protamine/siRNA mixture, mixed for 10 sec, incubated at room temperature for 5 min. Core+Trp2 particle size from TEM image was 102 ± 26 nm. C) (R)-DOTAP was added in a 2:1 molar ratio with Trp2 (7.5 µL added), mixed for 30 sec, allowed to incubate for 20 min at RT. TEM images showed oval shaped aggregates with the longest dimension 204 ± 86 nm and shorter dimension 120 ± 45 nm. D) (R)-DOTAP was added in a 4:1 molar ratio with Trp2 (15 µL added), mixed for 30 sec, allowed to incubate for 20 min at RT. 4:1TEM images showed small spherical particles (diameter 33 ± 14 nm) indicated by a white arrowhead and 7 % rod-shaped particles (length 216 ± 64 nm, width 44 ± 8 nm) indicated by a white arrow. E) (R)-DOTAP was added in a 6:1 molar ratio with Trp2 (22.5 µL added), mixed for 30 sec, allowed to incubate for 20 min at RT. 6:1TEM images showed small spherical particles (diameter: 30 ± 9 nm) and 7 % aggregated particles (length: 308 ± 122 nm, width: 117 ± 25 nm).

4.3.2 Uptake and Biodistribution of RTP particles

RTC particles were used to detect uptake in BMDCs (**Figure 3A)**. (R)-DOTAP(99 mol %)+NBD-DOPC(1 mol %) were used as the label for uptake. Endocytosis occurred very quickly with nearly 40 % cells NBD positive after 5 min, and stable both on the surface of the cell and endocytosed after 4 h.

C57BL/6 mice with trimmed abdomens were subcutaneously injected approximately 1 cm above the right inguinal lymph node with RT(TxR) particles at different time points (**Figure 3B)**. Mice were sacrificed and placed on their abdomens and imaged to analyze particle migration based on the TexasRed signal. After 20 min, the injection site is clearly visible. In the subsequent animal samples, one can observe the migration of the injection site towards the inguinal lymph node. After whole body imaging, the secondary lymph organs of interest were removed; spleen, left inguinal lymph node and right inguinal lymph node (**Figure 3C**). The right inguinal lymph node at 4 h showed a strong positive signal, while no other time points showed any fluorescence over background. Inguinal lymph nodes showed higher relative background compared to the spleens. Spleens never showed any fluorescence above background at any time points measured (up to 4 h). Excised spleens are shown in the left most column of **Figure 3C**.

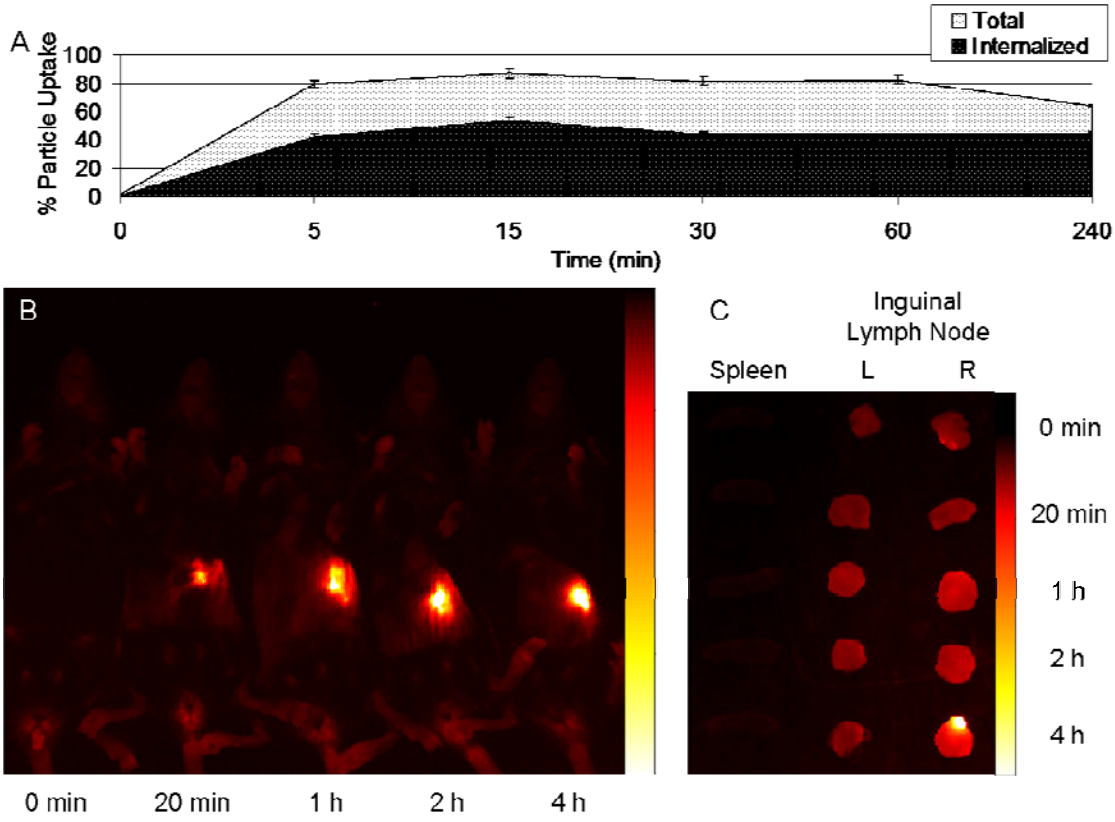

Figure 4.3 Delivery of RTP particles *in vitro* and *in vivo*.
A) 1e6 BMDCs cells were incubated with RTP or associated controls. BMDCs were treated with 25 μM RTP particles containing 1 mol % DOPC-NBD in the lipid bilayer to monitor uptake via flow cytometry. Internalized particles were estimated by running the same sample after the addition of 0.5 % Trypan blue in a 1:1 dilution. B) Six-week-old C57BL/6 mice were injected at different time points to evaluate RT (TexasRed oligos) drainage to lymph nodes. Twenty four μg TexasRed oligos were dosed per mouse. Mice were imaged using the Kodak In Vivo Imaging System. C) Spleen and both inguinal lymph nodes were removed to detect particles (TexasRed oligos), and imaged with the Kodak In Vivo Imaging System.

4.3.3 Surface molecule expression and toxicity of RTP in BMDCs

BMDCs were used to analyze the *in vitro* response of APCs to RTP particles (and associated controls) (**Figure 4**). BMDCs were analyzed for four different signals; CD86 to indicate activation of APCs, PD-L1 protein surface expression to analyze the effect of the siRNA delivery, H-2K^b surface expression to ensure the delivery vehicle would not cripple the APC ability to present Trp2 peptide, and finally, propidium iodide, to analyze the toxicity. Forty-eight h after stimulation with RTP (50 μM (R)-DOTAP, 12.5 μM Trp2, 250 nM PD-L1 siRNA), BMDCs showed the highest level of CD86-positive and H-2K^b-positive cells among all treated groups (**Figure 4A, 4C**). While RTP-treated cells also showed a 30 % decrease in PD-L1-positive cells, while RTC had a much more minor response (less than 10 % decrease) (**Figure 4B**). Toxicity of treatments was lower than 20 % of all treated groups, measured by PI positive cells. The treatments with the highest levels of toxicity were (R)-DOTAP as well as RTP particles, however, the difference was not statistically significant (**Figure 4D**).

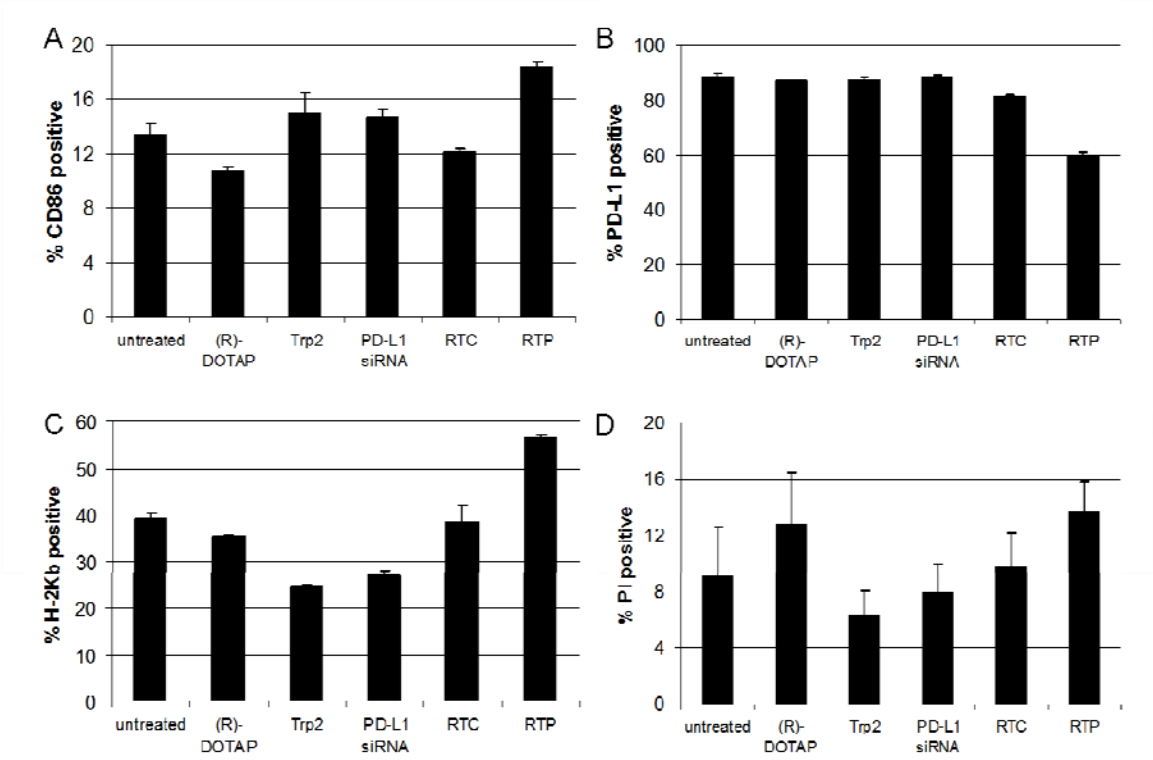

Figure 4.4 *In vitro* RTP characterization with BMDCs.
$1x10^6$ BMDCs were incubated for 48 h with 25 μM RTP and associated controls. After 48 h BMDCs were stained with corresponding antibodies (or propidium iodide) and monitored via flow cytometry for A) CD86 activation, B) PD-L1 surface expression, C) H-$2K^b$ surface expression, or D) toxicity (via PI positive cells, indicating cell permeability).

4.3.4 *In vitro* co-culture to determine RTP-treated BMDCs affect on splenocytes

Co-culture experiments were used to analyze the interactions between BMDCs and splenocytes to determine the efficiency of activating T cells after 36 h of co-incubation. CFSE-dye dilution showed that RTP and RTC both elicited dye-dilution, indicating cell expansion, with RTP at slightly higher levels (**Figure 5**). All the control groups in the dye-dilution study showed background levels of expansion, except for (R)-DOTAP which showed a slight increase over background. Light microscopy of these co-cultures showed obvious differences between RTP, RTC and the controls. While only RTP and RTC show clonal clusters of cells, RTP had larger clusters on average, compared to RTC. When the plates were gently washed to remove the clusters and collect the suspension cells, the resulting cells were analyzed for ability to identify Trp2 peptide by IFN-γ production. Cells were pulsed for 6 h with either OVA peptide or Trp2 peptide (both H-2K^b restricted). Both RTC and RTP showed increased IFN-γ secretion after Trp2 peptide pulse, however OVA-peptide pulse also showed a similar amount of IFN-γ in RTP treated samples. Untreated as well as (R)-DOTAP, Trp2 peptide and PD-L1 siRNA-treated samples all showed low levels of stimulation, relatively equal in both peptide-pulsed groups.

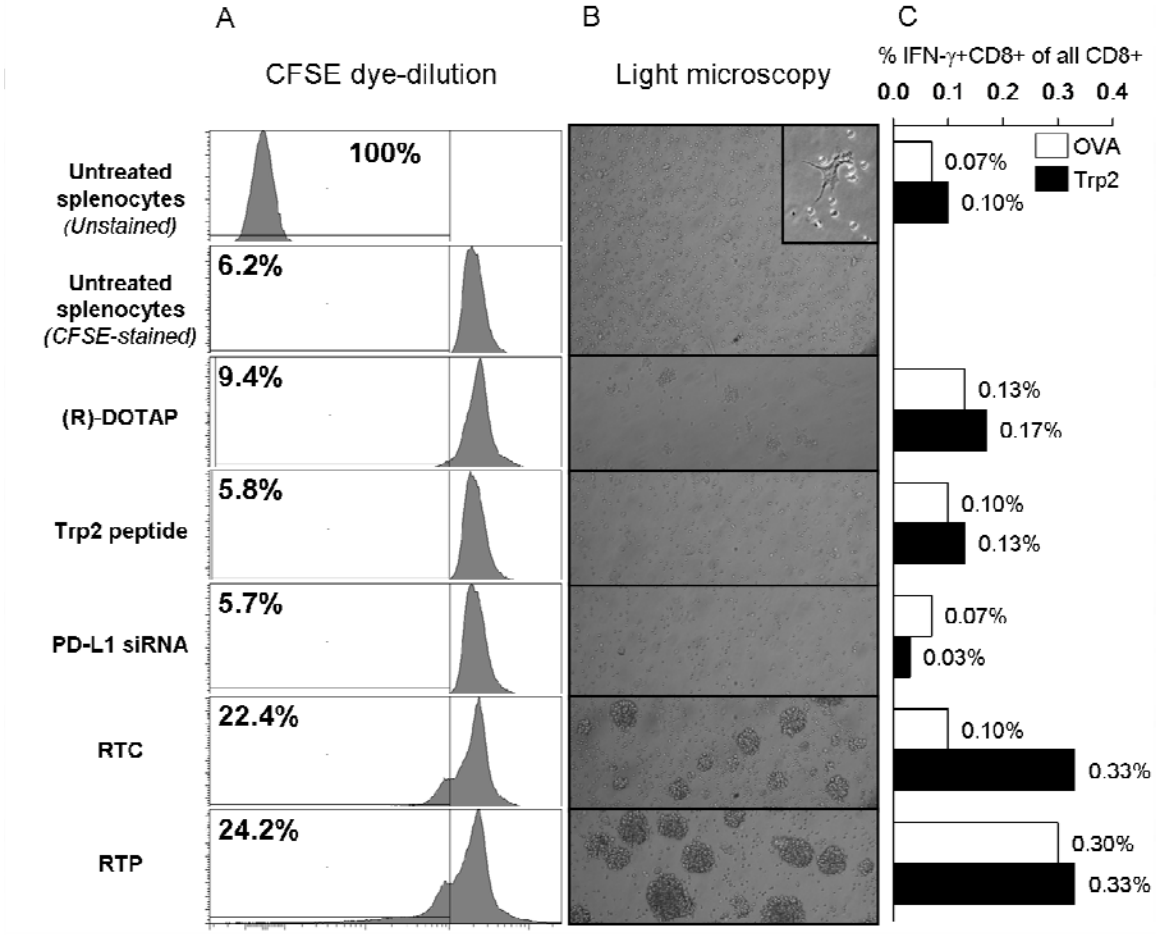

Figure 4.5 T cell activation and proliferation.
$2x10^6$ BMDCs were activated by incubating with RTP and associated controls for 24 h. Activated BMDCs were further incubated in 1:100 ratio with CSFE-stained splenocytes (unstained in C) for 36 h to evaluate the T-cell proliferation and IFN-γ secretion. A) Flow cytometry analysis of CFSE dye dilution. B) Light microscope images for T cell proliferation in cultures. One representative experiment is shown of three. (Inset picture represents an activated dendritic cell with T cells surrounding). C) Activated BMDCs were co cultured with unstained splenocytes (1:100 ratio) for 36 h. Splenocytes (suspension cells) were isolated and stimulated with target peptide (Trp2, filled bars) or untargeted peptide (OVA, open bars), IL-2 and Golgi stop for 12 h. The cells were stained with $CD8^+$ and IFN- γ antibodies and analyzed by flow cytometry.

4.3.5 RTP affects the IFN-γ production and PD-L1 surface expression *in vivo*

Mice were subcutaneously injected with RTP, RTC or associated controls and tested for an antigen-specific $CD8^+$ T cell response. Seven days after injection, mice were humanely sacrificed, and splenocytes were incubated with GolgiStop and pulsed with either OVA or Trp2 peptide for 6 h. Cells were then stained for surface expression of CD8 and intracellular IFN-γ. RTP and RTC treated-mice showed IFN-γ production greater than controls in Trp2 pulsed splenocytes, however RTC showed slightly higher levels, although not statistically different than RTP (**Figure 6A**). Tissue samples were taken from draining lymph nodes as well as spleen and analyzed for PD-L1 knockdown *in vivo* in both $CD11b^+$ (macrophages) and $CD11c^+$ (dendritic) cells. DLNs of mice treated with RTP showed lower levels of PD-L1 in both dendritic and macrophage cell compartments compared to RTC or control (**Figure 6B, 6C**). $CD11b^+$ splenocytes from mice treated with RTP had lower levels of PD-L1 compared to the other groups, however, $CD11c^+$ splenocytes had levels not different from RTC.

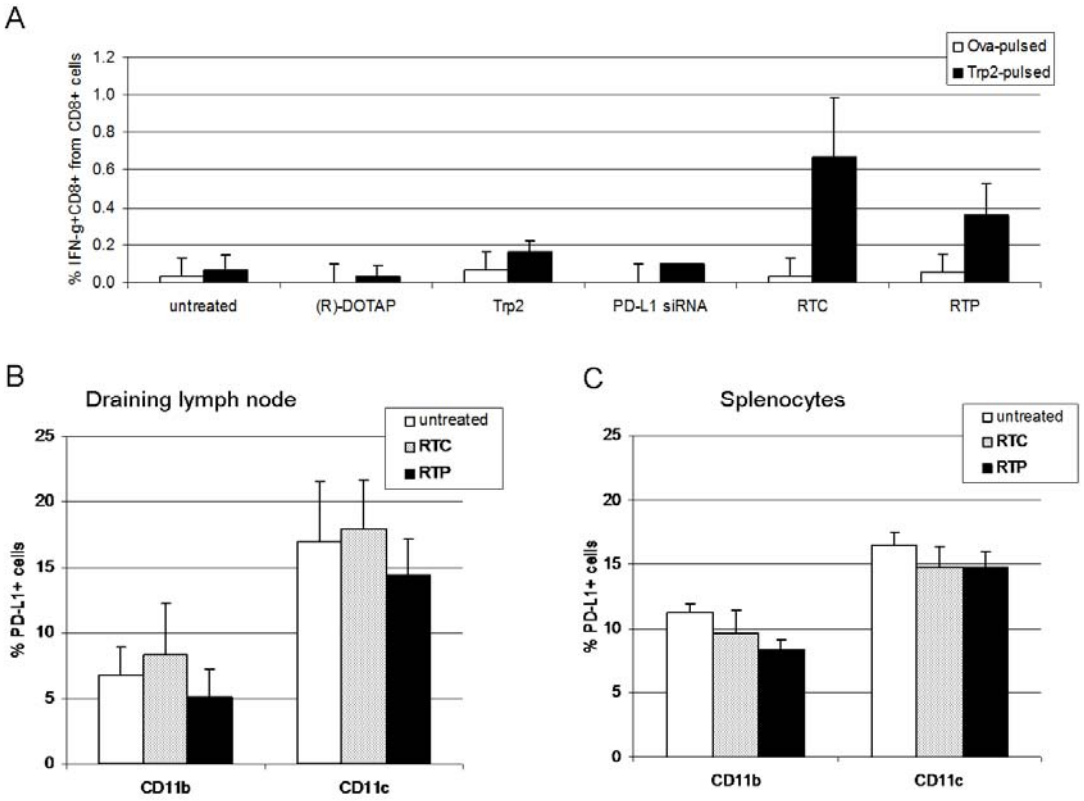

Figure 4.6 In vivo activity of RTP particles.
Six-week-old C57BL/6 mice were injected s.c. with RTC or RTP formulations. Eight days later, splenocytes were isolated and red blood cells lysed. A) Splenocytes were incubated with GolgiStop and pulsed with Ova or Trp2 for 6 h. Cells were then stained with anti-CD8 and anti-IFN-γ and examined via flow cytometry. B) Splenocytes were stained with anti-CD45, anti-CD11b, anti-CD11c, anti-PD-L1. Cells were gated on CD45 and CD11b or CD11b to select macrophage ($CD11b^+$) or dendritic cell ($CD11c^+$) populations, then examined for PD-L1 levels.

4.3.6 RTP delivery induces tumor growth delay

Mice were s.c. injected with B16F10 on day 0 on the left side of the abdomen, and tumor size and body weight was monitored for 20 days at which point all the mice in the study were sacrificed. On day 8, mice were injected with RTC, RTP or left untreated. Mice treated with RTP showed improved tumor growth delay compared to RTC or control mice (**Figure 7**). RTC did show some effect, but was not statistically significant from the untreated control. It was, however, statistically significantly different from tumor growth delay of RTP. The average body weight of the mice treated with RTP stayed fairly constant over time, while the body weight of RTC and control mice increased at the same relative rate, with no statistical differences between any groups.

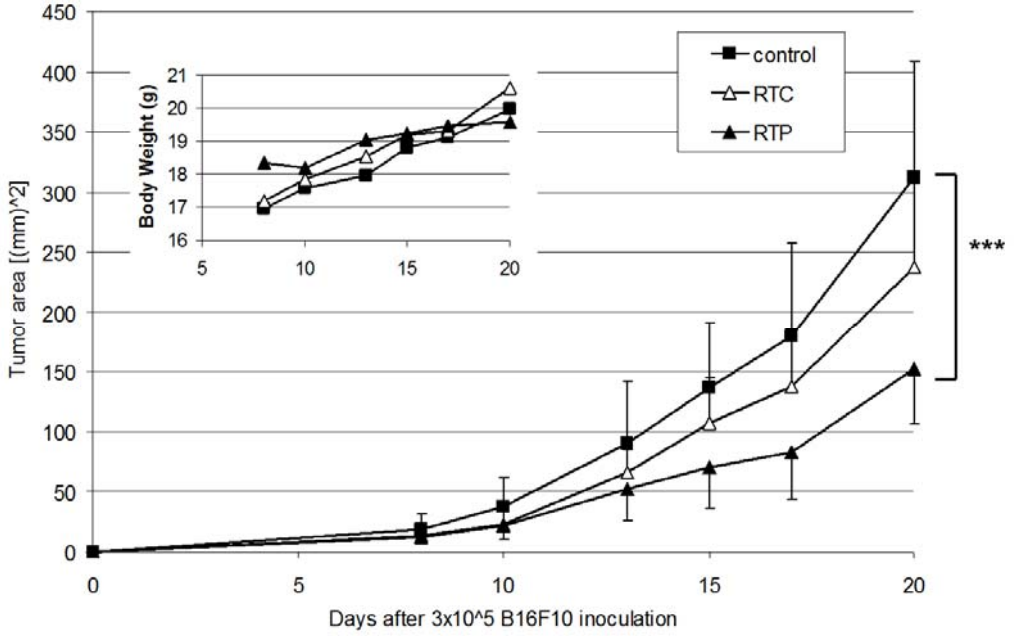

Figure 4.7 In vivo tumor growth delay after RTP administration.
Six-week-old C57BL/6 mice were inoculated with 3x105 B16F10 cells s.c. in the right side of the abdomen. Eight days later, mice were injected s.c. contra-laterally with RTC or RTP formulations, and tumor areas were measured for 20 days (n=5). Area was calculated by length x width ((mm) x (mm)). Inset is a chart of body weight. Weight was monitored after vaccination at every tumor measurement. ***: P=0.038 via repeated measures ANOVA

4.4 DISCUSSION

Subcutaneous delivery has long been used as a vaccination route studied in laboratories. However, it should be noted that most vaccines approved for use in humans are intramuscular, a simpler injection technique that promotes a stronger depot effect compared to subcutaneous that more easily facilitates lymph drainage. Subcutaneous drainage to lymph nodes is facilitated by two mechanisms. First, injection volume exerts a certain amount of interstitial pressure. Second, local inflammation by the injection or activation of APCs that are stationed in the skin or circulating nearby will sample their environment and if activated, drain to the lymph nodes. Macrophages have been shown to drive this process, even though dendritic cells are more effective as APCs.[299] We observed increased downregulation of PD-L1 in macrophages compared to dendritic cells and the difference in the type of cells facilitating uptake may be responsible. The downregulation in draining lymph nodes is not consistent across samples with no significant different which could be attributed to sporatic uptake from the injection site after dosing (**Figure 6B, 6C**).

Our data show that the downregulation of PD-L1 in dendritic cells does not to affect the clonal expansion of T cells *in vitro* (**Figure 5A).** The PD-1/PD-L1 (or PD-1/PD-L2) interaction stops the proliferation of T cells through the PI3K pathway, after silencing of PD-L1, we would expect to see an increase in proliferation.[300] However we did not observe a clonal expansion in the PD-L1 silenced population compared to RTC

treatment (**Figure 5A)**, as has been similarly observed by other investigators downregulating PD-L1 *in vitro*.[276] There may be engagement of PD-L2, or clonal expansion may only be observable *in vivo*, as the cell culture dish can not recreate the complex environment of the lymph node. With the knockdown of PD-L1 in DCs and subsequent removal of the PD-1/PD-L1 checkpoint, we hypothesize that the non-specific response seen in **Figure 5C** is due to natural killer T cells. In a PD-L1$^{-/-}$ knockout model, dendritic cells from the knockout were pulsed with melanoma antigen (and an adjuvant) and subsequently re-injecting into a donor mouse, which was inoculated with B16 melanoma cells the following day.[301] The mice that were treated with dendritic cells from the knockout had greater tumor growth delay compared to the mice treated with WT DCs pulsed similarly. This effect was attributed to the increased population of invariant natural killer T cells (iNKT). However, our experiments published here, are the first time this knockdown has be achieved *in vivo*, and with a therapeutic, rather than prophylactic model. The tumor microenvironment is much more challenging in therapeutic model, as mentioned previously.

The RTC platform takes advantage of molecular interactions to deliver nucleic acids, antigen and adjuvant. As dendritic cells drive the T cell priming process, more specifically controlling their signals could facilitate a bespoke response. The possibilities for the nucleic acid cargo are endless. Some other options to control the DC/T cell interaction would be to deliver siRNA against PD-L2 or IDO to prevent immunesuppression. Alternatively, the platform allows an opportunity to deliver genes to amplify the immune response, such as IL-2, GM-CSF, CD80/86, MHC I, or an additional antigen.

Trp2 peptide has very low solublity, and the interactions between the two negative charges with the positive core of protamine and siRNA anchors the peptide into the formulation, exposing the more hydrophobic residues to the aqueous solution, inducing aggregation. We see evidence of this, with the addition of (R)-DOTAP and hypothesize the aggregates are dispersed by the hydrophobic interactions of (R)-DOTAP interacting with the Trp2 hydrophobic resides.

Future advances in this formulation should address a new target, to see if more controlled growth reduction can be initiated due to the non-specific *in vivo* activation of T cells we observed (**Figure 5C**). Also, while the structural organization of the particles ensures the protection of the siRNA from the external solution by the layer of Trp2 and (R)-DOTAP, aggregates have shown more drainage into the lymph nodes. Therefore, certain techniques that could maintain the structural organization (and protection of the siRNA), potentially allowing the particles to associate in a network which would help delivery, faster drainage and immune response.

CHAPTER 5

DISCUSSION

5.1 DISCUSSION OF RESEARCH RESULTS AND FUTURE PLANS

The DOTAP enantiomers were investigated as adjuvants in an E7 peptide/lipid complex as a therapeutic vaccine in an established murine cervical cancer model. Delivery *in vivo* yielded tumor regression with (R)-DOTAP/E7 complexes similar to that with a racemic DOTAP with E7 peptide, in a dose-dependant fashion. These data are supported by IFN-γ production by $CD8^+$ splenocytes, in vivo cytotoxic T-lymphocytes (CTL) response, $CD8^+$ tumor-infiltrating lymphocytes (TIL), and IFN-γ production by $CD8^+$ TIL in (R)-DOTAP/E7-vaccinated mice. With (S)-DOTAP/E7 is delivered, tumor progression is delayed. While IFN-γ production is absent from $CD8^+$ splenocytes in mice vaccinated with (S)-DOTAP/E7, IFN-γ production by $CD8^+$ TIL is present, supporting our hypothesis that (S)-DOTAP has limited activity. Activation of bone marrow-derived dendritic cells by the enantiomeric formulations has also been evaluated, as well as cytokine production and toxicity with no considerable differences between the groups.

The results show the DOTAP enantiomers act differently as adjuvants in vivo, with (R)-DOTAP being more effective at stimulating a $CD8^+$ anti-tumor response. Investigation of the specific mechanism of (R)-DOTAP should be further explored. If there potentially exists a DOTAP-specific receptor, differences in affinity binding could explain the pharmacodynamic disparities between (R) and (S). However, and perhaps more interesting is if (S)-DOTAP stimulates an inhibitory immune response. This action would greatly expand the use of (S)-DOTAP into an adjuvant for autoimmune disease.

However, the differences *in vivo* between (R)- and (S)-DOTAP do not clearly explain why one enantiomer works and the other is less effective. We consider the role of (S)-DOTAP as less immunostimulatory, rather than wholly ineffective. This is supported by the statistically significant tumor growth delay of the (S)-DOTAP/E7 treated mouse compared to control (**Figure 2.1**). Also from the tumor growth delay data, we must consider that the racemic mixture of DOTAP/E7, contains 50% (S)-DOTAP. If the (S) enantiomer had immunosuppressive effects, we would expect to see less growth delay from the racemic mixture than from pure (R)-DOTAP.

It is plausible that a receptor or reaction exists that is stereospecific for DOTAP. This could occur in one of two ways; increased stability of the (R)-DOTAP lipid *in vivo* causing preferential cleavage of (S)-DOTAP or an immunostimulatory receptor for which (R)-DOTAP has higher affinity. Stereospecific activity of lipases has been established in the literature, and is the most likely cause of decreased (S)-DOTAP acitivty.[302; 303; 304; 305; 306] Under this hypothesis, enough (S)-DOTAP would be cleaved as to prevent specific interaction with APCs. Additionally, racemic DOTAP complexes would be able to retain enough (R)-DOTAP for eventual delivery an signally. It is unlikely that there is a specific

DOTAP receptor, but rather, DOTAP signals through an established pathway that is TNF-α independent (unpublished work by Wei-Yun Sheng, Huang Lab). DOTAP is most commonly used in immunology as a delivery vehicle for nucleic acids (particularly CpG), a specific DOTAP receptor has not been investigated. More could be understood on the location of DOTAP signaling (either intracellular, or extracellular) by the creation of particles with asymmetric bilayers, delivery *in vitro* and assessment of CD86 upregulation. Additionally, by parcing out the location of APC activation, the stereospecific lipase activity could be investigated in further depth, comparing lipase activity intracellularly, in cell culture media, in subcutaneous space, or after intravenous delivery. (R)- and (S)-DOTAP have not been compared via different methods of delivery and any new data from different delivery mechanisms may help explain the differences in activity.

Use of (R)-DOTAP was expanded to deliver self-antigen in an aggressive murine solid tumor melanoma model. (R)-DOTAP/Trp2 peptide complexes showed decreasing size and charge with increasing peptide concentration, taking a rod-shape at highest concentrations. The particles were stable for at 2 weeks at 4°C. A dose of 75nmol Trp2 (formulated in (R)-DOTAP) was able to show statistically significant tumor growth delay compared to lower doses of 5 and 25nmol which were no different than untreated tumors. (R)-DOTAP/Trp2 (75nmol) treated mice also showed increased T cell IFN-γ secretion after restimulation with Trp2, as well as CTL activity *in vivo.* This vaccination group also showed the highest population of functionally active tumor-infiltrating lymphocytes, indicated by IFN-γ secretion after restimulation with Trp2. We showed (R)-DOTAP able to break tolerance in an aggressive self-antigen tumor model.

The formulation of Trp2 peptide antigen posed interesting challenges in this work. Increasing the peptide solubility allowed for an increased deliverable dose. We hypothesize a specific interaction between the hydrophobic amino acids in the peptide and the hydrophobic tails of (R)-DOTAP due to the shape of the particles seen in **Figure 3.2D**. Previous examination of DOTAP and E7 peptide formulations had shown rounded complexes (data not shown). E7 peptide is highly soluble in aqueous solution but only 30 % of peptide is entrapped in DOTAP complexes, compared to nearly 100 % of Trp2 (**Table 2.1, Figure 3.2B)**. The role of hydrophobic interactions can increase peptide loading in lipid carriers, as we have seen with lipidated E7.[235] Understanding more about the characteristics of peptides that increase loading may facilitate identification of candidate antigens that would benefit most from lipid delivery. Trp2 peptide could be used as a model antigen to expanding the application of (R)-DOTAP/amplipathic peptide formulation. Selective modification of individual residues (either to glycine or phenylalanine) and a rapid screening process (such as the experiments presented in **Figure 3.2**), may lead to further understanding of ideal antigen candidates. By characterizing the structure-function relationship, only the most suitable peptides can be pursued. While we don't claim that lipid-based delivery is the best delivery option for every antigen in every situation; understanding how to maximize the potential of (R)-DOTAP could lead to many interesting projects in the future.

The (R)-DOTAP/Trp2 vaccine may be efficacious in models other than murine melanoma. The vaccine should be tested in additional murine tumor models that express Trp2, such as glioblastoma, to verify the robustness of the treatment. The Trp2 peptide epitope used, SVYDFFVWL, is also HLA-A2 restricted. Investigation with human

leukocytes *ex vivo* may increase understanding of the potential for expansion into clinical testing.

Expanding the versatility of (R)-DOTAP/Trp2, we developed a vaccine formulation to silencing the PD-L1 pathway in DCs, to amplify the immune response. The tri-modal vaccine, RTP, combined delivery of (R)-DOTAP, Trp2 peptide and PD-L1 siRNA to DCs. The spherical particles were stabilized by a layered approach, first charge-charge interactions to capture the siRNA, followed by hydrophobic interactions to complex the amphipathic peptide antigen, which interacted both with the positively charged core as well as the hydrophobic chains of the lipid adjuvant. The successful incorporation of siRNA into the particles yielded a versatile vehicle that could potentially deliver alternative siRNA sequences targeting other genes, or even deliver DNA to upregulate certain genes in DCs. (R)-DOTAP/Trp2/PD-L1 siRNA particles, termed RTP, were found to induce IFN-γ secretion *in vitro* and *in vivo*. Interestingly, the IFN-γ response was the same for target peptide (Trp2)-pulsed and off-target (Ova)-pulsed peptides, indicating the stimulation of a non-specific cell population, we hypothesize to be NKT cells. However, the *in vivo* result of tumor growth delay is puzzling as the IFN-γ production does not correlate. For further investigation, alternative genetic cargo may be of greater effect. Delivering plasmids of GM-CSF or IL-2 in the RT(DNA) particles could increase maturation of the APCs. Alternatively, a peptide and DNA vaccine could be directly compared, measuring the response to each antigen. The difficulty of the RTC formulation is the dependency of the particle on the structure of Trp2 peptide. As mentioned above, further investigation of the crucial number of hydrophobic resides would enable us to understand the anchorage of the peptide to (R)-DOTAP. For RTC

formulation, we hypothesize that the negative charge on the carboxylic acid at the distal end of the peptide assists in complexing the peptide to the protamine-DNA core.

Delivery is another opportunity to improve this formulation. After subcutaneous delivery, particles were found in draining lymph nodes. Macrophages and DCs showed down regulation of PD-L1 surface expression after *in vivo* dosing. However, consistent down regulation was not observed. This indicates a potential for improvement of the vaccine. While targeted or larger particles often yield higher uptake by APCs, protection of the siRNA cargo is paramount. Therefore, it would be valuable to investigate a way to network the small (80nm) spherical particles together to create larger aggregates, more attractive to APC uptake. By incorporating a biotinylated lipid into the (R)-DOTAP bilayer during particle coating, and subsequent incubation with avadin, we believe it possibility to produce large spiderweb-like networks of particles, with the siRNA protected in the particle core. In investigations of building liposomes-within-liposomes, a similar utilization of biotin-avidin was employed, creating web-like structures.[307; 308] Alternatively, targeting to macrophages using mannose or mannin has been widely investigated and could enhance in this formulation by surface coating of mannin, or incorporation of mannose-labeled lipids into the bilayer.

5.2 ENDING REMARKS

In closing, this work established the stereospecific adjuvanticity of (R)-DOTAP in several models. Investigation of (R)-DOTAP with different peptide antigens lead to diverse formulation characteristics. Further, incorporation of siRNA into the melanoma optimized particle created an increased tumor growth delay, and versatility of siRNA delivery cargo. Cancer immunotherapy is a field with growing clinical demand, and the next generation of treatments will evolve from novel investigations such as this.

REFERENCES

1. Alving, C. R. (1991). "Liposomes as carriers of antigens and adjuvants." J Immunol Methods **140**(1): 1-13.

2. Steers, N. J.,K. K. Peachman, et al. (2009). "Liposome-encapsulated HIV-1 Gag p24 containing lipid A induces effector CD4+ T-cells, memory CD8+ T-cells, and pro-inflammatory cytokines." Vaccine **27**(49): 6939-6949.

3. Bhowmick, S.,T. Mazumdar, et al. (2010). "Comparison of liposome based antigen delivery systems for protection against Leishmania donovani." J Control Release **141**(2): 199-207.

4. Paavonen, J.,D. Jenkins, et al. (2007). "Efficacy of a prophylactic adjuvanted bivalent L1 virus-like-particle vaccine against infection with human papillomavirus types 16 and 18 in young women: an interim analysis of a phase III double-blind, randomised controlled trial." Lancet **369**(9580): 2161-2170.

5. Romanowski, B.,P. C. de Borba, et al. (2009). "Sustained efficacy and immunogenicity of the human papillomavirus (HPV)-16/18 AS04-adjuvanted vaccine: analysis of a randomised placebo-controlled trial up to 6.4 years." Lancet **374**(9706): 1975-1985.

6. Ulrich, J. T. and K. R. Myers (1995). "Monophosphoryl lipid A as an adjuvant. Past experiences and new directions." Pharm Biotechnol **6**: 495-524.

7. Baldridge, J. R.,P. McGowan, et al. (2004). "Taking a Toll on human disease: Toll-like receptor 4 agonists as vaccine adjuvants and monotherapeutic agents." Expert Opin Biol Ther **4**(7): 1129-1138.

8. Mata-Haro, V.,C. Cekic, et al. (2007). "The vaccine adjuvant monophosphoryl lipid A as a TRIF-biased agonist of TLR4." Science **316**(5831): 1628-1632.

9. Casella, C. R. and T. C. Mitchell (2008). "Putting endotoxin to work for us: monophosphoryl lipid A as a safe and effective vaccine adjuvant." Cell Mol Life Sci **65**(20): 3231-3240.

10. Cekic, C.,C. R. Casella, et al. (2011). "MyD88-dependent SHIP1 regulates proinflammatory signaling pathways in dendritic cells after monophosphoryl lipid A stimulation of TLR4." J Immunol **186**(7): 3858-3865.

11. Duzgunes, N.,J. A. Goldstein, et al. (1989). "Fusion of liposomes containing a novel cationic lipid, N-[2,3-(dioleyloxy)propyl]-N,N,N-trimethylammonium: induction by multivalent anions and asymmetric fusion with acidic phospholipid vesicles." Biochemistry **28**(23): 9179-9184.

12. Christensen, D.,C. Foged, et al. (2010). "CAF01 liposomes as a mucosal vaccine adjuvant: In vitro and in vivo investigations." Int J Pharm **390**(1): 19-24.

13. Agger, E. M.,I. Rosenkrands, et al. (2008). "Cationic liposomes formulated with synthetic mycobacterial cordfactor (CAF01): a versatile adjuvant for vaccines with different immunological requirements." PLoS One **3**(9): e3116.

14. Henriksen-Lacey, M.,D. Christensen, et al. (2010). "Liposomal cationic charge and antigen adsorption are important properties for the efficient deposition of antigen at the injection site and ability of the vaccine to induce a CMI response." J Control Release **145**(2): 102-108.

15. Korsholm, K. S.,E. M. Agger, et al. (2007). "The adjuvant mechanism of cationic dimethyldioctadecylammonium liposomes." Immunology **121**(2): 216-226.

16. Henriksen-Lacey, M.,D. Christensen, et al. (2011). "Comparison of the depot effect and immunogenicity of liposomes based on dimethyldioctadecylammonium (DDA), 3beta-[N-(N',N'-Dimethylaminoethane)carbomyl] cholesterol (DC-Chol), and 1,2-Dioleoyl-3-trimethylammonium propane (DOTAP): prolonged liposome retention mediates stronger Th1 responses." Mol Pharm **8**(1): 153-161.

17. Higgins, R. J.,M. McKisic, et al. (2004). "Growth inhibition of an orthotopic glioblastoma in immunocompetent mice by cationic lipid-DNA complexes." Cancer Immunol Immunother **53**(4): 338-344.

18. Morrey, J. D.,N. E. Motter, et al. (2011). "Breaking B and T cell tolerance using cationic lipid--DNA complexes (CLDC) as a vaccine adjuvant with hepatitis B virus (HBV) surface antigen in transgenic mice expressing HBV." Antiviral Res **90**(3): 227-230.

19. Lay, M.,B. Callejo, et al. (2009). "Cationic lipid/DNA complexes (JVRS-100) combined with influenza vaccine (Fluzone) increases antibody response, cellular immunity, and antigenically drifted protection." Vaccine **27**(29): 3811-3820.

20. Kuramoto, Y.,S. Kawakami, et al. (2008). "Efficient peritoneal dissemination treatment obtained by an immunostimulatory phosphorothioate-type CpG DNA/cationic liposome complex in mice." J Control Release **126**(3): 274-280.

21. Freimark, B. D.,H. P. Blezinger, et al. (1998). "Cationic lipids enhance cytokine and cell influx levels in the lung following administration of plasmid: cationic lipid complexes." J Immunol **160**(9): 4580-4586.

22. Gao, X. and L. Huang (1991). "A novel cationic liposome reagent for efficient transfection of mammalian cells." Biochem Biophys Res Commun **179**(1): 280-285.

23. Li, S.,X. Gao, et al. (1996). "DC-Chol lipid system in gene transfer." Journal of Controlled Release **39**(2-3): 373-381.

24. Guy, B.,N. Pascal, et al. (2001). "Design, characterization and preclinical efficacy of a cationic lipid adjuvant for influenza split vaccine." Vaccine **19**(13-14): 1794-1805.

25. Myschik, J.,W. T. McBurney, et al. (2008). "Immunostimulatory lipid implants containing Quil-A and DC-cholesterol." Int J Pharm **363**(1-2): 91-98.

26. Pialoux, G.,H. Hocini, et al. (2008). "Phase I study of a candidate vaccine based on recombinant HIV-1 gp160 (MN/LAI) administered by the mucosal route to HIV-seronegative volunteers: the ANRS VAC14 study." Vaccine **26**(21): 2657-2666.

27. Brunel, F.,A. Darbouret, et al. (1999). "Cationic lipid DC-Chol induces an improved and balanced immunity able to overcome the unresponsiveness to the hepatitis B vaccine." Vaccine **17**(17): 2192-2203.

28. Vangala, A.,V. W. Bramwell, et al. (2007). "Comparison of vesicle based antigen delivery systems for delivery of hepatitis B surface antigen." J Control Release **119**(1): 102-110.

29. Walker, C.,M. Selby, et al. (1992). "Cationic lipids direct a viral glycoprotein into the class I major histocompatibility complex antigen-presentation pathway." Proc Natl Acad Sci U S A **89**(17): 7915-7918.

30. Chen, W.,W. Yan, et al. (2008). "A simple but effective cancer vaccine consisting of an antigen and a cationic lipid." Cancer Immunol Immunother **57**(4): 517-530.

31. Yan, W.,W. Chen, et al. (2008). "Reactive oxygen species play a central role in the activity of cationic liposome based cancer vaccine." J Control Release **130**(1): 22-28.

32. Yan, W.,W. Chen, et al. (2007). "Mechanism of adjuvant activity of cationic liposome: phosphorylation of a MAP kinase, ERK and induction of chemokines." Mol Immunol **44**(15): 3672-3681.

33. Vasievich, E. A.,W. Chen, et al. (2011). "Enantiospecific adjuvant activity of cationic lipid DOTAP in cancer vaccine." Cancer Immunol Immunother **60**(5): 629-638.

34. Dileo, J.,R. Banerjee, et al. (2003). "Lipid-protamine-DNA-mediated antigen delivery to antigen-presenting cells results in enhanced anti-tumor immune responses." Mol Ther **7**(5 Pt 1): 640-648.

35. Cui, Z.,S. J. Han, et al. (2004). "Coating of mannan on LPD particles containing HPV E7 peptide significantly enhances immunity against HPV-positive tumor." Pharm Res **21**(6): 1018-1025.

36. Cui, Z.,S. J. Han, et al. (2005). "Immunostimulation mechanism of LPD nanoparticle as a vaccine carrier." Mol Pharm **2**(1): 22-28.

37. Cui, Z. and L. Huang (2005). "Liposome-polycation-DNA (LPD) particle as a carrier and adjuvant for protein-based vaccines: therapeutic effect against cervical cancer." Cancer Immunol Immunother **54**(12): 1180-1190.

38. Vangasseri, D. P.,S. J. Han, et al. (2005). "Lipid-protamine-DNA-mediated antigen delivery." Curr Drug Deliv **2**(4): 401-406.

39. Vangasseri, D. P.,Z. Cui, et al. (2006). "Immunostimulation of dendritic cells by cationic liposomes." Mol Membr Biol **23**(5): 385-395.

40. Whitmore, M. M.,S. Li, et al. (2001). "Systemic administration of LPD prepared with CpG oligonucleotides inhibits the growth of established pulmonary metastases by stimulating innate and acquired antitumor immune responses." Cancer Immunol Immunother **50**(10): 503-514.

41. Ma, Z.,J. Li, et al. (2005). "Cationic lipids enhance siRNA-mediated interferon response in mice." Biochem Biophys Res Commun **330**(3): 755-759.

42. Yan, W. and L. Huang (2009). "The effects of salt on the physicochemical properties and immunogenicity of protein based vaccine formulated in cationic liposome." Int J Pharm **368**(1-2): 56-62.

43. Hawkins, L. D.,S. T. Ishizaka, et al. (2002). "A novel class of endotoxin receptor agonists with simplified structure, toll-like receptor 4-dependent immunostimulatory action, and adjuvant activity." J Pharmacol Exp Ther **300**(2): 655-661.

44. Lincopan, N.,N. M. Espindola, et al. (2009). "Novel immunoadjuvants based on cationic lipid: Preparation, characterization and activity in vivo." Vaccine **27**(42): 5760-5771.

45. Lincopan, N.,M. R. Santana, et al. (2009). "Silica-based cationic bilayers as immunoadjuvants." BMC Biotechnol **9**: 5.

46. Tanaka, T.,A. Legat, et al. (2008). "DiC14-amidine cationic liposomes stimulate myeloid dendritic cells through Toll-like receptor 4." Eur J Immunol **38**(5): 1351-1357.

47. Sasaki, S.,J. Fukushima, et al. (1997). "Human immunodeficiency virus type-1-specific immune responses induced by DNA vaccination are greatly enhanced by mannan-coated diC14-amidine." Eur J Immunol **27**(12): 3121-3129.

48. Faisal, S. M.,J. W. Chen, et al. (2011). "Immunostimulatory and antigen delivery properties of liposomes made up of total polar lipids from non-pathogenic bacteria leads to efficient induction of both innate and adaptive immune responses." Vaccine **29**(13): 2381-2391.

49. Lee, Y. S.,K. A. Lee, et al. (2011). "An alpha-GalCer analogue with branched acyl chain enhances protective immune responses in a nasal influenza vaccine." Vaccine **29**(3): 417-425.

50. Lin, Y. F.,M. C. Deng, et al. (2011). "Adjuvant effect of liposome in chicken result from induction of nitric oxide." Biomed Mater **6**(1): 015011.

51. Wakefield, A. J.,S. H. Murch, et al. (1998). "Ileal-lymphoid-nodular hyperplasia, non-specific colitis, and pervasive developmental disorder in children." Lancet **351**(9103): 637-641.

52. Wakefield, A. J. (1999). "MMR vaccination and autism." Lancet **354**(9182): 949-950.

53. Wakefield, A. (2004). "A statement by Dr Andrew Wakefield." Lancet **363**(9411): 823-824.

54. Wakefield, A. J.,P. Harvey, et al. (2004). "MMR--responding to retraction." Lancet **363**(9417): 1327-1328; discussion 1328.

55. Triozzi, P. L.,W. Aldrich, et al. (2010). "Regulation of the activity of an adeno-associated virus vector cancer vaccine administered with synthetic Toll-like receptor agonists." Vaccine.

56. Coussens, L. M. and Z. Werb (2002). "Inflammation and cancer." Nature **420**(6917): 860-867.

57. Zijlmans, H. J.,G. J. Fleuren, et al. (2006). "The absence of CCL2 expression in cervical carcinoma is associated with increased survival and loss of heterozygosity at 17q11.2." J Pathol **208**(4): 507-517.

58. Miotto, D.,P. Boschetto, et al. (2007). "CC ligand 2 levels are increased in LPS-stimulated peripheral monocytes of patients with non-small cell lung cancer." Respir Med **101**(8): 1738-1743.

59. Kuroda, T.,Y. Kitadai, et al. (2005). "Monocyte chemoattractant protein-1 transfection induces angiogenesis and tumorigenesis of gastric carcinoma in nude mice via macrophage recruitment." Clin Cancer Res **11**(21): 7629-7636.

60. Loberg, R. D.,C. Ying, et al. (2007). "CCL2 as an important mediator of prostate cancer growth in vivo through the regulation of macrophage infiltration." Neoplasia **9**(7): 556-562.

61. Bailey, C.,R. Negus, et al. (2007). "Chemokine expression is associated with the accumulation of tumour associated macrophages (TAMs) and progression in human colorectal cancer." Clin Exp Metastasis **24**(2): 121-130.

62. Kagaya, T.,Y. Nakamoto, et al. (2006). "Monocyte chemoattractant protein-1 gene delivery enhances antitumor effects of herpes simplex virus thymidine kinase/ganciclovir system in a model of colon cancer." Cancer Gene Ther **13**(4): 357-366.

63. Kross, K. W.,J. H. Heimdal, et al. (2007). "Tumour-associated macrophages secrete IL-6 and MCP-1 in head and neck squamous cell carcinoma tissue." Acta Otolaryngol **127**(5): 532-539.

64. Roca, H.,Z. S. Varsos, et al. (2009). "CCL2 and interleukin-6 promote survival of human CD11b+ peripheral blood mononuclear cells and induce M2-type macrophage polarization." J Biol Chem **284**(49): 34342-34354.

65. Allavena, P.,A. Sica, et al. (2008). "The inflammatory micro-environment in tumor progression: The role of tumor-associated macrophages." Crit Rev Oncol Hematol **66**(1): 1-9.

66. Balkwill, F. and A. Mantovani (2001). "Inflammation and cancer: back to Virchow?" Lancet **357**(9255): 539-545.

67. Klimp, A. H.,E. G. de Vries, et al. (2002). "A potential role of macrophage activation in the treatment of cancer." Crit Rev Oncol Hematol **44**(2): 143-161.

68. Werno, C.,H. Menrad, et al. (2010). "Knockout of HIF-1alpha in tumor-associated macrophages enhances M2 polarization and attenuates their pro-angiogenic responses." Carcinogenesis **31**(10): 1863-1872.

69. Koga, M.,H. Kai, et al. (2008). "Mutant MCP-1 therapy inhibits tumor angiogenesis and growth of malignant melanoma in mice." Biochem Biophys Res Commun **365**(2): 279-284.

70. Gazzaniga, S.,A. I. Bravo, et al. (2007). "Targeting tumor-associated macrophages and inhibition of MCP-1 reduce angiogenesis and tumor growth in a human melanoma xenograft." J Invest Dermatol **127**(8): 2031-2041.

71. Guiducci, C.,A. P. Vicari, et al. (2005). "Redirecting in vivo elicited tumor infiltrating macrophages and dendritic cells towards tumor rejection." Cancer Res **65**(8): 3437-3446.

72. Luo, Y.,H. Zhou, et al. (2006). "Targeting tumor-associated macrophages as a novel strategy against breast cancer." J Clin Invest **116**(8): 2132-2141.

73. Gabrilovich, Y. (2010). Eur J Immunol.

74. Yang, R. and R. Roden (2007). Cancer Res **67**: 426.

75. Yang, R.,Z. Cai, et al. (2006). "CD80 in immune suppression by mouse ovarian carcinoma-associated Gr-1+CD11b+ myeloid cells." Cancer Res **66**(13): 6807-6815.

76. Movahedi, K.,M. Guilliams, et al. (2008). "Identification of discrete tumor-induced myeloid-derived suppressor cell subpopulations with distinct T cell-suppressive activity." Blood **111**(8): 4233-4244.

77. Habibi, M.,M. Kmieciak, et al. (2009). "Radiofrequency thermal ablation of breast tumors combined with intralesional administration of IL-7 and IL-15 augments anti-tumor immune responses and inhibits tumor development and metastasis." Breast Cancer Res Treat **114**(3): 423-431.

78. Yang, L.,J. Huang, et al. (2008). "Abrogation of TGF beta signaling in mammary carcinomas recruits Gr-1+CD11b+ myeloid cells that promote metastasis." Cancer Cell **13**(1): 23-35.

79. Kim, H. S.,H. M. Park, et al. (2010). "Dendritic cell vaccine in addition to FOLFIRI regimen improve antitumor effects through the inhibition of immunosuppressive cells in murine colorectal cancer model." Vaccine.

80. Murdoch, C.,M. Muthana, et al. (2008). "The role of myeloid cells in the promotion of tumour angiogenesis." Nat Rev Cancer **8**(8): 618-631.

81. Du, W.-J.,J.-P. Yu, et al. (2010). Chinese Journal of Cancer Biotherapy **17**(5).

82. Kusmartsev, S.,Y. Nefedova, et al. (2004). "Antigen-specific inhibition of CD8+ T cell response by immature myeloid cells in cancer is mediated by reactive oxygen species." J Immunol **172**(2): 989-999.

83. Li, H.,Y. Han, et al. (2009). "Cancer-expanded myeloid-derived suppressor cells induce anergy of NK cells through membrane-bound TGF-beta 1." J Immunol **182**(1): 240-249.

84. Song, X.,Y. Krelin, et al. (2005). "CD11b+/Gr-1+ immature myeloid cells mediate suppression of T cells in mice bearing tumors of IL-1beta-secreting cells." J Immunol **175**(12): 8200-8208.

85. Young, M. R.,K. Kolesiak, et al. (1999). "Chemoattraction of femoral CD34+ progenitor cells by tumor-derived vascular endothelial cell growth factor." Clin Exp Metastasis **17**(10): 881-888.

86. Bronte, V.,E. Apolloni, et al. (2000). "Identification of a CD11b(+)/Gr-1(+)/CD31(+) myeloid progenitor capable of activating or suppressing CD8(+) T cells." Blood **96**(12): 3838-3846.

87. Serafini, P.,R. Carbley, et al. (2004). "High-dose granulocyte-macrophage colony-stimulating factor-producing vaccines impair the immune response through the recruitment of myeloid suppressor cells." Cancer Res **64**(17): 6337-6343.

88. Sinha, P.,V. K. Clements, et al. (2007). "Cross-talk between myeloid-derived suppressor cells and macrophages subverts tumor immunity toward a type 2 response." J Immunol **179**(2): 977-983.

89. Ohkusu-Tsukada, K.,S. Ohta, et al. (2011). "Adjuvant effects of formalin-inactivated HSV through activation of dendritic cells and inactivation of myeloid-derived suppressor cells in cancer immunotherapy." Int J Cancer **128**(1): 119-131.

90. Mirza, N.,M. Fishman, et al. (2006). "All-trans-retinoic acid improves differentiation of myeloid cells and immune response in cancer patients." Cancer Res **66**(18): 9299-9307.

91. Gonzalez-Aparicio, M.,P. Alzuguren, et al. (2010). "Oxaliplatin in combination with liver-specific expression of interleukin 12 reduces the immunosuppressive microenvironment of tumours and eradicates metastatic colorectal cancer in mice " Gut.

92. Suzuki, E.,V. Kapoor, et al. (2005). "Gemcitabine selectively eliminates splenic Gr-1+/CD11b+ myeloid suppressor cells in tumor-bearing animals and enhances antitumor immune activity." Clin Cancer Res **11**(18): 6713-6721.

93. Yang and Ansell (2009). Amer J Immunol.

94. Ahmadzadeh, M.,A. Felipe-Silva, et al. (2008). "FOXP3 expression accurately defines the population of intratumoral regulatory T cells that selectively accumulate in metastatic melanoma lesions." Blood.

95. Goforth, R.,A. K. Salem, et al. (2008). "Immune stimulatory antigen loaded particles combined with depletion of regulatory T-cells induce potent tumor specific immunity in a mouse model of melanoma." Cancer Immunol Immunother.

96. Woo, E. Y.,C. S. Chu, et al. (2001). "Regulatory CD4(+)CD25(+) T cells in tumors from patients with early-stage non-small cell lung cancer and late-stage ovarian cancer." Cancer Res **61**(12): 4766-4772.

97. Lagouros, E.,D. Salomao, et al. (2009). "Infiltrative T regulatory cells in enucleated uveal melanomas." Trans Am Ophthalmol Soc **107**: 223-228.

98. Valdman, A.,S. J. Jaraj, et al. (2010). "Distribution of Foxp3-, CD4- and CD8-positive lymphocytic cells in benign and malignant prostate tissue." APMIS **118**(5): 360-365.

99. El Andaloussi, A.,Y. Han, et al. (2006). "Prolongation of survival following depletion of CD4+CD25+ regulatory T cells in mice with experimental brain tumors." J Neurosurg **105**(3): 430-437.

100. Kobayashi, N.,N. Hiraoka, et al. (2007). "FOXP3+ regulatory T cells affect the development and progression of hepatocarcinogenesis." Clin Cancer Res **13**(3): 902-911.

101. Eikawa, S. (2010). J Immunol.

102. Curiel, T. J.,G. Coukos, et al. (2004). "Specific recruitment of regulatory T cells in ovarian carcinoma fosters immune privilege and predicts reduced survival." Nat Med **10**(9): 942-949.

103. Jacobs, J. F.,A. J. Idema, et al. (2010). "Prognostic significance and mechanism of Treg infiltration in human brain tumors." J Neuroimmunol **225**(1-2): 195-199.

104. Mailloux, A. W.,A. M. Clark, et al. (2010). "NK depletion results in increased CCL22 secretion and Treg levels in Lewis lung carcinoma via the accumulation of CCL22-secreting CD11b+CD11c+ cells." Int J Cancer **127**(11): 2598-2611.

105. Tan, M. C.,P. S. Goedegebuure, et al. (2009). "Disruption of CCR5-dependent homing of regulatory T cells inhibits tumor growth in a murine model of pancreatic cancer." J Immunol **182**(3): 1746-1755.

106. Mellor, A. L. and D. H. Munn (2004). "IDO expression by dendritic cells: tolerance and tryptophan catabolism." Nat Rev Immunol **4**(10): 762-774.

107. Levings, M. K. and M. G. Roncarolo (2000). "T-regulatory 1 cells: a novel subset of CD4 T cells with immunoregulatory properties." J Allergy Clin Immunol **106**(1 Pt 2): S109-112.

108. O'Garra, A.,P. L. Vieira, et al. (2004). "IL-10-producing and naturally occurring CD4+ Tregs: limiting collateral damage." J Clin Invest **114**(10): 1372-1378.

109. Curtin, J. F.,M. Candolfi, et al. (2008). "Treg depletion inhibits efficacy of cancer immunotherapy: implications for clinical trials." PLoS One **3**(4): e1983.

110. Jacobs, C.,P. Duewell, et al. (2010). "An ISCOM vaccine combined with a TLR9 agonist breaks immune evasion mediated by regulatory T cells in an orthotopic model of pancreatic carcinoma." Int J Cancer.

111. Rech, A. J. and R. H. Vonderheide (2009). "Clinical use of anti-CD25 antibody daclizumab to enhance immune responses to tumor antigen vaccination by targeting regulatory T cells." Ann N Y Acad Sci **1174**: 99-106.

112. Morse, M. A.,A. C. Hobeika, et al. (2008). "Depletion of human regulatory T cells specifically enhances antigen-specific immune responses to cancer vaccines." Blood **112**(3): 610-618.

113. Rasku, M. A.,A. L. Clem, et al. (2008). "Transient T cell depletion causes regression of melanoma metastases." J Transl Med **6**: 12.

114. Matsushita, N.,S. A. Pilon-Thomas, et al. (2008). "Comparative methodologies of regulatory T cell depletion in a murine melanoma model." J Immunol Methods **333**(1-2): 167-179.

115. Quezada, S. A.,K. S. Peggs, et al. (2006). "CTLA4 blockade and GM-CSF combination immunotherapy alters the intratumor balance of effector and regulatory T cells." J Clin Invest **116**(7): 1935-1945.

116. Kraman, M.,P. J. Bambrough, et al. (2010). "Suppression of Antitumor Immunity by Stromal Cells Expressing Fibroblast Activation Protein-{alpha}." Science **330**(6005): 827-830.

117. Kircheis, R.,A. Kichler, et al. (1997). "Coupling of cell-binding ligands to polyethylenimine for targeted gene delivery." Gene Ther **4**(5): 409-418.

118. Houk, B. E.,G. Hochhaus, et al. (1999). "Kinetic modeling of plasmid DNA degradation in rat plasma." AAPS PharmSci **1**(3): E9.

119. Papahadjopoulos, D.,T. M. Allen, et al. (1991). "Sterically stabilized liposomes: improvements in pharmacokinetics and antitumor therapeutic efficacy." Proc Natl Acad Sci U S A **88**(24): 11460-11464.

120. Woodle, M. C. and D. D. Lasic (1992). "Sterically stabilized liposomes." Biochim Biophys Acta **1113**(2): 171-199.

121. Woodle, M. C.,K. K. Matthay, et al. (1992). "Versatility in lipid compositions showing prolonged circulation with sterically stabilized liposomes." Biochim Biophys Acta **1105**(2): 193-200.

122. Woodle, M. C.,G. Storm, et al. (1992). "Prolonged systemic delivery of peptide drugs by long-circulating liposomes: illustration with vasopressin in the Brattleboro rat." Pharm Res **9**(2): 260-265.

123. Seymour, L. W. (1992). "Passive tumor targeting of soluble macromolecules and drug conjugates." Crit Rev Ther Drug Carrier Syst **9**(2): 135-187.

124. Jain, R. K. (1997). "Delivery of molecular and cellular medicine to solid tumors." Adv Drug Deliv Rev **26**(2-3): 71-90.

125. Eatock, M. M.,A. Schatzlein, et al. (2000). "Tumour vasculature as a target for anticancer therapy." Cancer Treat Rev **26**(3): 191-204.

126. Maeda, H.,J. Wu, et al. (2000). "Tumor vascular permeability and the EPR effect in macromolecular therapeutics: a review." J Control Release **65**(1-2): 271-284.

127. Yuan, F.,M. Leunig, et al. (1994). "Microvascular permeability and interstitial penetration of sterically stabilized (stealth) liposomes in a human tumor xenograft." Cancer Res **54**(13): 3352-3356.

128. Gabizon, A.,R. Catane, et al. (1994). "Prolonged circulation time and enhanced accumulation in malignant exudates of doxorubicin encapsulated in polyethylene-glycol coated liposomes." Cancer Res **54**(4): 987-992.

129. Khalil, I. A.,K. Kogure, et al. (2006). "Uptake pathways and subsequent intracellular trafficking in nonviral gene delivery." Pharmacol Rev **58**(1): 32-45.

130. Godbey, W. T.,K. K. Wu, et al. (1999). "Tracking the intracellular path of poly(ethylenimine)/DNA complexes for gene delivery." Proc Natl Acad Sci U S A **96**(9): 5177-5181.

131. Zuhorn, I. S. and D. Hoekstra (2002). "On the mechanism of cationic amphiphile-mediated transfection. To fuse or not to fuse: is that the question?" J Membr Biol **189**(3): 167-179.

132. Douglas, K. L.,C. A. Piccirillo, et al. (2008). "Cell line-dependent internalization pathways and intracellular trafficking determine transfection efficiency of nanoparticle vectors." Eur J Pharm Biopharm **68**(3): 676-687.

133. Mukherjee, A.,T. K. Prasad, et al. (2005). "Haloperidol-associated stealth liposomes: a potent carrier for delivering genes to human breast cancer cells." J Biol Chem **280**(16): 15619-15627.

134. Dauty, E. and A. S. Verkman (2005). "Actin cytoskeleton as the principal determinant of size-dependent DNA mobility in cytoplasm: a new barrier for non-viral gene delivery." J Biol Chem **280**(9): 7823-7828.

135. Lukacs, G. L.,P. Haggie, et al. (2000). "Size-dependent DNA mobility in cytoplasm and nucleus." J Biol Chem **275**(3): 1625-1629.

136. Hebert, E. (2003). "Improvement of exogenous DNA nuclear importation by nuclear localization signal-bearing vectors: a promising way for non-viral gene therapy?" Biol Cell **95**(2): 59-68.

137. Pante, N. and M. Kann (2002). "Nuclear pore complex is able to transport macromolecules with diameters of about 39 nm." Mol Biol Cell **13**(2): 425-434.

138. Felgner, P. L.,T. R. Gadek, et al. (1987). "Lipofection: a highly efficient, lipid-mediated DNA-transfection procedure." Proc Natl Acad Sci U S A **84**(21): 7413-7417.

139. Quattrone, A.,L. Papucci, et al. (1994). "Inhibition of MDR1 gene expression by antimessenger oligonucleotides lowers multiple drug resistance." Oncol Res **6**(7): 311-320.

140. Faneca, H.,A. S. Cabrita, et al. (2007). "Evaluation of the antitumoral effect mediated by IL-12 and HSV-tk genes when delivered by a novel lipid-based system." Biochim Biophys Acta **1768**(5): 1093-1102.

141. Schenkman, S.,P. S. Araujo, et al. (1981). "Effects of temperature and lipid composition on the serum albumin-induced aggregation and fusion of small unilamellar vesicles." Biochim Biophys Acta **649**(3): 633-647.

142. Lee, R. J. and L. Huang (1996). "Folate-targeted, anionic liposome-entrapped polylysine-condensed DNA for tumor cell-specific gene transfer." J Biol Chem **271**(14): 8481-8487.

143. Li, S. D.,S. Chono, et al. (2008). "Efficient oncogene silencing and metastasis inhibition via systemic delivery of siRNA." Mol Ther **16**(5): 942-946.

144. Kim, J.,W. J. Kim, et al. (2006). "Release characteristics of quinupramine from the ethylene-vinyl acetate matrix." Int J Pharm **315**(1-2): 134-139.

145. Li, S.,W. Dong, et al. (2007). "Polyethylenimine-complexed plasmid particles targeting focal adhesion kinase function as melanoma tumor therapeutics." Mol Ther **15**(3): 515-523.

146. Coll, J. L.,P. Chollet, et al. (1999). "In vivo delivery to tumors of DNA complexed with linear polyethylenimine." Hum Gene Ther **10**(10): 1659-1666.

147. Rozema, D. B.,D. L. Lewis, et al. (2007). "Dynamic PolyConjugates for targeted in vivo delivery of siRNA to hepatocytes." Proc Natl Acad Sci U S A **104**(32): 12982-12987.

148. Gonzalez, H.,S. J. Hwang, et al. (1999). "New class of polymers for the delivery of macromolecular therapeutics." Bioconjug Chem **10**(6): 1068-1074.

149. Bellocq, N. C.,S. H. Pun, et al. (2003). "Transferrin-containing, cyclodextrin polymer-based particles for tumor-targeted gene delivery." Bioconjug Chem **14**(6): 1122-1132.

150. Hu-Lieskovan, S.,J. D. Heidel, et al. (2005). "Sequence-specific knockdown of EWS-FLI1 by targeted, nonviral delivery of small interfering RNA inhibits tumor growth in a murine model of metastatic Ewing's sarcoma." Cancer Res **65**(19): 8984-8992.

151. Bartlett, D. W. and M. E. Davis (2007). "Physicochemical and biological characterization of targeted, nucleic acid-containing nanoparticles." Bioconjug Chem **18**(2): 456-468.

152. Yockman, J. W.,A. Maheshwari, et al. (2003). "Tumor regression by repeated intratumoral delivery of water soluble lipopolymers/p2CMVmIL-12 complexes." J Control Release **87**(1-3): 177-186.

153. Omidi, Y.,A. J. Hollins, et al. (2005). "Polypropylenimine dendrimer-induced gene expression changes: the effect of complexation with DNA, dendrimer generation and cell type." J Drug Target **13**(7): 431-443.

154. Behr, J. P. (1997). "The proton sponge: A trick to enter cells the viruses did not exploit." Chimia **51**(1-2): 34-36.

155. Manunta, M.,P. H. Tan, et al. (2004). "Gene delivery by dendrimers operates via a cholesterol dependent pathway." Nucleic Acids Res **32**(9): 2730-2739.

156. Manunta, M.,B. J. Nichols, et al. (2006). "Gene delivery by dendrimers operates via different pathways in different cells, but is enhanced by the presence of caveolin." J Immunol Methods **314**(1-2): 134-146.

157. Zhang, X. Q.,J. Intra, et al. (2007). "Conjugation of polyamidoamine dendrimers on biodegradable microparticles for nonviral gene delivery." Bioconjug Chem **18**(6): 2068-2076.

158. Zhang, X. Q.,X. L. Wang, et al. (2005). "In vitro gene delivery using polyamidoamine dendrimers with a trimesyl core." Biomacromolecules **6**(1): 341-350.

159. Morris, M. C.,E. Gros, et al. (2007). "A non-covalent peptide-based carrier for in vivo delivery of DNA mimics." Nucleic Acids Res **35**(7): e49.

160. Kumar, P.,H. Wu, et al. (2007). "Transvascular delivery of small interfering RNA to the central nervous system." Nature **448**(7149): 39-43.

161. Liu, F.,Y. K. Song, et al. (1999). "Hydrodynamics-based transfection in animals by systemic administration of plasmid DNA." Gene Therapy **6**(7): 1258-1266.

162. Pirollo, K. F.,G. Zon, et al. (2006). "Tumor-targeting nanoimmunoliposome complex for short interfering RNA delivery." Hum Gene Ther **17**(1): 117-124.

163. Wu, J.,M. H. Nantz, et al. (2002). "Targeting hepatocytes for drug and gene delivery: emerging novel approaches and applications." Front Biosci **7**: d717-725.

164. Yu, F.,T. Jiang, et al. (2007). "Galactosylated liposomes as oligodeoxynucleotides carrier for hepatocyte-selective targeting." Pharmazie **62**(7): 528-533.

165. Cotten, M.,F. Langle-Rouault, et al. (1990). "Transferrin-polycation-mediated introduction of DNA into human leukemic cells: stimulation by agents that affect the survival of transfected DNA or modulate transferrin receptor levels." Proc Natl Acad Sci U S A **87**(11): 4033-4037.

166. Stavridis, J. C.,G. Deliconstantinos, et al. (1986). "Construction of transferrin-coated liposomes for in vivo transport of exogenous DNA to bone marrow erythroblasts in rabbits." Exp Cell Res **164**(2): 568-572.

167. Joshee, N.,D. R. Bastola, et al. (2002). "Transferrin-facilitated lipofection gene delivery strategy: characterization of the transfection complexes and intracellular trafficking." Hum Gene Ther **13**(16): 1991-2004.

168. Cheng, P. W. (1996). "Receptor ligand-facilitated gene transfer: enhancement of liposome-mediated gene transfer and expression by transferrin." Hum Gene Ther **7**(3): 275-282.

169. Rettig, W. J.,P. Garin-Chesa, et al. (1988). "Cell-surface glycoproteins of human sarcomas: differential expression in normal and malignant tissues and cultured cells." Proc Natl Acad Sci U S A **85**(9): 3110-3114.

170. Campbell, I. G.,T. A. Jones, et al. (1991). "Folate-binding protein is a marker for ovarian cancer." Cancer Res **51**(19): 5329-5338.

171. Coney, L. R.,A. Tomassetti, et al. (1991). "Cloning of a tumor-associated antigen: MOv18 and MOv19 antibodies recognize a folate-binding protein." Cancer Res **51**(22): 6125-6132.

172. Weitman, S. D.,R. H. Lark, et al. (1992). "Distribution of the folate receptor GP38 in normal and malignant cell lines and tissues." Cancer Res **52**(12): 3396-3401.

173. Garin-Chesa, P.,I. Campbell, et al. (1993). "Trophoblast and ovarian cancer antigen LK26. Sensitivity and specificity in immunopathology and molecular identification as a folate-binding protein." Am J Pathol **142**(2): 557-567.

174. Franklin, W. A.,M. Waintrub, et al. (1994). "New anti-lung-cancer antibody cluster 12 reacts with human folate receptors present on adenocarcinoma." Int J Cancer Suppl **8**: 89-95.

175. Holm, J.,S. I. Hansen, et al. (1994). "Folate receptor of human mammary adenocarcinoma." Apmis **102**(6): 413-419.

176. Ross, J. F.,P. K. Chaudhuri, et al. (1994). "Differential regulation of folate receptor isoforms in normal and malignant tissues in vivo and in established cell lines. Physiologic and clinical implications." Cancer **73**(9): 2432-2443.

177. Zhao, X. B.,N. Muthusamy, et al. (2007). "Cholesterol as a bilayer anchor for PEGylation and targeting ligand in folate-receptor-targeted liposomes." J Pharm Sci **96**(9): 2424-2435.

178. Wang, S. and P. S. Low (1998). "Folate-mediated targeting of antineoplastic drugs, imaging agents, and nucleic acids to cancer cells." J Control Release **53**(1-3): 39-48.

179. Guo, W. and R. L. Lee (1999). "Receptor-targeted gene delivery via folate-conjugated polyethylenimine." AAPS PharmSci **1**(4): E19.

180. Mislick, K. A.,J. D. Baldeschwieler, et al. (1995). "Transfection of folate-polylysine DNA complexes: evidence for lysosomal delivery." Bioconjug Chem **6**(5): 512-515.

181. Wolfe, S. A., Jr.,S. G. Culp, et al. (1989). "Sigma-receptors in endocrine organs: identification, characterization, and autoradiographic localization in rat pituitary, adrenal, testis, and ovary." Endocrinology **124**(3): 1160-1172.

182. Hellewell, S. B.,A. Bruce, et al. (1994). "Rat liver and kidney contain high densities of sigma 1 and sigma 2 receptors: characterization by ligand binding and photoaffinity labeling." Eur J Pharmacol **268**(1): 9-18.

183. Novakova, M.,V. Bruderova, et al. (2007). "Modulation of expression of the sigma receptors in the heart of rat and mouse in normal and pathological conditions." Gen Physiol Biophys **26**(2): 110-117.

184. Vilner, B. J.,C. S. John, et al. (1995). "Sigma-1 and sigma-2 receptors are expressed in a wide variety of human and rodent tumor cell lines." Cancer Res **55**(2): 408-413.

185. Vilner, B. J.,B. R. de Costa, et al. (1995). "Cytotoxic effects of sigma ligands: sigma receptor-mediated alterations in cellular morphology and viability." J Neurosci **15**(1 Pt 1): 117-134.

186. Mach, R. H.,Y. Huang, et al. (2004). "Conformationally-flexible benzamide analogues as dopamine D3 and sigma 2 receptor ligands." Bioorg Med Chem Lett **14**(1): 195-202.

187. Banerjee, R.,P. Tyagi, et al. (2004). "Anisamide-targeted stealth liposomes: a potent carrier for targeting doxorubicin to human prostate cancer cells." Int J Cancer **112**(4): 693-700.

188. Li, S. D. and L. Huang (2006). "Surface-modified LPD nanoparticles for tumor targeting." Ann N Y Acad Sci **1082**: 1-8.

189. Li, S. D.,Y. C. Chen, et al. (2008). "Tumor-targeted Delivery of siRNA by Self-assembled Nanoparticles." Mol Ther **16**(1): 163-169.

190. Li, S. D.,S. Chono, et al. (2007). "Efficient gene silencing in metastatic tumor by siRNA formulated in surface-modified nanoparticles." J Control Release.

191. Kunath, K.,T. Merdan, et al. (2003). "Integrin targeting using RGD-PEI conjugates for in vitro gene transfer." J Gene Med **5**(7): 588-599.

192. Ruoslahti, E. (1996). "RGD and other recognition sequences for integrins." Annu Rev Cell Dev Biol **12**: 697-715.

193. Tamura, T.,T. Nishi, et al. (2001). "Intratumoral delivery of interleukin 12 expression plasmids with in vivo electroporation is effective for colon and renal cancer." Hum Gene Ther **12**(10): 1265-1276.

194. Zaharoff, D. A.,R. C. Barr, et al. (2002). "Electromobility of plasmid DNA in tumor tissues during electric field-mediated gene delivery." Gene Ther **9**(19): 1286-1290.

195. McCray, A. N.,K. E. Ugen, et al. (2006). "Complete regression of established subcutaneous B16 murine melanoma tumors after delivery of an HIV-1 Vpr-expressing plasmid by in vivo electroporation." Mol Ther **14**(5): 647-655.

196. Takahashi, Y.,M. Nishikawa, et al. (2006). "Suppression of tumor growth by intratumoral injection of short hairpin RNA-expressing plasmid DNA targeting beta-catenin or hypoxia-inducible factor 1alpha." J Control Release **116**(1): 90-95.

197. Duvshani-Eshet, M.,O. Benny, et al. (2007). "Therapeutic ultrasound facilitates antiangiogenic gene delivery and inhibits prostate tumor growth." Mol Cancer Ther **6**(8): 2371-2382.

198. Henshaw, J. W.,D. A. Zaharoff, et al. (2007). "Electric field-mediated transport of plasmid DNA in tumor interstitium in vivo." Bioelectrochemistry **71**(2): 233-242.

199. Niidome, T. and L. Huang (2002). "Gene therapy progress and prospects: nonviral vectors." Gene Ther **9**(24): 1647-1652.

200. Mir, L. M.,P. H. Moller, et al. (2005). "Electric pulse-mediated gene delivery to various animal tissues." Adv Genet **54**: 83-114.

201. Favard, C.,D. S. Dean, et al. (2007). "Electrotransfer as a non viral method of gene delivery." Curr Gene Ther **7**(1): 67-77.

202. Boussif, O.,F. Lezoualc'h, et al. (1995). "A versatile vector for gene and oligonucleotide transfer into cells in culture and in vivo: polyethylenimine." Proc Natl Acad Sci U S A **92**(16): 7297-7301.

203. Sonawane, N. D.,J. R. Thiagarajah, et al. (2002). "Chloride concentration in endosomes measured using a ratioable fluorescent Cl- indicator: evidence for chloride accumulation during acidification." J Biol Chem **277**(7): 5506-5513.

204. Lewis, R. N. and R. N. McElhaney (2000). "Surface charge markedly attenuates the nonlamellar phase-forming propensities of lipid bilayer membranes: calorimetric and (31)P-nuclear magnetic resonance studies of mixtures of cationic, anionic, and zwitterionic lipids." Biophys J **79**(3): 1455-1464.

205. Sakae, M.,T. Ito, et al. (2008). "Highly efficient in vivo gene transfection by plasmid/PEI complexes coated by anionic PEG derivatives bearing carboxyl groups and RGD peptide." Biomed Pharmacother.

206. Buerli, T.,C. Pellegrino, et al. (2007). "Efficient transfection of DNA or shRNA vectors into neurons using magnetofection." Nat Protoc **2**(12): 3090-3101.

207. Scherer, F.,M. Anton, et al. (2002). "Magnetofection: enhancing and targeting gene delivery by magnetic force in vitro and in vivo." Gene Ther **9**(2): 102-109.

208. Xenariou, S.,U. Griesenbach, et al. (2006). "Using magnetic forces to enhance non-viral gene transfer to airway epithelium in vivo." Gene Ther **13**(21): 1545-1552.

209. Lee, C. H.,E. Y. Kim, et al. (2008). "Simple, efficient, and reproducible gene transfection of mouse embryonic stem cells by magnetofection." Stem Cells Dev **17**(1): 133-141.

210. Schlemmer, M.,L. H. Lindner, et al. (2004). "[Principles, technology and indication of hyperthermia and part body hyperthermia]." Radiologe **44**(4): 301-309.

211. Chen, T. H.,Y. Bae, et al. (2008). "Intelligent Biosynthetic Nanobiomaterials (IBNs) for Hyperthermic Gene Delivery." Pharm Res **25**(3): 683-691.

212. Zintchenko, A.,M. Ogris, et al. (2006). "Temperature dependent gene expression induced by PNIPAM-based copolymers: potential of hyperthermia in gene transfer." Bioconjug Chem **17**(3): 766-772.

213. McKenzie, D. L.,K. Y. Kwok, et al. (2000). "A potent new class of reductively activated peptide gene delivery agents." J Biol Chem **275**(14): 9970-9977.

214. Kwok, K. Y.,Y. Park, et al. (2003). "In vivo gene transfer using sulfhydryl cross-linked PEG-peptide/glycopeptide DNA co-condensates." J Pharm Sci **92**(6): 1174-1185.

215. Lee, H.,H. Mok, et al. (2007). "Target-specific intracellular delivery of siRNA using degradable hyaluronic acid nanogels." J Control Release **119**(2): 245-252.

216. Xiong, M. P.,M. L. Forrest, et al. (2007). "Biotin-triggered release of poly(ethylene glycol)-avidin from biotinylated polyethylenimine enhances in vitro gene expression." Bioconjug Chem **18**(3): 746-753.

217. Wang, J.,M. Jiang, et al. (2000). "On-demand electrochemical release of DNA from gold surfaces." Bioelectrochemistry **52**(1): 111-114.

218. Blay, J. (2000). "Technology evaluation: GEM-231, Hybridon Inc." Curr Opin Mol Ther **2**(4): 468-472.

219. Agrawal, S.,E. R. Kandimalla, et al. (2002). "GEM 231, a second-generation antisense agent complementary to protein kinase A RIalpha subunit, potentiates antitumor activity of irinotecan in human colon, pancreas, prostate and lung cancer xenografts." Int J Oncol **21**(1): 65-72.

220. Kaushik, A. (2001). "Leuvectin Vical Inc." Curr Opin Investig Drugs **2**(7): 976-981.

221. Gleich, L. L.,J. L. Gluckman, et al. (1998). "Alloantigen gene therapy for squamous cell carcinoma of the head and neck: results of a phase-1 trial." Arch Otolaryngol Head Neck Surg **124**(10): 1097-1104.

222. Palena, C. and J. Schlom (2010). "Vaccines against human carcinomas: strategies to improve antitumor immune responses." J Biomed Biotechnol **2010**: 380697.

223. Hsu, F. J.,C. Benike, et al. (1996). "Vaccination of patients with B-cell lymphoma using autologous antigen-pulsed dendritic cells." Nat Med **2**(1): 52-58.

224. Syrengelas, A. D.,T. T. Chen, et al. (1996). "DNA immunization induces protective immunity against B-cell lymphoma." Nat Med **2**(9): 1038-1041.

225. Nestle, F. O.,S. Alijagic, et al. (1998). "Vaccination of melanoma patients with peptide- or tumor lysate-pulsed dendritic cells." Nat Med **4**(3): 328-332.

226. De Gregorio, E.,E. Tritto, et al. (2008). "Alum adjuvanticity: unraveling a century old mystery." Eur J Immunol **38**(8): 2068-2071.

227. Harper, D. M.,E. L. Franco, et al. (2004). "Efficacy of a bivalent L1 virus-like particle vaccine in prevention of infection with human papillomavirus types 16 and 18 in young women: a randomised controlled trial." Lancet **364**(9447): 1757-1765.

228. (1992). "FDA's policy statement for the development of new stereoisomeric drugs." Chirality **4**(5): 338-340.

229. Francotte, E. R. (2001). "Enantioselective chromatography as a powerful alternative for the preparation of drug enantiomers." J Chromatogr A **906**(1-2): 379-397.

230. Simonyi, M. (1984). "On chiral drug action." Med Res Rev **4**(3): 359-413.

231. Schlossman, S. F.,J. Herman, et al. (1969). "Antigen recognition: in vitro studies on the specificity of the cellular immune response." J Exp Med **130**(5): 1031-1045.

232. Barbier, P. and C. Benezra (1982). "Stereospecificity of allergic contact dermatitis (ACD) induced by two natural enantiomers, (+)- and (-)-frullanolides, in guinea pigs." Naturwissenschaften **69**(6): 296-297.

233. Lin, K. Y.,F. G. Guarnieri, et al. (1996). "Treatment of established tumors with a novel vaccine that enhances major histocompatibility class II presentation of tumor antigen." Cancer Res **56**(1): 21-26.

234. Byers, A. M.,C. C. Kemball, et al. (2003). "Cutting edge: rapid in vivo CTL activity by polyoma virus-specific effector and memory CD8+ T cells." J Immunol **171**(1): 17-21.

235. Chen, W. and L. Huang (2008). "Induction of cytotoxic T-lymphocytes and antitumor activity by a liposomal lipopeptide vaccine." Mol Pharm **5**(3): 464-471.

236. Xu, Y. and F. C. Szoka, Jr. (1996). "Mechanism of DNA release from cationic liposome/DNA complexes used in cell transfection." Biochemistry **35**(18): 5616-5623.

237. Flaherty, K. T. (2010). "Narrative review: BRAF opens the door for therapeutic advances in melanoma." Ann Intern Med **153**(9): 587-591.

238. Hersey, P. (2010). "Immunotherapy of melanoma." Asia Pac J Clin Oncol **6 Suppl 1**: S2-8.

239. Ko, J. M. and D. E. Fisher (2011). "A new era: melanoma genetics and therapeutics." J Pathol **223**(2): 241-250.

240. Davies, H.,G. R. Bignell, et al. (2002). "Mutations of the BRAF gene in human cancer." Nature **417**(6892): 949-954.

241. Puzanov, I. and K. T. Flaherty (2010). "Targeted molecular therapy in melanoma." Semin Cutan Med Surg **29**(3): 196-201.

242. Fedorenko, I. V.,K. H. Paraiso, et al. "Acquired and intrinsic BRAF inhibitor resistance in BRAF V600E mutant melanoma." Biochem Pharmacol **82**(3): 201-209.

243. Grauer, O. M.,R. P. Sutmuller, et al. (2008). "Elimination of regulatory T cells is essential for an effective vaccination with tumor lysate-pulsed dendritic cells in a murine glioma model." Int J Cancer **122**(8): 1794-1802.

244. Jakobisiak, M. and J. Golab (2010). "Genetic modification of T cells improves the effectiveness of adoptive tumor immunotherapy." Arch Immunol Ther Exp (Warsz) **58**(5): 347-354.

245. Liu, G.,H. T. Khong, et al. (2003). "Molecular and functional analysis of tyrosinase-related protein (TRP)-2 as a cytotoxic T lymphocyte target in patients with malignant glioma." J Immunother **26**(4): 301-312.

246. McCormick, A. A.,T. A. Corbo, et al. (2006). "Chemical conjugate TMV-peptide bivalent fusion vaccines improve cellular immunity and tumor protection." Bioconjug Chem **17**(5): 1330-1338.

247. McWilliams, J. A.,S. M. McGurran, et al. (2006). "A modified tyrosinase-related protein 2 epitope generates high-affinity tumor-specific T cells but does not mediate therapeutic efficacy in an intradermal tumor model." J Immunol **177**(1): 155-161.

248. Kou, G.,S. Shi, et al. (2007). "Preparation and characterization of recombinant protein ScFv(CD11c)-TRP2 for tumor therapy from inclusion bodies in Escherichia coli." Protein Expr Purif **52**(1): 131-138.

249. Tang, Y.,Z. Lin, et al. (2007). "An altered peptide ligand for naive cytotoxic T lymphocyte epitope of TRP-2(180-188) enhanced immunogenicity." Cancer Immunol Immunother **56**(3): 319-329.

250. Jerome, V.,A. Graser, et al. (2006). "Cytotoxic T lymphocytes responding to low dose TRP2 antigen are induced against B16 melanoma by liposome-encapsulated TRP2 peptide and CpG DNA adjuvant." J Immunother **29**(3): 294-305.

251. Mansour, M.,B. Pohajdak, et al. (2007). "Therapy of established B16-F10 melanoma tumors by a single vaccination of CTL/T helper peptides in VacciMax." J Transl Med **5**: 20.

252. Triozzi, P. L.,W. Aldrich, et al. (2010). "Regulation of the activity of an adeno-associated virus vector cancer vaccine administered with synthetic Toll-like receptor agonists." Vaccine **28**(50): 7837-7843.

253. Vasievich, E. A.,W. Chen, et al. (2011). "Enantiospecific adjuvant activity of cationic lipid DOTAP in cancer vaccine." Cancer Immunol Immunother.

254. Chono, S.,S. D. Li, et al. (2008). "An efficient and low immunostimulatory nanoparticle formulation for systemic siRNA delivery to the tumor." J Control Release **131**(1): 64-69.

255. Li, S. D.,S. Chono, et al. (2008). "Efficient gene silencing in metastatic tumor by siRNA formulated in surface-modified nanoparticles." J Control Release **126**(1): 77-84.

256. Rosenberg, S. A. and D. E. White (1996). "Vitiligo in patients with melanoma: normal tissue antigens can be targets for cancer immunotherapy." J Immunother Emphasis Tumor Immunol **19**: 81-84.

257. Wang, H. Y.,T. Fu, et al. (2002). "Induction of CD4(+) T cell-dependent antitumor immunity by TAT-mediated tumor antigen delivery into dendritic cells." J Clin Invest **109**(11): 1463-1470.

258. Shibagaki, N. and M. C. Udey (2003). "Dendritic cells transduced with TAT protein transduction domain-containing tyrosinase-related protein 2 vaccinate against murine melanoma." Eur J Immunol **33**(4): 850-860.

259. Vasievich, E. A. and L. Huang (2011). "The Suppressive Tumor Microenvironment: A Challenge in Cancer Immunotherapy." Mol Pharm.

260. Singh, V.,Q. Ji, et al. (2009). "Melanoma progression despite infiltration by in vivo-primed TRP-2-specific T cells." J Immunother **32**(2): 129-139.

261. Calabro, L.,R. Danielli, et al. (2010). "Clinical studies with anti-CTLA-4 antibodies in non-melanoma indications." Semin Oncol **37**(5): 460-467.

262. Gajewski, T. F.,Y. Meng, et al. (2006). "Immune suppression in the tumor microenvironment." J Immunother **29**(3): 233-240.

263. Vasievich, E. A. and L. Huang (2011). "The suppressive tumor microenvironment: a challenge in cancer immunotherapy." Mol Pharm **8**(3): 635-641.

264. Graziani, G.,L. Tentori, et al. (2011). "Ipilimumab: A novel immunostimulatory monoclonal antibody for the treatment of cancer." Pharmacol Res.

265. Lipson, E. J. and C. G. Drake (2011). "Ipilimumab: an Anti-CTLA-4 Antibody for Metastatic Melanoma." Clin Cancer Res.

266. Hodi, F. S.,S. J. O'Day, et al. (2010). "Improved survival with ipilimumab in patients with metastatic melanoma." N Engl J Med **363**(8): 711-723.

267. Schwartz, R. H. (2003). "T cell anergy." Annu Rev Immunol **21**: 305-334.

268. Wang, L.,R. Han, et al. (2007). "Programmed cell death 1 (PD-1) and its ligand PD-L1 are required for allograft tolerance." Eur J Immunol **37**(10): 2983-2990.

269. Benedict, C. A.,A. Loewendorf, et al. (2008). "Dendritic cell programming by cytomegalovirus stunts naive T cell responses via the PD-L1/PD-1 pathway." J Immunol **180**(7): 4836-4847.

270. Fife, B. T. and J. A. Bluestone (2008). "Control of peripheral T-cell tolerance and autoimmunity via the CTLA-4 and PD-1 pathways." Immunol Rev **224**: 166-182.

271. Groschel, S.,K. D. Piggott, et al. (2008). "TLR-mediated induction of negative regulatory ligands on dendritic cells." J Mol Med (Berl) **86**(4): 443-455.

272. Gajewski, T. F. (2007). "Failure at the effector phase: immune barriers at the level of the melanoma tumor microenvironment." Clin Cancer Res **13**(18 Pt 1): 5256-5261.

273. Tomihari, M.,J. S. Chung, et al. (2010). "DC-HIL/glycoprotein Nmb promotes growth of melanoma in mice by inhibiting the activation of tumor-reactive T cells." Cancer Res **70**(14): 5778-5787.

274. Breton, G.,B. Yassine-Diab, et al. (2009). "siRNA knockdown of PD-L1 and PD-L2 in monocyte-derived dendritic cells only modestly improves proliferative responses to Gag by CD8(+) T cells from HIV-1-infected individuals." J Clin Immunol **29**(5): 637-645.

275. Borkner, L.,A. Kaiser, et al. (2010). "RNA interference targeting programmed death receptor-1 improves immune functions of tumor-specific T cells." Cancer Immunol Immunother **59**(8): 1173-1183.

276. Hobo, W.,F. Maas, et al. (2010). "siRNA silencing of PD-L1 and PD-L2 on dendritic cells augments expansion and function of minor histocompatibility antigen-specific CD8+ T cells." Blood **116**(22): 4501-4511.

277. Kantoff, P. W.,C. S. Higano, et al. (2010). "Sipuleucel-T immunotherapy for castration-resistant prostate cancer." N Engl J Med **363**(5): 411-422.

278. Jaeger, E.,H. Bernhard, et al. (1996). "Generation of cytotoxic T-cell responses with synthetic melanoma-associated peptides in vivo: implications for tumor vaccines with melanoma-associated antigens." Int J Cancer **66**(2): 162-169.

279. Maeurer, M. J.,W. J. Storkus, et al. (1996). "New treatment options for patients with melanoma: review of melanoma-derived T-cell epitope-based peptide vaccines." Melanoma Res **6**(1): 11-24.

280. Rosenberg, S. A.,J. C. Yang, et al. (1998). "Immunologic and therapeutic evaluation of a synthetic peptide vaccine for the treatment of patients with metastatic melanoma." Nat Med **4**(3): 321-327.

281. Schwartzentruber, D. J.,D. H. Lawson, et al. (2011). "gp100 peptide vaccine and interleukin-2 in patients with advanced melanoma." N Engl J Med **364**(22): 2119-2127.

282. Yang, J. C. (2011). "Melanoma vaccines." Cancer J **17**(5): 277-282.

283. High, W. A.,D. Stewart, et al. (2005). "Completely regressed primary cutaneous malignant melanoma with nodal and/or visceral metastases: a report of 5 cases and assessment of the literature and diagnostic criteria." J Am Acad Dermatol **53**(1): 89-100.

284. Arpaia, N.,N. Cassano, et al. (2006). "Regressing cutaneous malignant melanoma and vitiligo-like depigmentation." Int J Dermatol **45**(8): 952-956.

285. Kalialis, L. V.,K. T. Drzewiecki, et al. (2009). "Spontaneous regression of metastases from melanoma: review of the literature." Melanoma Res **19**(5): 275-282.

286. Pique-Duran, E.,S. Palacios-Llopis, et al. (2011). "Complete regression of melanoma associated with vitiligo." Dermatol Online J **17**(1): 4.

287. Vasievich, E. A.,S. Ramishetti, et al. (2011). "Trp2 peptide vaccine adjuvanted with (R)-DOTAP inhibits tumor growth in an advanced melanoma model." Mol Pharm **(accepted)**.

288. Parkhurst, M. R.,E. B. Fitzgerald, et al. (1998). "Identification of a shared HLA-A*0201-restricted T-cell epitope from the melanoma antigen tyrosinase-related protein 2 (TRP2)." Cancer Res **58**(21): 4895-4901.

289. Ducat, E.,J. Deprez, et al. (2011). "Nuclear delivery of a therapeutic peptide by long circulating pH-sensitive liposomes: Benefits over classical vesicles." Int J Pharm **420**(2): 319-332.

290. Kang, M. J.,S. Lee, et al. (2011). "Pep-1 Peptide-modified liposomal carriers for intracellular delivery of gold nanoparticles." Chem Pharm Bull (Tokyo) **59**(1): 109-112.

291. Wieber, A.,T. Selzer, et al. (2011). "Characterisation and stability studies of a hydrophilic decapeptide in different adjuvant drug delivery systems: A comparative study of PLGA nanoparticles versus chitosan-dextran sulphate microparticles versus DOTAP-liposomes." Int J Pharm.

292. Gao, X. and L. Huang (1996). "Potentiation of cationic liposome-mediated gene delivery by polycations." Biochemistry **35**(3): 1027-1036.

293. Li, S. and L. Huang (1997). "In vivo gene transfer via intravenous administration of cationic lipid-protamine-DNA (LPD) complexes." Gene Ther **4**(9): 891-900.

294. Tan, Y.,M. Whitmore, et al. (2002). "LPD nanoparticles--novel nonviral vector for efficient gene delivery." Methods Mol Med **69**: 73-81.

295. Chen, Y.,S. R. Bathula, et al. (2010). "Targeted nanoparticles deliver siRNA to melanoma." J Invest Dermatol **130**(12): 2790-2798.

296. Chen, Y.,J. J. Wu, et al. (2010). "Nanoparticles targeted with NGR motif deliver c-myc siRNA and doxorubicin for anticancer therapy." Mol Ther **18**(4): 828-834.

297. Tomihari, M.,J. S. Chung, et al. "DC-HIL/glycoprotein Nmb promotes growth of melanoma in mice by inhibiting the activation of tumor-reactive T cells." Cancer Res **70**(14): 5778-5787.

298. Zhang, X.,Z. G. Chen, et al. (2005). "Tumor growth inhibition by simultaneously blocking epidermal growth factor receptor and cyclooxygenase-2 in a xenograft model." Clin Cancer Res **11**(17): 6261-6269.

299. Peyre, M.,R. Fleck, et al. (2004). "In vivo uptake of an experimental microencapsulated diphtheria vaccine following sub-cutaneous immunisation." Vaccine **22**(19): 2430-2437.

300. Keir, M. E.,M. J. Butte, et al. (2008). "PD-1 and its ligands in tolerance and immunity." Annu Rev Immunol **26**: 677-704.

301. Durgan, K.,M. Ali, et al. (2011). "Targeting NKT cells and PD-L1 pathway results in augmented anti-tumor responses in a melanoma model." Cancer Immunol Immunother **60**(4): 547-558.

302. Paltauf, F.,F. Esfandi, et al. (1974). "Stereospecificity of lipases. Enzymic hydrolysis of enantiomeric alkyl diacylglycerols by lipoprotein lipase, lingual lipase and pancreatic lipase." FEBS Lett **40**(1): 119-123.

303. Akesson, B.,S. Gronowitz, et al. (1976). "Stereospecificity of hepatic lipases." FEBS Lett **71**(2): 241-244.

304. Paltauf, F. and E. Wagner (1976). "Stereospecificity of lipases. Enzymatic hydrolysis of enantiomeric alkyldiacyl- and dialkylacylglycerols by lipoprotein lipase." Biochim Biophys Acta **431**(2): 359-362.

305. Somerharju, P.,T. Kuusi, et al. (1978). "Stereospecificity of lipoprotein lipase is an intrinsic property of the active site of the enzyme protein." FEBS Lett **96**(1): 170-172.

306. Zandonella, G.,L. Haalck, et al. (1995). "Inversion of lipase stereospecificity for fluorogenic alkyldiacyl glycerols. Effect of substrate solubilization." Eur J Biochem **231**(1): 50-55.

307. Lasic, D. D. (1997). "Colloid chemistry. Liposomes within liposomes." Nature **387**(6628): 26-27.

308. Walker, S. A.,M. T. Kennedy, et al. (1997). "Encapsulation of bilayer vesicles by self-assembly." Nature **387**(6628): 61-64.